

**An ultra scale-down tool for the predictive
design of a filtration procedure for
preparation of human cell therapies**

A thesis submitted to University College London for
the degree of Doctor of Engineering in Biochemical
Engineering

By

Chris Longster

The Advanced Centre of Biochemical
Engineering
Department of Biochemical Engineering
University College London

September 2015

*To my family, Longster,
O'Neill, Parsons.....*

Declaration

I hereby declare that the work presented in this thesis is solely my own work and that to the best of my knowledge the work is original except where otherwise indicated by reference to other authors.

Chris Longster

05/09/15

Abstract

With the potential to provide a cure as oppose to a treatment, human cell therapies offer an exciting alternative to biopharmaceuticals. However the challenges associated with whole cell bioprocessing are one of the main issues hindering human cell therapies from becoming commonplace in modern medicine.

An ultra scale-down approach to dead end filtration for the recovery of adherent cells for therapy is presented.

Initial viable cell yields were low and a number of methods were used in an attempt to improve recovery, with little success. It was possible to recover approximately 85% of the cells but only when the number of cells loaded was low ($< 1 \times 10^6$ cells), when a higher number of cells were loaded $> 1 \times 10^6$ cells, the recoveries were significantly lower.

A model is proposed which describes two distinct cell populations; surface cells (T_{SURF}) which reside on the surface of the filter after loading and are almost entirely recovered and filtered cells (T_{FILT}) which enter the filter and are extremely difficult to recover. Results showed that on average $35\% \pm 11\%$ of filtered cells (T_{FILT}) are recovered regardless of the number of cells loaded.

Scanning electron microscopy was used to image the cells residing within the filter. The images showed the cells wrapping around and entangling themselves within the fibres of the filter demonstrating why they are difficult to recover.

Finally a method is presented which uses a layer of glass beads on the surface of the filter to prevent the cells coming into contact with filter. By stopping the cells becoming trapped within the filter there was a significant increase in the viable cell recoveries. Using this method it was possible to recover on average $84\% \pm 6\%$.

Acknowledgements

This project was funded by the EPSRC IDTC in collaboration with Pall Life Sciences.

I would like to thank my supervisor Mike Hoare for his unwavering support and expertise throughout the research. It has been an honour to work alongside a true expert in the field and the lessons I have learned from you stretch far beyond the boundaries of this research and will stay with me for the rest of my career.

I wish to thank Peter Levison my co-supervisor at Pall, you have provided constant direction and support to the project. In our first meeting together you said that our relationship over the duration of the project would progress from “supervisor – student” to colleagues. I hope that I can now consider you a friend and a colleague and I wish you all the best for the future.

I would also like to thank my secondary supervisor Dr Ivan Wall you have provided valuable input throughout the project and have been an ever present source of support and ideas. The project has also benefitted from the input and expertise of a number of others including Dr Kate Lawrence, Dr Jennifer Man, Ludmila Ruban and Dr Brian O’Sullivan, your input has been invaluable.

My time at UCL has been thoroughly enjoyable thanks to the many good friends and colleagues I have made during the past 4 years. I would like to thank Kate Lawrence, it’s amazing how so much knowledge can be stored in something so small; you really are the Tardis of cell biology!! Fernanda Masri, “Julio Arca’s cousin” for sharing my love of trashy TV and Karaoke, Alex “the Charlatan” Chatel for introducing me to the art of Quackery and less so the art of time keeping, “Chen” Man for fun San Diego times, you are one in a billion, and Delahaye for a number of reasons but mainly for giving me that cracked version of Champ Man 01/02 for my laptop, cheers pal!! Dougie

and Rhys for making lunch breaks entertaining with our crosswords and incessant mocking of Rhys' spelling and general lack of vowels.

To everyone else who made my time at UCL a real pleasure, Hughson, Sara, Aaron, Rooni, Asma, Bettsy, Jayan, Daria, Dave, Adam, Helmi and countless others (no doubt some of whom I've missed!!) I thank you.

Away from UCL, Rob, Marty, Cloughy and Ossie you haven't really done a lot but felt like I should include you somehow. Cheers!

I would like to thank Karen, David and family. From giving me a home and welcoming me into the family during my MSc to your constant support throughout my studies (whilst only rarely mentioning the fact I didn't have a "proper job"), I could not have done any of it without you.

To my Nan and Grandad, Grandma and Grandad, sister Jo, aunties, uncles and family your continuing interest and backing in everything I do gave me the energy to keep going. Thank you!!

To my mam and dad, I cannot thank you enough for everything you have done for Jo and I. Your hard work has allowed us the fantastic opportunities we've had and I am eternally grateful. You are true role models in every sense of the word.

Finally Charley, you are my rock and my soul mate. For the sacrifices you have made over the past 5 years I cannot thank you enough, you are incredible. As I finish this thesis we now start a new chapter in our lives together in more ways than one and it is one which I cannot wait to explore with you, I feel that this is the best time, to tell you that I love you, all the time.

Contents

Abstract	4
Acknowledgements	5
List of figures	10
List of tables	14
Abbreviations	15
Nomenclature	17
1. Introduction.....	21
1.1. Thesis overview.....	21
1.2. Cell therapy	22
1.2.1. Allogeneic therapies.....	22
1.2.2. Autologous therapies.....	23
1.2.3. Tissue engineering	24
1.2.4. Whole cell therapies.....	25
1.2.5. Stem cell therapies	26
1.2.6. Whole cell vaccines.....	28
1.3. Whole cell bioprocessing	29
1.3.1. Cell culture	29
1.1. Primary recovery	35
1.1.1. Depth filtration	35
1.1.2. Tangential flow filtration	37
1.1.3. Batch centrifugation	38
1.1.4. Continuous Centrifugation.....	39
1.2. Effect of bioprocessing on cell quality.....	40
1.2.1. Physiological conditions	41
1.3. Analysing cell quality.....	42
1.3.1. Membrane integrity and viability.....	42
1.3.2. Apoptosis	44
1.3.3. Cell Morphology	45
1.3.4. Cell surface markers.....	46
1.4. Ultra scale-down technology.....	46
1.4.1. Shear devices.....	47
1.4.2. Tangential flow filtration (TFF).....	48

1.4.3.	Normal flow filtration (NFF)	49
1.5.	Project aims	50
2.	Materials and methods	53
2.1.	Introduction	53
2.2.	Cell lines	53
2.2.1.	HCA2	53
2.2.2.	CTX0E03	53
2.3.	Cell culture	54
2.3.1.	HCA2	54
2.3.2.	CTX0E03 (CTX).....	55
2.4.	Dead end ultra scale-down filtration and cell recovery.....	56
2.4.1.	Device design	56
2.4.2.	Device Operation	57
2.4.3.	Filter preparation.....	59
2.5.	Backflush buffer preparation.....	59
2.5.1.	Rheology studies	59
2.5.2.	Sample collection.....	60
2.5.3.	Centrifugation control	60
2.6.	Cell analysis	61
2.6.1.	Cell membrane integrity.....	61
2.6.2.	Lactate dehydrogenase	61
2.6.3.	Particle size distribution.....	63
2.6.4.	Cell morphology analysis.....	63
2.6.5.	Cell death analysis.....	64
2.6.6.	BCA total protein analysis	67
2.7.	Microscopy.....	67
2.7.1.	Fluorescent microscopy	67
2.7.2.	Scanning electron microscopy	68
3.	Development of an ultra scale-down filtration process for the recovery of human cells for therapy.....	71
3.1.	Introduction	71
3.2.	Establishing and optimising operating conditions.....	71
3.2.1.	Syringe hold time	71
3.2.2.	Backflush conditions.....	74

3.2.3.	Backflush buffer	81
3.2.4.	Effect of loading conditions on recovery of HCA2 cells	87
3.3.	Chapter Discussion	100
4.	Mechanisms affecting the recovery of high quality adherent cells during filtration	105
4.1.	Locating and quantifying the unrecovered cells	105
4.1.1.	Lactate dehydrogenase	105
4.1.2.	Cryosectioning and fluorescent microscopy	109
4.1.3.	Effect of filter geometry on cell recovery	109
4.1.4.	Scanning electron microscopy	118
4.2.	Impact of processing on the quality of recovered cells	122
4.2.1.	Continuous culture of processed cells	127
4.2.2.	Effects of process hold times	129
4.2.1.	Removal of protein during processing	133
4.1.	Chapter Discussion	142
5.	Maximising cell recovery	147
5.1.	Membrane filtration	147
5.2.	Gravity settling as a method of loading to increase cell recovery	149
5.3.	Using glass beads to prevent cell loss during filtration	155
5.4.	Effect of glass bead ‘pre-filter’ on total cell recovery	157
5.5.	Why do the beads work?	160
5.6.	Effect of flux on the recovery of cells during glass bead filtration	161
5.7.	Effect of flux rate on cell quality	163
5.8.	Protein removal	167
5.9.	Effect of a glass bead ‘pre-filter’ during membrane filtration.	167
5.9.1.	Reasons for cell loss during membrane bead filtration	172
5.9.2.	Bead layers	175
5.9.3.	Effect of flux on the recovery of cells during glass bead membrane filtration	177
5.10.	Chapter discussion	179
6.	Conclusion	183
7.	Future Work	186
	References	196

List of figures

Figure 1.1 - - Purchase cost of MF/UF hardware adapted from Petrides (2003).....	46
Figure 1.2 – Schematic diagram of a rotating drum filter (not to scale).....	46
Figure 1.3 – Flux- pressure profiles for constant pressure filtration (a) and constant flux filtration (b).	46
Figure 2.1 – Schematic diagram of the USD filtration set up including syringe pump, with magnetic stirrer, filter housing and digital pressure sensor (Not to scale).....	58
Figure 2.2 –Flow diagram detailing the categorisation process undertaken by the software when analysing objects within the images taken from the ViCell XR.....	65
Figure 3.1 – Total cell concentration and viability of cells delivered by the syringe when maintained in suspension by the magnetic stirrer for three repeat tests.....	73
Figure 3.2 – Cell death analysis of cells maintained in suspension within the syringe barrel.	75
Figure 3.3 – Effect of backflush flow rate on total cell recovery.	77
Figure 3.4 - Effect of backflush flow rate on the membrane integrity of recovered cells.	79
Figure 3.5 – Proportion of recoverable cells recovered in each section of the backflush buffer.....	80
Figure 3.6 – Effect of dextran concentration on rheology of backflush buffer; 10% (◆), 20%(◆) and 30%(◆) dextran in DPBS.....	82
Figure 3.7 – Effect of elution buffer on total cell recovery and viability of recovered cells.	85
Figure 3.8 – Particle size analysis of recovered samples.....	86
Figure 3.9 – Effect of number of total cells loaded on the number of total cells recovered.....	89

Figure 3.10 - Effect of number of cells loaded on the proportion of total cells recovered.	90
Figure 3.11 - Effect of number of load cell number on the proportion of cells in the permeate.	91
Figure 3.12 – Effect of load cell number on the viability of the recovered cells.....	92
Figure 3.13 – Proportion of “filtered” cells which are recovered (see Equation 3.4 and Equation 3.5).	95
Figure 3.14 – Effect of the number of total cells loaded on the number of total cells recovered.	96
Figure 3.15 – Effect of volume of cell suspension loaded on recovery of “filtered” cells.	98
Figure 3.16 – Effect of cell concentration in the feed on the recovery of “filtered” cells.	99
Figure 4.1 – Schematic of LDH mass balance.	107
Figure 4.2 – LDH accountability.	108
Figure 4.3 – Fluorescent microscopy images of cryosectioned filters.....	110
Figure 4.4 – Schematic drawing of the hypothesised mechanism which causes cells to become trapped within ‘dead zones’ in the filter.	112
Figure 4.5 – Effect of reuse of filter on increase in total cell recovery.....	113
Figure 4.6 – Effect of filter housing geometry on total cell recovery.....	117
Figure 4.7 – Scanning electron microscopy of filter cross sections.....	119
Figure 4.8 - Scanning electron microscopy of filter surface.....	121
Figure 4.9 – Cellular interaction with filter fibres.	123
Figure 4.10 – Cell death caspase assay results for the effect of processing on the quality of recovered cells.	124

Figure 4.11 - Cell death caspase assay results for the effect of processing on HCA2 and CTX0E03 cells	126
Figure 4.12 – Effect of processing on the quality of recovered cells.....	128
Figure 4.13 –Growth curves and specific growth constants for processed HCA2 cells.	130
Figure 4.14 – Effect of a 24 hour hold time on the quality of recovered HCA2 cells. .	132
Figure 4.15 – Effect of a pre-backflush forward wash step on protein removal.....	135
Figure 4.16 – Protein removal: filtration vs centrifugation.....	137
Figure 4.17 – Effect of wash buffer volume on total cell recovery	138
Figure 4.18 –Effect of a forward wash step on cell morphology.....	140
Figure 4.19 – Effect of forward washing on the quality of recovered cells.....	141
Figure 5.1 - Membrane vs depth filtration	148
Figure 5.2 – Effect of load cell number on the total cell recovery.....	150
Figure 5.3 – Schematic drawing of gravity settling filtration set up.....	152
Figure 5.4 – Effect of settling times on the recovery of cells from the filter.....	154
Figure 5.5 – Overview of gravity settling filtration experiments	156
Figure 5.6 – Mastersizer 2000 particle size data distribution profile for the glass beads.	158
Figure 5.7 – Impact of glass bead pre-filter layer on the recovery of total cells.	159
Figure 5.8 –Effective pore size created by the glass beads.....	162
Figure 5.9 - Schematic drawing of gravity settling filtration set up.	164
Figure 5.10 – Effect of filtration rate on the proportion of total cells recovered during gravity settling filtration.....	165
Figure 5.11 – Effect of flux rate during processing on the quality of recovered cells..	166

Figure 5.12 –Comparison of protein removal capacity for three different methods of primary recovery.	168
Figure 5.13 –Effect of a forward wash step on protein removal during ‘glass bead filtration’.	169
Figure 5.14 – Effect of glass bead ‘pre-filter’ on total cell recovery.....	171
Figure 5.15 – SEM images of glass beads post filtration.....	174
Figure 5.16 – Effect of glass bead pre-filter depth on the total cell recovery.....	176
Figure 5.17 - Effect of filtration rate on the total cell recovery	178

List of tables

Table 1.1 - Comparison of cell properties for the three cell types used in this research (CHO, HCA2 and CTX0E03) and other cell types relevant to the bioprocessing industry	30
Table 3.1 – Rheological properties of dextran solutions using power law model, $\tau = k\gamma^n$	82
Table 4.1- Scale up of processing conditions for different filter housing geometries..	115
Table 6.1 – Theoretical scale up of bead filtration process.....	190

Abbreviations

4-OHT – 4-hydroxy-tamoxifen

BCA assay - Bicinchoninic acid assay

bFGF – basic fibroblast growth factor

BSA – bovine serum albumin

cDMEM – complete Dulbecco's Modified Eagles Medium

CGM – complete growth medium

CQA – critical quality attribute

DAPI – 4', 6-diamidino Modified Eagles Medium

DMSO – dimethyl sulfoxide

DPBS – Dulbecco's phosphate buffer saline

DTI – defined trypsin inhibitor

EGF – epidermal growth factor

FCS – foetal calf serum

FLICA® - Fluorescent labelled inhibitor of caspases

GMP – Good manufacturing practice

HAS – human serum albumin

HBSS – Hanks balanced salt solution

hESC – human embryonic stem cells

INT – tetrazolium salts

iPS – induced pluripotent stem cells

LDH – lactate dehydrogenase

PI – propidium iodide

RMM – reduced modified medium

SEM – Scanning electron microscopy

TFF – tangential flow filtration

UCL – University College London

USD – ultra scale-down

Nomenclature

[T_L] - Total cell concentration of loading suspension (cells mL⁻¹)

[T_R] - Total cell concentration of recovered suspension (cells mL⁻¹)

Δp - Pressure drop across the filter (bar)

A – Area of filter (m²)

A_{Bead} - Cross sectional area of a glass bead (μm²)

C – Confluency (-)

d_{Bead} - Mean average diameter, volume basis (μm)

d_c – Mean cell diameter, number basis (μm)

K - Consistency index (N sⁿ m⁻²)

k – specific growth constant (h⁻¹)

K_v - Particle shape (-)

LDH_{Total} - Total amount of LDH present (internal and external)

M_{Beads} - Mass of beads on the filter surface (g)

M_c - Total mass of solids within the filter (g)

n - Degree of non-Newtonian behaviour (-)

N_{vc} – Number of viable cells

PLDH_{TOTAL} - Percentage of total LDH recovered (%)

PT_P – Percentage of total cells in the permeate (%)

PT_R – Percentage of total cells recovered (%)

PT_R^* - % of total filtered cells recovered by backflush (%)

rcf – Relative centrifugal force (xg)

r_m - Filter medium resistance (m^{-1})

s – Filter cake compressibility (-)

SA_{PART} – Specific particle surface area (-)

t – Time (s)

T_{FILT} – Number of total cells residing within the filter after loading (#)

T_L – Number of total cells loaded (#)

T_P – Number of total cells in the permeate (#)

T_R – Number of total cells recovered (#)

t_{SET} – Settling time (mins)

T_{SURF} – Number of total cells residing on the filter surface after loading (#)

V_{Bed} - Volume of the bed created by the bead layers (m^3)

V_c – Volume of filter cake (m^3)

V_f – Volume of filtrate (m^3)

V_{PART} - Particle volume (m^3)

V_{sol} – Total volume of solids within the filter cake (m^3)

α - Average specific cake resistance ($m\ kg^{-1}$)

γ - Shear rate (s^{-1})

ε - Filter cake porosity (-)

μ_f - Viscosity of the filtrate (Nsm^{-2})

ρ_{Bead} - Density of glass beads ($g\ m^{-3}$)

ρ_p - Particle density ($kg\ m^{-3}$)

τ - Shear stress ($N\ m^{-2}$)

Chapter 1: Introduction

1. Introduction

1.1. Thesis overview

This thesis will have the following structure:

Chapter 1 will present a review of the literature detailing the research into the production of cellular therapies for the biopharmaceutical sector. This chapter will cover the types of cell therapies currently under research and available on the market, the cells used to produce these therapies and the challenges associated with manufacturing them. It will also cover the use of ultra scale-down technologies to develop these therapies in the lab.

Chapter 2 will detail the methods and standard operating procedures used to carry out the work presented in this thesis. The materials used, are also presented to allow the work to be repeated in future if needed.

Chapter 3 documents the initial development of the ultra scale-down device used to carry out the early research.

Chapter 4 investigates the mechanisms and interactions which influence the recovery of cells from the filter and the quality of those cells post processing. The chapter looks at the reasons behind poor performance and aims to provide a solution to the low recoveries.

Chapter 5 proposes a solution to the recovery problems associated with the earlier devices. The solution takes the form of an ultra scale-down filter system which uses a permeable glass bead pre-filter layer to prevent the cells becoming trapped on or within the filter.

Chapter 6 provides some final thoughts on how the research developed and whereabouts there is potential room for future work.

Chapter 0 covers the process validation which would need to be undertaken in order to use the filtration process described in the commercial manufacture of cells for therapy.

1.2. Cell therapy

With the potential to provide a cure as oppose to a treatment, human cell therapies offer an exciting alternative to biopharmaceuticals. However, the challenges associated with whole cell bioprocessing are one of the main issues hindering human cell therapies from becoming commonplace in modern medicine (Raviv and Carnieli, 2014).

The idea of culturing cells for tissue replacement or regeneration evolved in the 1930's and research began with the start-up of the tissue engineering industry in the late part of the 20th century (Nerem, 2010). Recent times have seen the arrival of the first human cell therapeutics to market, applicable for a wide variety of conditions including treatment of ulcers as a result of diabetes (Zhou et al., 2016), whole cell vaccines against cancer (Bencherif et al., 2015) and cartilage repair in joint injuries (Fellows et al., 2016).

Regenerative medicine and cell therapy can be roughly divided into 4 main categories; tissue engineering, whole cell therapies, stem cell therapies and whole cell vaccines. The source of the cells used for the therapy determines whether the therapy is deemed allogeneic or autologous.

1.2.1. Allogeneic therapies

Allogeneic cell therapies involve the transplantation of cells or tissues derived from another human being; they are not the patient's own cells. Allogeneic cell therapies have the potential to treat a number of diseases, such as chronic liver disease (Than et al., 2016), Hodgkin Lymphoma (Gauthier et al., 2017), heart disease (Oh et al., 2016), hip osteonecrosis (Stanovici et al., 2016) and spinal cord injury (Bretzner et al., 2011).

1.2.2. Autologous therapies

There are currently a number of autologous therapies on the market, treating a wide number of diseases such as, peripheral arterial disease, diabetes, neurodegenerative disorders, liver disease, bone repair, and spinal cord injuries (Hourd et al., 2014)

Multiple sclerosis is an inflammatory disease affecting the myelin sheath coating the axons within the brain and spinal cord preventing communication between the two. The myelin sheath is attacked by the patient's own immune system causing damage and scarring (Colmone, 2015). According to statistics the disease affects as many as 1 in 1000 people in the western world (Chwastiak et al., 2014). Current research into possible autologous therapies is looking at the possibility of using autologous haematopoietic stem cells to treat the disease. Studies have shown that implanting the cells into the patient, following a period of chemotherapy to suppress the patient's immune system, provides the patient with a new myelin sheath that is more 'tolerant to the immune system'.(Blanco et al., 2005, Llufriu et al., 2014)

As previously mentioned there are a number of benefits associated with using autologous therapies. The fact that they are the patient's own cells that are taken out and cultured before being transplanted back into the patient provides a number of biological advantages in terms of infection and the immune response from the patient, which is often a major problem with human cell therapies. However, there are also bioprocessing

advantages in terms of getting regulatory approval for the therapy. The regulations tend to be slightly more relaxed for autologous therapies, as opposed to allogeneic therapies, as the patient is being administered their own cells and there is no need for immunosuppression (Knoepfler, 2015). The initial sourcing of the cells for the therapy is less problematic too, as there are no issues associated with finding a donor or any ethical issues associated with harvesting from the blastocyst, as is the case with human embryonic therapies (Munsie and Hyun, 2014).

There are, however, a number of disadvantages associated with manufacturing autologous therapies. Each cell batch is patient specific, so all batches must be kept completely separate throughout manufacture. This means separate hoods, incubators, single use filters and separate storage. This becomes a major issue when looking to treat high numbers of patients. The therapies are required to be manufactured in multiple small batches meaning there is no benefit from economies of scale making production time consuming and expensive (Jones et al., 2012). Research indicates that the average cost to produce an autologous cell therapy can be more than double the cost per dose when compared to allogeneic cell therapies (Malik, 2012). The relatively small lot sizes for individual therapies may also mean that there are not enough cells to spare for comprehensive biopotency and efficacy assays (Ährlund-Richter et al., 2009).

1.2.3. Tissue engineering

Tissue engineering is the *in vitro* production of new tissues using donor cells usually grown on a collagen scaffold, in order to repair or replace damaged tissue within a patient. The scaffold plays an important role mimicking the extra cellular matrix (ECM) which the tissues grow on *in vivo*. The ECM provides the stimuli necessary for cells within the tissue to divide and differentiate (Jakab et al., 2015).

One of the most promising developments in tissue engineering is tracheal transplants used to treat tracheal stenosis. Tracheal stenosis is the narrowing of the trachea and can occur for a number of different reasons, including blunt trauma and compression from congenital cardiovascular abnormalities (He et al., 2012).

The first tracheal transplantation was carried out in June 2008 on a 30 year old female with end stage bronchomalacia (Macchiarini et al., 2008). A healthy trachea from a human donor was decellularised to remove cells as well as the MHC antigens. The trachea was then colonised with cells taken from the recipient and expanded. The new airway was used to replace the patients damaged left main bronchus and provided the recipient with a functional airway and improved quality of life. After 4 months the implanted airway showed normal appearance and mechanical properties. Complete removal of the donor cells and antigens from the donated trachea meant that the patient did not require any immuno-suppression (Macchiarini et al., 2008).

Despite this recent success a number of challenges still remain. A full understanding of the many factors which have a major impact on the development and sustainability of tissues, as well as the complex cell-cell interactions which occur within tissues, is required if the potential of tissue engineering is to be fully achieved (Berthiaume et al., 2011).

1.2.4. Whole cell therapies

The U.S Food and Drug Administration (FDA) define cell therapy as ‘the prevention, treatment, cure or mitigation of disease or injuries in humans by the administration of autologous, allogeneic or xenogeneic cells that have been manipulated or altered *ex vivo*’ (FDA, 1997).

The earliest examples of cell therapies date back to the first successful bone marrow transplantations in humans in the 1960's (Starzl, 2000, Baptista and Atala, 2014). Since then whole cell therapies have sparked an entire new industry with over 30,000 autologous bone marrow transplants alone carried out by the start of the 21st century (Mason and Hoare, 2007).

Cell therapies have been used to treat a number of conditions, including cartilage damage, with chondrocyte implant therapies, such as Chondrocelect® being available since the late 1980's (Minas and Peterson, 2000) and the potential to treat many others, including inflammatory conditions, such as graft vs host disease and Crohn's disease (Newman et al., 2009).

1.2.5. Stem cell therapies

Amongst all the therapies and treatments associated with regenerative medicine none provide quite the same level of excitement, potential or controversy as stem cell therapies (Ilic and Ogilvie, 2017). Stem cells are biological cells which have the potential to differentiate into adult cells when the correct stimuli are present. The level of differentiation that the cell is capable of, in terms of the number of potential lineages they can follow, is dependent on the type of stem cell. Totipotent cells have the ability to differentiate into any cell or cell precursor found within the human body and so by definition have the potential to form a whole organism. The fertilised egg or zygote cell is an example of a totipotent cell (Zhou and Dean, 2015). Pluripotent cells such as embryonic stem cells can differentiate into any of the cells derived from the three germ layers. Multipotent and oligopotent stem cells have a select number of differentiation pathways dependent on the cell type (oligopotent cells have less differentiation potential than multipotent cells). For instance, haematopoietic stem cells are multipotent adult

stem cells which give rise to the different types of blood cells (Morrison and Scadden, 2014).

The ability of these cells to differentiate provides extraordinary therapeutic potential, which, as yet, has not fully been recognised. However, there have been a number of recent breakthroughs and we are now beginning to see the first few stem cell therapies move into and through clinical trials. In 2009 the FDA approved the first ever clinical trial for an embryonic stem cell therapy, a phase I clinical safety trial for Geron Corps' treatment for spinal cord injury (Mothe and Tator, 2012). However, the trial was eventually abandoned and there have been no more embryonic stem cell trials since. Multipotent adult stem cell applications however, have proved much more successful. There is always likely to be a high level of risk and ethical controversy surrounding any human embryonic stem cell therapy and going forward I see the focus of stem cell therapies going more in the direction of some of the newer technologies such as induced pluripotent stem cells (IPS).

IPS cells like embryonic stem cells are pluripotent however they are generated from directly from adult cells and therefore do not require the harvesting of an embryo thus reducing the level of ethical controversy which has surrounded human embryonic stem cells. In 2006 (Takahashi and Yamanaka) successfully transformed mouse fibroblasts into pluripotent stem cells using a combination of 4 transcription factors. They were subsequently able to use the same transcription factors to produce human IPS cells from human dermal fibroblasts (Takahashi et al., 2008). Since this breakthrough a number of human cell types have been transformed back to a pluripotent state including T-lymphocytes, neural stem cells and adipose tissue (Youssef et al., 2016).

Whilst there are still some safety concerns surrounding the use of IPS cells for therapy in particular around teratoma formation, they are undoubtedly less controversial and have the potential to treat a number of diseases such as cirrhosis of the liver which is currently one of the leading causes of death in the world (Hansel et al., 2016).

1.2.6. Whole cell vaccines

The understanding that cancer and the progression of cancer is often due to the bodies inability to produce an immune response in order to target the cancer cells has led to a significant developments in the search for new ways to treat cancer (Katz et al., 2014). The use of cancer cells in whole cell vaccines marks a significant step change in the approach to treating cancer (Lokhov and Balashova, 2010). Whole cell cancer vaccines use either autologous or allogeneic cancer cells, which have identical, or at least similar, antigenic proteins to the patient's tumour (Ramirez-Montagut, 2014). The main advantage of whole cell vaccines over other target specific therapies is the ability to target multiple and even unidentified cell markers. However, research into potential cancer vaccines has been carried out over the last few decades with little breakthrough (De Gruijl et al., 2008). One of the reasons for this is that only a small number of the molecules expressed on the surface of the tumour cells are specific to the cancerous cells. This means that when patients are injected with a whole cell vaccine, the immune response that the vaccination induces is not strong enough to eliminate the cancer cells (Cohen et al., 2009). In order to be effective, cancer vaccines need to identify cells which only express molecules that are not found on the surface of normal cells. The proteins and carbohydrates found on normal cells dilute the proportion of cancer specific surface molecules and weaken the immune response (Abercrombie and Ambrose, 1962).

One method of improving the immune response to the vaccines is to use vaccines made up solely of the cancer specific antigens. Hollinshead et al first proposed the use of soluble membrane antigens isolated from cancer cells as a cancer vaccine (Hollinshead et al., 1974a, Hollinshead et al., 1974b).

For many years this method has proved unsuccessful due to the damage caused to the antigens during isolation. However, this method has been developed and recently Petr (2010) presented a method of using cell surface antigens proteolytically cleaved from the surface of live tumour cells as a cancer vaccine. Results showed that when compared to a cell lysate based vaccine the cleaved antigens induced an immune response up to 40% greater, whilst using a much lower concentration of protein (2 µg/mL compared to 270 µg/mL) (Petr, 2010).

1.3. Whole cell bioprocessing

As with any new therapy, the bioprocessing and manufacturing of these therapies reveal a unique set of challenges; this is especially relevant with whole cell bioprocessing. Whereas with the traditional bioprocessing of cells for the preparation of proteins, any damage caused to the cells in the process environment is only a concern in the culture stages and generally has little or no effect on the final product. With human cell therapies, the cell itself is the product and therefore it is essential that damage is kept to a minimum (Mason and Hoare, 2007).

1.3.1. Cell culture

1.3.1.1. 2D cell culture

Traditionally at lab scale, adherent cells are grown in polystyrene tissue culture flasks known as T-flasks. Cells are grown surface attached until confluent and then

enzymatically detached. The flasks vary depending on the size of the area they have available for growth and can range from 25 cm² to 500 cm², with typical cell densities of around 1 x 10⁵ cells cm⁻² (Lapinskas, 2010). As therapies move towards clinical trials and eventual commercialisation the demand for large numbers of cells makes the use of T-flasks unfeasible with cell dose sizes varying from 10⁴ to 10⁶ in the case of some cardiac cell therapies and even 10⁹ cells per dose for blood therapies. At this stage simply scaling out the cell expansion process by increasing the number of T-flasks becomes unrealistic in terms of operator variability as well as regulatory and physical limitations (Lapinskas, 2010).

Scale up of 2D culture is possible by increasing the number of growth surfaces available and essentially stacking them up, these multi-layered culture systems are known as cell stacks or cell factories. The Cell Cube and the CellSTACK (Corning, New York, USA) as well as the Cell Factory (Nunc; Thermo, Strasbourg, France) are good examples of these, offering surface growth areas of up to 25,000 cm². However, for commercial production, large clean rooms or buildings would still need to be filled with these factories in order to meet the numbers of cells required for clinical trial doses (Brandenberger et al., 2011).

Although anchorage dependant cells are traditionally expanded in a two dimensional culture environment *in vitro*, this is far from the case *in vivo*. In the human body cells grow as part of 3D matrices, organised into tissues and surrounded by other cells. It is the interactions within these matrices that govern the behaviour of the surrounding cells and subtle changes within these environments determine whether or not a cell proliferates or differentiates or even if it enters apoptosis. In a 2D culture environment some of these interactions are lost and there are increasing numbers of studies

suggesting that cells grown in 2D systems can express differences in phenotype and drug responses (Keiran et al., 2006).

The most appealing aspect of 2D cell culture is its simplicity; cell seeding, cell harvesting and liquid handling are all straight forward and relatively low cost. However, there is also a distinct lack of process control. Flasks/factories are stored within humidified and temperature controlled incubators and the air within the incubators is maintained at a constant level, outside of this there is little or no control on the process environments. Despite work being carried out in laminar flow hoods, there is still an inherent risk of contamination as the cells are exposed to an open environment making regulatory compliance difficult.

The passaging process is also a very manual and labour intensive process. This makes operator variability a big issue and complicates process validation.

Automation of cell culture in a controlled environment would help to remove the operator variability and could also be carried out in a closed environment. Automated cell culture has thus far not been significantly used in the cell therapy industry for a number of reasons including the initial cost of the automation equipment. The Automation Partnership (TAP, now part of the Sartorius Stedim Biotech Group) has two automated cell culture platforms; the Cellmate™ and the more recent SelecT.

The Cellmate™ was developed in the late 1980's and there are over 70 installed worldwide fulfilling a number of manufacturing purposes. The Cellmate™ works with flasks or roller bottles feeding them into the laminar flow hood and processing them dependant on pre-defined user protocols. The Cellmate™ can handle 20-1000 roller flasks and can culture up to 10 different cell lines in parallel (Kempner and Felder, 2002).

The SelecT system is a fully automated cell culture system which includes a robotic arm which is used to access a humidified incubator with a maximum capacity of 90 x T175 flasks. The system also incorporates a Cedex automated cell counting system within the laminar flow safety cabinet (Thomas et al., 2009).

1.3.1.2. Microcarriers

Traditionally adherent cells have been grown using two dimensional culture methods as described previously. Such methods although extremely reliable and well understood, are heavily labour intensive and unfeasible to scale up (Rowley et al., 2012). The ability to scale up and manufacture cells on a large scale is essential with certain applications such as the transplantation of fully differentiated cells requiring in excess of 10^{10} cells (Kirouac and Zandstra, 2008). It is for this reason that a large proportion of the research carried out in this area has been aimed at the 3D culture of adherent cells in a suspension culture environment, with arguably the most successful method being the use of microcarriers.

Microcarriers are small spherical particles usually ranging from 125-250 μm in diameter. They are manufactured in a range of materials including natural materials, such as collagen and synthetic materials, such as polystyrene. Pall SoloHill® Plastic Plus Fact III and Hillex II are solid core microcarriers with a positively charged surface allowing cells to rapidly attach (Szczyepka et al., 2014). Solohill microcarriers have been used successfully in the proliferation of adherent human mesenchymal stem cells in a 3D stirred tank culture system; cell densities of up to 3.5×10^5 cells mL^{-1} were achieved within 8 days of seeding (Carmelo et al., 2015).

The ability to grow anchorage dependant human cells on microcarriers was first demonstrated using human embryonic lung cells grown on positively charged DEAE-

Sephadex beads (van Wezel, 1967). Van Wezel noted that within 20 hours of inoculation the cells began to adhere to the beads and gradually a monolayer was formed entirely covering the microcarrier.

Microcarriers have a much higher surface to volume ratio in comparison to 2D culture flasks making them ideal for large scale culture of anchorage dependant cells. 1L of Cytodex™ microcarriers at a concentration of 3 mg mL⁻¹ can provide a surface growth area equivalent to 75 x T175 flasks (Chen et al., 2013).

Microcarriers are usually cultured in stirred tank reactors which allow for tight control of multiple physiological parameters, such as pH and DO. This also means the cultures can be easily scaled up using either traditional stainless steel or disposable vessels. One issue with using stirred tank reactors is the damage caused to the cells by the shear stresses induced by the stirrer, however, it has been shown that some microcarriers can help to protect the cells from such damage (Ng et al., 1996).

1.3.1.3. Hollow fibres

Hollow fibre bioreactors use semi permeable fibres as a growing surface for adherent cells. This creates a 3D tissue culture platform allowing high density culture of adherent cells. The Hollow Fibre Perfusion Bioreactor (HFPB; Frederick, Maryland, USA) is a high density, single use continuous perfusion culture system allowing 3D culture of adherent cells in a controlled single use environment. The bioreactor consists of a number of semi permeable hollow fibres arranged in parallel within a tubular cartridge. Liquid, including complete growth media, is pumped in through the end of the cartridge and flows through the interior of the fibres. The cells are seeded within the tubular cartridge, outside of the hollow fibres. The HFPB has a cell growth area of 3000cm² with the capacity to culture up to 2 x 10⁹ cells. Pumping media through the fibres allows

nutrients and oxygen to diffuse through the fibres. Diffusion can take place in both directions meaning waste products can also diffuse out into the media stream. Once medium exits the cartridge it can either be re-oxygenated and re-circulated or collected as waste and replaced with fresh medium (Whitford Sr et al., 2014).

The hollow fibre reactors have been used in a number of different applications, including in vitro toxicology and in the production of recombinant proteins and monoclonal antibodies (Cadwell, 2011, Hugo et al., 1994).

The HFBR system has also been used as an in vitro bone marrow model in the evaluation of myeloid leukaemia. Human marrow stromal HS-5 cells were cultured in the HFBR to establish a supporting stroma. They were then co-cultured along with erythroleukemia K562 cells to generate a myelo-leukemic model which could be used to analyse the proliferation and differentiation which takes place in patients suffering from myeloid leukaemia. In comparison to cells cultured on standard tissue culture polystyrene the HFBR produced a 3,130 fold expansion of the leukemic cells compared with a 43 fold expansion on the tissue culture polystyrene. Due to the increased cell growth area capacity in the HFBR, it was also able to achieve a much greater number of cells (Usuludin et al., 2012).

The iCellis® (Pall Life Sciences) is the first commercially available fully integrated high density bioreactor for the proliferation of adherent cells. A compact matrix of polyethylene terephthalate microfibers comprise a fixed bed providing up to 500 m² of growth area in a 25 L volume (DePalma, 2014).

The iCellis has been used to successfully produce adenovirus vectors for gene therapies. Initial scale-down studies were carried out in the lab scale iCellis® Nano (Pall Life Sciences) with a culture area of 4 m². HEK293 were cultured infected and harvested within the reactor producing maximum yields of 1.6×10^{14} viral particles (vp) per batch.

The process was replicated in large scale iCellis with a culture area of 500 m² producing yields of up to 6.1 x 10¹⁵ vp. The number of virus particles produced per area of growth surface were comparable between the two systems demonstrating successful scale up as well as a successful method of producing large scale batches of adenoviral vectors (Lesch et al., 2015).

1.1. Primary recovery

1.1.1. Depth filtration

For decades dead end filtration has been used in water treatment plants for the removal of particular contaminants from wastewater (Jeannie et al., 1991) and has also long been a common method of primary clarification in traditional bioprocesses. It is a simple and well understood process which provides consistent results; at least for non-adherent cell bioprocesses, such as microbial and mammalian. The cells are applied perpendicular to the filter, as opposed to the tangential nature of the feed in a cross flow filtration system. Simple dead end or normal flow filtration offers high levels of recovery over a wide range of cell densities.

The processing volume of the filtration process is ultimately determined by the size of the filtration area (Burke et al., 2004). Dead end filtration has its limitations when using large volumes of high density material due to the formation of a filter cake. This fouling of the filter causes a decline in the rate of filtration increasing processing times and in some cases preventing further filtration (Russotti et al., 1995). There are a number of methods which can be used to reduce the decline in flux due to filter cake formation. Inclined dead end filtration, angles the filter and allows a higher filtration rate over a prolonged period of time (Iritani et al., 2012). A vibrating medium can also be used to reduce the levels of filter fouling. Studies have shown that at a critical vibration

amplitude, a dramatic increase in the filtration rate can be observed; in some cases almost as high as when the filter was in its original clean state. Vibration of the particles on the filter in some cases can be large enough to counteract the compressive nature of the feed flow causing fluidisation of the particles on the filter (Gundogdu et al., 2003). It is important for the fouling mechanisms to be fully understood at a process development level in order to effectively predict manufacturing filtration areas (Laska et al., 2005). It is also important to understand that the methods described above have only proved successful at preventing filters from fouling when the filtrate contents are non-adherent. I believe the added complication of filtering cells which are looking to adhere any surfaces they come in to contact with, will not only have an impact on levels of recovery but will also mean it is harder to prevent the filters from fouling.

Although commonly used in bioprocessing, the use of dead end filtration for the recovery of cells is not a process which is common practice. However, it may be able to provide a viable option for the primary recovery of cells for therapy. Studies have already shown that filtration can be a suitable option in the recovery of non-adherent cells from human umbilical cord blood (Sowemimo-Coker et al., 2009). The study showed that the red cell volume reduction system that was developed was capable of an 85% depletion of red blood cells, with a greater than 10 fold overall reduction in volume. The retrograde rinsing of the filter with an isotonic solution allowed recovery of up to 99.9% of CD34+ and haematopoietic clonogenic progenitor cells, thus concentrating the cells of interest and removing the majority of contaminant cells. Also, the mean viability of the processed human umbilical cord blood showed no significant difference from the unprocessed control blood, showing that filtration is a suitable option for the primary recovery of non-adherent human cells (Sowemimo-Coker et al., 2009) . Whilst this method does offer some proof of concept in terms of using depth

filtration to recover cells, using this method for the recovery of adherent cells may prove more complex. The research presented in this paper does not explore the interactions between the cells and the filter which may or may not impact recovery. It will be important to understand some of these mechanisms if we are to successfully recover adherent human cells.

Depth filtration has been used successfully to separate cells from micro-carriers with minimal cell loss (<5%) (Cunha et al., 2015b), however tangential flow filtration was then needed in order to concentrate the cells and remove the growth media. The benefit of using depth filtration to capture the cells and remove the growth medium is that primary recovery can be achieved in a single step process.

1.1.2. Tangential flow filtration

Tangential flow filtration (TFF) provides an attractive alternative to depth filtration as a method of primary recovery as the tangential nature of the flow reduces the level of fouling on the filter membrane. As well as reduced levels of fouling, the continuous nature of TFF is making the process more and more popular in industry. The ability to run the process continuously means that large volumes of material can be processed. Wash steps can also be included in 'diafiltration' or 'buffer exchange' modes allowing for the removal of contaminants carried over from the earlier cell expansion and cell harvest phases of the process (Pattasseril et al., 2013).

Rowley et al. (2012) demonstrated the ability to process mammalian cells using tangential flow filtration to reduce the total volume and concentrate the cells to a final concentration of approximately 5×10^6 cells mL⁻¹. More importantly, the method was able to recover over 90% of the cells whilst maintaining a minimum cell viability of 90%.

The ease at which TFF can be scaled up to process large volumes of material and the single use nature of some of the systems makes TFF a desirable choice for downstream processing of human cells for therapy (Cunha et al., 2015a). Studies have also shown that TFF is the most cost effective option when compared to the other systems which are commercially available for primary recovery of adherent cells for therapy such as fluidised bed centrifugation systems (Hassan et al., 2015). Systems such as the PureTec Tangential Flow Filtration System (SciLog, Wisconsin, USA) and the Akta Crossflow (GE Healthcare, Amersham, UK) offer feasible solutions to the primary recovery of adherent cells for therapy. It is important to note that within the lab team at UCL, research into the use of TFF as a method for the primary recovery of human cells for therapy was running in parallel to this piece of work.

1.1.3. Batch centrifugation

Traditionally batch centrifugation has been the method of choice for the primary recovery of whole cell therapeutics following harvest of adherent cells. During batch centrifugation cells are pooled usually in disposable bottles and spun until the cells form a pellet. The supernatant is discarded and the cells manually resuspended before undergoing a number of washing and resuspension steps. The simplicity and low cost nature of the operation makes it ideal for small scale initial studies. However, the open nature of the process carries an inherent risk of contamination making it unsuitable for large scale manufacture (Hitchcock, 2009).

One of the main benefits of batch centrifugation as a method of primary recovery is the relatively high recovery rates which are achievable ($\approx 95\%$). However, it has been shown that at certain centrifuge speeds, processing times and operating temperatures there can be extensive damage to the cells resulting in cell losses of up to 25% (Wong,

2009). Whilst batch centrifugation may be a viable option for cell recovery at lab scale it is not a reliable option for larger scale process due to some of the reasons mentioned above. This is one of the main reasons behind the need for an alternative method of primary recovery and for this research.

1.1.4. Continuous Centrifugation

A more recent option for primary recovery of cells for therapy is single use fluidized bed centrifugation. The KSep® (KBI Biopharma, Durham, North Carolina, USA) is a single use continuous centrifuge system offering a closed, low shear system for the clarification, washing, concentration and separation of whole cells.

The system works by balancing two forces; the centrifugal force and the fluid flow. In a standard batch centrifuge the centrifugal force determines the settling velocity of the cells, causing them to pellet out at the bottom of the centrifuge tube. In the KSep® the settling of the cells caused by the centrifugal force is counteracted by the fluid flow, creating a fluidised cell bed whilst the supernatant is discharged from the chamber.

The system contains 4 x 100 mL chambers each with a maximum capacity of approximately 10×10^9 cells. When used to harvest 5 CHO populations from 5 different bioreactors varying in batch size, cell density and cell viability the KSep® recovered on average 97% of the cells. There was also no significant increase in LDH or residual DNA levels post processing compared to pre-processing controls, demonstrating that the cells are exposed to a minimal amount of shear stress (Ko and Bhatia, 2012).

The single use nature of the KSep® system means that the cycle times are reduced as there is no need for lengthy CIP/SIP procedures. The risk of batch to batch contamination is also significantly reduced.

The KSep® is also scalable and as well as the 400mL system described above (KSep400), a 6000mL (KSep6000) version is also available with the capacity to harvest up to 1200×10^9 cells (KBI-Biopharma, 2014).

Whilst the KSep® is scalable to deal with larger volumes of feed material, it has yet to be scaled down to allow for full process development at lab scale. This is a disadvantage as it means the cost of process development could be significantly increased. Producing an ultra scale-down model for this process would allow multiple experiments to be carried out using minimal numbers of cells to identify optimum processing conditions. UCL Biochemical Engineering has acquired a significant amount of knowledge and expertise in the development of ultra scale-down tools and therefore continuous centrifugation could be an area that they look to expand into.

1.2. Effect of bioprocessing on cell quality

When cells are processed at large scale they are often subjected to mechanical and physiochemical stresses which are not experienced during the development stages at lab-scale. These stresses can have a damaging effect on the cells leading to a reduction in cell quality and efficacy.

Hydrodynamic shear stresses are often present during large scale processing, whether it is on entry to a disk stack centrifuge or whilst being pumped through a narrow channel the cells will at some point be exposed to these forces. This can cause changes in the cells which are not observed during the preliminary investigations at small scale.

There have been numerous studies to show the harmful effect of exposure to shear stress during processing (McCoy et al., 2009, Delahaye et al., 2015, Acosta-Martinez et al., 2010, Dhondalay et al., 2014). The damaging effects ranged from complete disruption

of the cell membrane rendering the cell non-viable to more subtle but none the less significant effects, such as the loss of key cell surface markers.

It has also been shown that in certain cell lines, such as multipotent mesenchymal cell lines, that exposure to shear stresses can induce differentiation. Yourek et al. (2010) demonstrated that exposure to shear stress stimulated the differentiation of human mesenchymal stem cells towards an osteoblastic phenotype. This is a concern during processing of cell therapies when it is essential that a purely homogenous population of cells are administered to a patient. Injecting patients with the wrong type of cell could have a significant effect on the safety of the recipient.

1.2.1. Physiological conditions

During every stage of processing the physiological conditions including temperature, dissolved oxygen, nutrient concentration and pH must be accurately controlled (Ozturk et al., 1997). Physiological conditions can have a huge impact on cell viability and critical quality attributes.

Temperature is an important factor in maintaining cell homeostasis. During processing cells can often undergo transitions between temperature extremes which will induce adaptive responses from the cells potentially causing irreparable cell damage rendering the therapy ineffective (Kregel, 2002, Kühl and Rensing, 2000). Many steps are taken during processing to ensure cells are not exposed to extreme temperature changes, such as the use of cryoprotectants during freezing and storage of therapies.

Dissolved oxygen concentration also has a significant effect on cell quality if it is not tightly regulated and too little (hypoxia) or too much (hyperoxia) can cause harm (Pandian et al., 2003, Wenger, 2000). It is important to control and regulate the

dissolved oxygen concentrations throughout the process. During upstream processing increasing numbers of cells can rapidly deplete the oxygen supply as the cells proliferate. Further downstream compacted cell pellets, for example during filter cake formation, can limit gas exchange leading to a state of hypoxia.

1.3. Analysing cell quality

Before any process the main parameters that define the final product need to be established. These critical quality attributes (CQA's) can include product purity, identity and viability amongst many others. Maintaining CQA's whilst scaling up cell processes provides a major challenge to commercial manufacturing of cell based therapies (Carmen et al., 2011). Every product will have its own specific set of attributes and a toolkit of analytical techniques with which to measure them. Identifying the CQA's and the specific assays for a particular product is a major part of process development and can often be a highly expensive and time consuming process. That being said, it is the responsibility of the manufacturer to ensure that the final product is both safe and effective as a therapy. The following sections outline some of the CQA's associated with cell based therapeutics and the assays used to measure them.

1.3.1. Membrane integrity and viability

The determination of cell viability is essential in tissue culture and cytotoxicity testing; however, it is also essential in bioprocessing (Wiegand and Hipler, 2008). It is important that engineers understand the effect that processing has on the cells; cell viability testing is a good way of understanding this. When assessing cell viability the first point of call is to define what distinguishes a cell as being viable. The current techniques for assessing cell viability label a cell as being viable if its cell membrane is

intact. Compromised membranes lose the ability to exclude certain dyes, for example trypan blue or propidium iodide, this principle forms the basis of a number of key analysis techniques (Stromer, 1997).

The two most commonly used tests for cell viability work on the dye exclusion theory, using either trypan blue or propidium iodide as the dyes. In the case of trypan blue the cells that have lost the ability to exclude the dye appear blue under the microscope. Another dye often used is propidium iodide. Propidium iodide works in a similar way to the trypan blue test; the dead cells lose the ability to expel the dye from the membrane. There are a number of issues surrounding the use of the dye exclusion method as an indicator of cell viability. There are cases when cells are non-viable as they can no longer grow or replicate, however, their membranes are still perfectly intact. In contrast there are also examples of cells with damaged membranes that are capable of repairing, but they temporarily cannot exclude the dye.

It has also been shown that with trypan blue staining, the count must be taken within a few minutes of staining, due to an increased number of cells taking up the dye over time (Jones, 1985).

The main difference between the two dyes is the location of the staining. Both the dyes stain cells when the cell membrane has lost its ability to expel the dye. The trypan blue stains the entire contents of the cell, showing up as an entirely blue circle on the microscope. Propidium iodide on the other hand intercalates itself into the DNA of the cell, staining the nucleus.

By viewing the cells under a microscope, the ratio of viable and non-viable cells can be analysed to give percentage viability.

There are a number of automated machines which can now run multiple dye exclusion experiments to test the sample viability and produce information on cell numbers, size and viability. The ViCell XR cell viability analyser, automates the trypan blue exclusion testing and can be used for the analysis of yeast, insect and mammalian cells. The sample is taken up by the machine, it is then analysed in a flow cell using a camera. The camera and the software use the difference in the grey scale of the live and dead images to ascertain information on cell size, roundness, cell numbers and viability (Beckman, 2006).

1.3.2. Apoptosis

Apoptosis is a programmed mode of cell death, often caused during processing as a response to physical or chemical stress. Cells often condense and bud as the main organelles are encapsulated within the membranes of apoptotic bodies before being phagocytised by other cells (Kerr et al., 1994). Aside from cells sometimes reducing in size there is often no visual indication that a cell is in a state of apoptosis, it may also not be picked up using standard membrane integrity based cell viability assays as apoptotic cells may still possess an intact membrane.

It is for this reason that recent years have seen the need to develop more advanced cytometric assays based on measuring levels of specific proteins, which are known to be expressed during apoptosis (Darzynkiewicz and Pożarowski, 2007).

Caspases are cysteine proteases which play a key role in the apoptosis pathways. Fluorochrome-Labeled Inhibitors of Caspases (FLICA) have been used to measure the level of caspase activity in situ. They bind specifically to the active centre of the active caspase enzymes and the fluorescent labelling allows the intensity to be measured in

direct correlation to caspase activity. This method allows for a quick and simple measurement of apoptosis activity within individual cells (Bedner et al., 2000).

Furthermore, this method can be used in tandem with a secondary stain such as propidium iodide (section 1.3.1) to identify necrotic cells. Whilst still a mode of cell death, necrosis differs from apoptosis as it is a premature and unprogrammed death resulting from external harm or injury. Unlike with apoptosis there is inflammation and swelling caused by metabolic collapse and unregulated digestion of organelles. The inflammation prevents the phagocytic cells from digesting the dead cell resulting in the leak of toxins into the surrounding area. If not removed this can cause damage to surrounding cells which is what happens in diseases such as gangrene (Dive et al., 1992).

Cells that stain positive for both FLICA and propidium iodide are classed as late apoptotic; they are cells in a state of apoptosis to the extent at which they have begun to break down the cell membrane. Necrotic cells will stain negative for FLICA as they do not follow the apoptosis pathway and activate the caspase enzymes. Necrotic cells will stain positive for propidium iodide only.

1.3.3. Cell Morphology

Identification and characterisation can also serve as an important marker for cell damage and stress. As well as more complex changes, such as protein expression and cell surface markers, cells which are exposed to damaging levels of stress can also demonstrate alterations in size and morphology which are visible under a microscope (Needham et al., 1991, Al-Rubeai et al., 1995). The change in morphology can also provide some detail on the physical state of the cell. For example, cells which are terminally damaged and are necrotic will cause inflammation and swell resulting in an

increase in size (Dive et al., 1992), whereas cells which are apoptotic tend to condense and show signs of budding, resulting in a decrease in cell size (Bedner et al., 2000, Kumar et al., 2007).

1.3.4. Cell surface markers

Identification of specific surface markers is a powerful tool in the characterisation and identification of cells. In particular when differentiating human embryonic stem cells as part of a therapy, the final identity of the differentiated cells is a key CQA. There are a number of surface protein markers that can be used to identify human embryonic stem cells (Kolle et al., 2009). The cell surface markers provide an accurate method for identifying human embryonic stem cells, as well as the lineage of the cell during differentiation. When culturing human embryonic stem cells it is important to be able to prove that the cells have remained pluripotent and are not differentiated. One way of achieving this is by staining for the appropriate cell surface markers. Oct 4 and SSEA-1 are markers for pluripotency, whereas Tra-160 is a marker for differentiation (Kim et al., 2009). Human embryonic stem cell populations should stain positive for SSEA-1 and Oct-4 but negatively for Tra-160. SSEA-1 and Tra-160 are both external markers while Oct-4 is an internal marker, this means that the cell must be permeabilised before the last marker can be stained for.

1.4. Ultra scale-down technology

Ultra scale-down mimics of bioprocess unit operations have been successfully used in research. Studies have shown that centrifugation clarification (Tait et al., 2009), tangential flow diafiltration (Ma et al., 2009) and normal flow microfiltration (Jackson et al., 2006, Kong et al., 2010) can all be mimicked at small scale and be accurately

modelled to predict how the operation will perform at the large scale. Work has also been carried out to show how shear stresses common in large scale processes can affect cells (Acosta-Martinez et al., 2010, McCoy et al., 2009, McCoy et al., 2010).

Ultra scale-down studies allow the optimisation of manufacturing processes without the need for large quantities of expensive material, enabling high throughput screening of potential operating conditions.

1.4.1. Shear devices

1.4.1.1. Rotating disc

The ability to mimic the shear stresses which cells are exposed to during large scale bioprocessing is imperative when developing ultra scale down devices. The use of a rotating disc to impart shear stress on cells was first described by Levy (1999) to examine the effect of shear on plasmid DNA. The device consisted of 3 cm diameter aluminium alloy flat disc contained within an air tight Perspex chamber with a diameter of 4 cm and a height of 1.5 cm. The shaft connected to the disc extended out of the top of the chamber and connected to a high speed motor. The motor was used to rotate the disc at 6 different fixed speeds ranging from 5000 RPM to 28000 RPM. The chamber was completely filled with material and sheared for a fixed period of time between 5 – 25 seconds (Levy et al., 1999).

The rotating disc shear device has been used to investigate the effect of shear in a number of different environments, including the effect of shear imparted from impellers in stirred tank reactors on mammalian cell cultures (Hu et al., 2011) and the shear cells are exposed to in large scale centrifugation (Tait et al., 2009). Tait et al, used the rotating disc shear device alongside a microwell centrifugation plate to accurately mimic large scale centrifugation of mammalian cell broths. This ultra scale-down

approach allowed for full analysis of a wide range of operating conditions which might not normally be feasible at a larger scale.

1.4.1.2. Capillary based

Hydrodynamic shear can affect cells in a number of operations, at all stages of the process. Aspiration, pumping and resuspension all exert hydrodynamic shear on the cells and so it is important to determine how they will respond. By using a syringe pump to force cellular suspensions through a microscale capillary with internal diameters of 250 μ m and less, it is possible to expose the cells to hydrodynamic stresses comparable to those faced in large scale operation (Acosta-Martinez et al., 2010). Using results from these small scale studies, it is then possible to predict how different cell lines will behave and react in a large scale process. The studies showed that the cell lines had a stress limit beyond which, they demonstrated a 'significant loss of integrity'. The cells were also analysed for the presence of several cell surface markers. These markers were CD9, CD44, CD59, CD81, CD147 and MHC-1. The markers displayed varying degrees of sensitivity to the exposure to shear. In terms of the final biopotency of the product, the immunological effect of the vaccine in this case will be a result of one of, or a combination of these markers. Therefore there is a critical need to understand, on a small scale, how these environmental factors can affect the product in a large scale manufacturing process (Acosta-Martinez et al., 2010).

1.4.2. Tangential flow filtration (TFF)

Tangential flow filtration (TFF) or crossflow filtration (CFF) is currently being used in the large scale primary recovery of adherent cells for therapy. The main benefits of TFF over normal flow filtration are the fact that the flow of material parallel to the

membrane limits the level of fouling on the membrane, compared to when the feed is applied perpendicular to the membrane, as is the case with normal flow filtration. However, as with any process, it is important to be able to understand the performance at manufacturing scale and be able to accurately mimic the operation at the process development stages.

Ma et al. (2010) developed a rotating disk filter (RDF) device capable of accurately mimicking large scale diafiltration processes using only 1.5 mL of material. This is especially beneficial for adherent cell research considering the difficulties associated with cell expansion.

The RDF is designed with a sealed chamber housing a rotating 15 mm diameter stainless steel conical disc. The chamber had an internal diameter of 25 mm and had capacity for a 25 mm membrane with an effective filtration area of 3.64 cm². A cooling coil positioned around the motor and two cooling jackets on the top and bottom of the chamber were used to maintain the temperature at 20°C ± 1°C. Ports were installed to allow collection of permeate samples as well as to monitor trans-membrane pressure (TMP) throughout the process.

Hydrodynamic shear stress across the membrane which is a factor in large scale TFF was mimicked using the shear created by the rotating disk. Wall shear rates were then correlated to large scale using a lab scale TFF cassette, combined with CFD simulation.

The USD TFF membrane device was used to successfully predict flux rates and transmission in a process whereby Fab' was recovered from an *E. coli* feed lysate (Ma et al., 2009).

1.4.3. Normal flow filtration (NFF)

A high throughput automated depth filtration platform was developed by Jackson and Lye (2006) using an automated vacuum manifold (Tecan VacS two-position vacuum manifold; Tecan, Reading, UK) to draw the filtrate through the filter. The system was operated with both a 96 well plate, as well as a custom designed 8-24 well plate, allowing parallel analysis of complex microbial broths, as well as the performance of various membranes and filters. The manifold resides on top of a fully automated liquid handling system (Tecan Freedom EVO[®] liquid handling system) which enables automated liquid sensing and continuous loading, as well as integrated analysis. In comparison to commercial multi-well filters the system was shown to minimise errors associated with scale down filtration experiments and when combined with microwell fermentation techniques provided a tool for small scale optimisation of upstream and downstream processes (Jackson et al., 2006).

The system has since been optimised and used for a variety of purposes, including sterile filtration of plasmid DNA (Kong et al., 2010).

1.5. Project aims

The aim of this research is to create a novel ultra scale-down investigative procedure to help understand the relationship between cell line selection, filter (material) selection and operating conditions required for the successful recovery of human adherent cells for therapeutic use. The ability to work with micro-scale quantities of cells within whole bioprocess mimics will offer a novel means of early selection of filtration methods for cell recovery and contaminant removal.

The thesis aims to combine the in-house expertise of Pall Life Sciences and UCL Biochemical Engineering in order to guide, inform and develop the research

The initial part of this research will look at developing and establishing an ultra scale-down filtration device, which is capable of loading accurately small volumes of homogenous cell suspension onto a filter, before recovering a high proportion of good quality cells via flushing the filter in the opposite direction to which it was loaded with an elution buffer.

The aim will then be to optimise this process and begin to understand the interactions which occur between the cells and the filter material during process and what impact this can have on the proportion of cells recovered, as well as the quality of these cells.

Chapter 2: Materials and methods

2. Materials and methods

2.1. Introduction

This chapter describes the standard operating procedures used throughout this body of work from culturing and maintaining the various cell lines, to processing the cells and analysing the quality of those cells post processing.

2.2. Cell lines

2.2.1. HCA2

The HCA2 cells are an immortalised human fibroblast cell line, gifted to us by Professor David Kipling of the University of Cardiff. The cells were immortalised by infection with an amphotropic retrovirus expressing hTERT. The retrovirus was constructed by cloning the EcoRI insert of pGRN121 into the retroviral vector pBABE-puro to produce pBABE-hTERT. hTERT is the catalytic protein subunit of human telomerase and when infected into the HCA2 cells induces telomerase activity (McSharry et al., 2001). A working cell bank was created in house from the cells provided by the University of Cardiff. Cells were frozen down in 1mL of FCS supplemented with 10% dimethyl sulphoxide (DMSO, Sigma-Aldrich, Ayrshire, UK) at a concentration of 5×10^6 cells mL⁻¹ and stored in liquid nitrogen.

2.2.2. CTX0E03

The CTX0E03 (CTX) cells are a clonal cortical multipotential stem cell line, derived by ReNeuron Group plc for the treatment of ischemic brain injury. The cells are derived from first trimester foetal brain tissue and are conditionally immortalised via the integration of the c-mycER^{TAM} fusion gene (Pollock et al., 2006). The c-mycER^{TAM} is delivered via retroviral infection (Stevanato et al., 2009). Activation of this protein is

achieved via the addition of 4-hydroxy-tamoxifen (4-OHT) to the culture medium (Stroemer et al., 2009). A frozen vial of cells provided by ReNeuron Group plc and consisting of 5×10^6 cells in 1 mL of RMM (see section 2.3.2) supplemented with 10% (v/v) DMSO was used to produce a further working cell bank. (The working cell bank was established in house by Dr. Katherine Lawrence). The vials of the working cell bank were stored in liquid nitrogen.

2.3. Cell culture

2.3.1. HCA2

HCA2 cells from the working cell bank were revived at 37°C for 2 mins. Dulbecco's modified Eagle medium (DMEM, Life Technologies, Paisley, Scotland, UK) was supplemented with 10% v/v foetal calf serum and 1% v/v L-glutamine (Life Technologies, Paisley, Scotland, UK). This supplemented medium will be referred to as the complete Dulbecco's modified Eagle medium (cDMEM). Thawed cells were transferred to a 15 mL Falcon tube and cDMEM was added to a final volume of 10 mL. The revived cells were then centrifuged at 500 x g for 3 mins before the supernatant was removed. The cells were then resuspended in 2 mL of cDMEM. 175 cm² tissue culture flasks (Greiner, Sigma-Aldrich, Ayrshire, UK) were loaded with 42mL of cDMEM and the HCA2 cells were inoculated at a seeding density of 30-40 x 10³ cells cm⁻². The flasks were incubated at 37°C with the internal air containing 5% CO₂. The cells were passaged every 3-4 days at 70-80% confluency. Revived cells were at passage 11 and were cultured on average for a period of 2 months or 15 passages.

During passaging the spent medium was removed and discarded and the cells were washed with 10 mL Dulbecco's phosphate buffered saline (DPBS, Sigma-Aldrich, Ayrshire, UK). The cells were then enzymatically detached from the surface using 5 mL

TrypLE[®] Select (Life Technologies, Paisley, Scotland, UK) at 37°C for 7 mins or until completely detached when viewed microscopically. The enzyme was quenched using 5 mL of cDMEM and the suspension centrifuged (Heraeus Multifuge X3R centrifuge, Thermo, Strasbourg, France) at 500 x g for 3 mins at 21°C. The supernatant was removed and the pellet re-suspended in cDMEM. Cells were then re-seeded into T175 flasks at a minimum seeding density of 10,000 cells cm⁻², this equated to a 1:10 split.

When harvesting cells for filtration studies cells were resuspended in cDMEM at the required concentration as opposed to being re-seeded in the flasks. Although the aim of the research is to provide an alternative to centrifugation, at this stage the cells must still be centrifuged and resuspended in order to provide a single cell suspension of known concentration for accurate filtration studies. All work was carried out in a class II safety cabinet (Walker, Derbyshire, UK).

2.3.2. CTX0E03 (CTX)

CTX cells frozen in liquid nitrogen at a concentration of 5x10⁶ cells mL⁻¹ were revived at 37°C for 2 mins. DMEM:F12 (Life Technologies, Paisley, Scotland, UK) was supplemented with human serum albumin (HSA; 0.03%; Octopharma, Manchester, UK); L-Glutamine (2 mM; Life Technologies, Paisley, Scotland, UK); human transferrin (100 µg mL⁻¹; Millipore, Hertfordshire, UK); putrescine dihydrochloride (16.2 µg/mL; Sigma-Aldrich, Ayrshire, UK); human insulin (5 µg mL⁻¹; Sigma-Aldrich, Ayrshire, UK); progesterone (60 ng mL⁻¹; Sigma-Aldrich, Ayrshire, UK); sodium selenite (selenium; 40 ng mL⁻¹ Sigma-Aldrich, Ayrshire, UK); basic fibroblast growth factor (bFGF; 10 ng mL⁻¹; Life Technologies, Paisley, Scotland, UK) and epidermal growth factor (EGF; 20 ng mL⁻¹; Sigma-Aldrich, Ayrshire, UK). This supplemented medium will be referred to RMM. Immediately prior to use 4-hydroxy-tamoxifen (4-

OHT; Sigma-Aldrich, Ayrshire, UK) was added to the RMM at a final concentration of 100 nM. Cells were thawed for 2 mins before being transferred to a 15 mL Falcon tube, RMM + 4-OHT was then gently added to a final volume of 10 mL. The revived cells were then centrifuged at 500 x g for 3 mins before the supernatant was removed. The cells were then resuspended in 2 mL of RMM + 4-OHT.

Prior to inoculation, the growth surface of the T175 flask was coated with 20 mL of DMEM:F12 containing 10 $\mu\text{g mL}^{-1}$ laminin (AMS Biotechnology, Oxford, UK) for a minimum of 1 hour in an incubator maintained at 37°C, 5% CO₂. Before the cells were seeded, the 10 $\mu\text{g mL}^{-1}$ laminin solution was aspirated off and the flask was washed with 20 mL of DMEM:F12 medium. Cells were seeded at an approximate density of 10-20x10³ cells cm⁻² and split 1:2 every 3-4 days or when a confluency of 70-80% had been achieved. Cells were cultured in a 37°C incubator in 5% CO₂, 95% air.

Cells were harvested by aspirating the spent medium and washing with 15 mL of Hank's balanced salt solution (HBSS, Sigma-Aldrich, Ayrshire, UK). 5 mL of a trypsin based enzyme (TrypZean, Lonza, Slough, UK) was added and the cells were incubated at 37°C for 6 minutes in order to enzymatically detach the cells. Once detached, the enzyme was quenched using 5 mL of defined trypsin inhibitor (DTI, Life Technologies, Paisley, Scotland, UK) supplemented with 20 units per mL of benzonase (Benz, Merck, Nottingham, UK). The resulting suspension was then centrifuged at 800 x g for 5 mins at 21°C (Heraeus Multifuge X3R centrifuge, Thermo, Strasbourg, France). The supernatant was then decanted and the cells were resuspended in RMM. All work was carried out in a class II safety cabinet.

2.4. Dead end ultra scale-down filtration and cell recovery

2.4.1. Device design

For a schematic diagram of the device see Figure 2.1. The device consisted of a 13 mm Swinney filter housing (Pall, Portsmouth, UK) containing the cell capture filter media (Pall, Portsmouth, UK). A syringe pump (Harvard PHD Ultra, Harvard Apparatus, Massachusetts, USA) was used to control the flow from a 100 mL disposable syringe (BD, New Jersey, USA). A metal T-junction containing a pressure sensor linked the syringe to the filter housing (Figure 2.1). The pressure device consisted of an amplified pressure gauge sensor (Part number - 667-0914, RS Components Ltd, Northants, UK) linked to a 12-Bit, 10 kS/s low-cost multifunction data acquisition device (Part number - 193132-02, National Instruments Corporation Ltd, Berkshire, UK). The pressure device was powered by a power-pack with a USB connection built in house at the UCL Rapid Design and Fabrication Facility. The pressure readings were logged using software supplied with the data acquisition device (LabVIEW SignalExpress, National Instruments Corporation Ltd, Berkshire, UK). The pressure sensor had a range of 7-700x10³ Pa, with a sensitivity of ±7000 Pa. A magnetic stirrer built in house at the UCL Rapid Design and Fabrication Facility was used to maintain the cells in suspension whilst in the syringe (Figure 2.1). The stirrer consisted of a 20 mm diameter metal disk with three paddles. The disk also had three extra arms holding magnetic fleas. The stirrer was turned using a mechanically driven rotating magnet on the outside of syringe.

2.4.2. Device Operation

Before loading the sample, DPBS was passed through the filter at a flow rate of 0.003 mL s⁻¹ (150 LMH) for 300 s in order to wet the filter. The DPBS containing syringe barrel was then disconnected and replaced by a second identical syringe barrel containing the cells suspended in complete growth media (cDMEM or RMM),

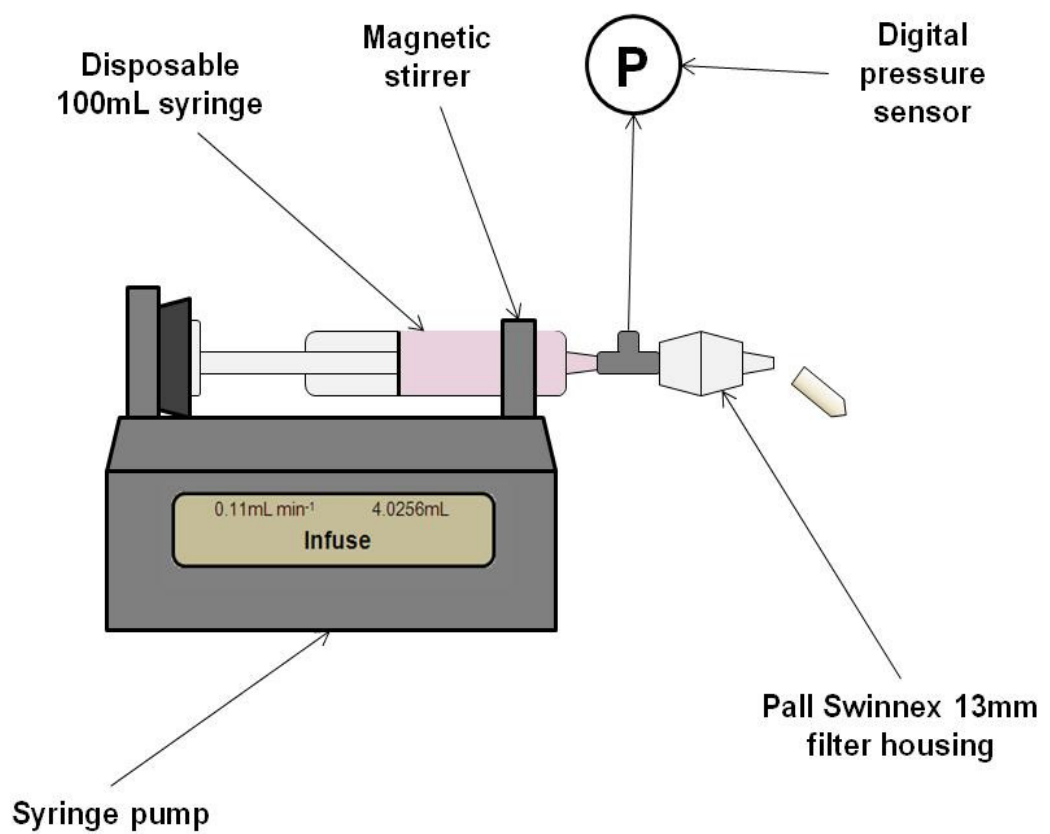


Figure 2.1 – Schematic diagram of the USD filtration set up including syringe pump, with magnetic stirrer, filter housing and digital pressure sensor (Not to scale).

harvested as previously stated in the cell culture section 2.3. The sample was left in the barrel with the magnetic stirrer rotating in order to ensure even mixing. The set volume of sample was then loaded onto the filter at a constant controlled flow rate of 3.0×10^{-3} mL s⁻¹ (150 LMH). Following the filtration process the syringe was replaced with a syringe containing the elution buffer (proprietary formulation, Pall, Portsmouth, UK). The filter housing was disconnected and re-attached in the opposite direction (so that the elution buffer entered through the retentate side of the filter). The elution buffer was then applied to the filter at a rate of 1.0 mL s⁻¹ (45,000 LMH); this was termed the back flush sample.

2.4.3. Filter preparation

Filters were cut from a sheet of filter material provided by Pall Life Sciences. Filter disks were cut using a 13 mm diameter steel cork borer. Disks were cut fresh at the beginning of each experiment and loaded into the filter housings with metal tweezers.

2.5. Backflush buffer preparation

Standard elution buffer consisted of 10% dextran (Sigma-Aldrich, Gillingham, UK) in PBS. 4g of dextran 40 from *Leuconostoc spp.* was measured and added to 30 mL of PBS. The solution was mixed until all the dextran had dissolved (at higher dextran concentrations it was mixed at 37°C to achieve total dissolution) and then topped up to 40 mL with PBS. The buffer was then sterile filtered through a 0.22 µm membrane to remove any contaminants. Buffer was stored at 4°C and brought back to room temperature before each experiment.

2.5.1. Rheology studies

The viscosity of the elution buffers was measured using a cup and bob viscometer (Brookfield QV2, Brookfield Viscometers LTD, Essex, UK). 1 mL of sample was placed in the cup and the bob was rotated at 10 rpm. The speed of the bob was increased to vary the torque (without exceeding 100% torque) and then decreased back to 10 rpm. Measurements were taken at regular intervals when the torque reading was stabilised with the optimum range for measurement being between 50% and 80% torque. The viscometer is accurate to within $\pm 1\%$. The temperature of the sample was maintained at $21^{\circ}\text{C} \pm 1^{\circ}\text{C}$.

2.5.2. Sample collection

Prior to loading the filter, a 300 μL sample was taken from the syringe and analysed by trypan blue exclusion (ViCell XR (see section 2.6.1)) to provide an accurate figure for the number of cells loaded onto the filter. Throughout the filtration the permeate was collected and again analysed using the ViCell XRTM to check whether any cells were breaking through the filter and ending up in the permeate. Finally the backflushed retentate was collected and the number of cells recovered was determined using the ViCell XR.

$$PT_R = \frac{T_R}{T_L - T_P} \times 100$$

Equation 2.1

Where, PT_R is the percentage of total cells recovered and T_R is the number of total cells recovered in the backflush. The total number of cells loaded onto the filter is equal to the initial number of cells loaded T_L , minus the number of total cells in the permeate T_P .

2.5.3. Centrifugation control

Following filtration studies, 1 mL of HCA2 cell suspension was collected from the syringe in a 15 mL centrifuge tube. The sample was then centrifuged at 500 x g for 5 mins (Thermo, Strasbourg, France). The supernatant was then aspirated off and the pellet resuspended in 10 mL of the elution buffer.

2.6. Cell analysis

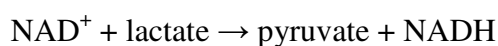
2.6.1. Cell membrane integrity

Samples were collected for the load, permeate and backflush and cells within these were counted within 10 mins of collection. Samples were counted in triplicate using an automated cell counter (ViCell XR, Beckman Coulter, High Wycombe, UK). The system performs an automated trypan blue exclusion test and measures cell numbers from images taken inside a quartz flow cell. The system was programmed to capture 50 images and record both total and viable cell numbers as well as percentage viability. The ViCell XR has an acceptable concentration range of 50×10^3 cells mL^{-1} to 50×10^6 cells mL^{-1} outside of this range the results are deemed unreliable.

2.6.2. Lactate dehydrogenase

The lactate dehydrogenase (LDH) assay was carried out using the Promega CytoTox 96 non – radioactive cytotoxicity assay kit (Promega UK, Southampton, UK) according to the manufacturer’s instructions. LDH from experimental cell samples catalyses the conversion of lactate to pyruvate, in the same reaction NAD^+ is reduced to NADH. NADH then combines with tetrazolium salts (INT) resulting in the formation of a red compound, formazan.

LDH



Diaphorase



LDH activity is calculated by measuring the absorbancy levels of red formazan product at 490 nm. As well as the LDH released from damaged cells ($\text{LDH}_{\text{External}}$), the internal LDH ($\text{LDH}_{\text{Internal}}$) of intact cells was also measured by chemically lysing the cells in the samples to give a value for the total amount of LDH present ($\text{LDH}_{\text{Total}}$). Samples were collected from the load, permeate and the backflush. The housing was also immersed in TrypLE™ Select in order to detach any cells stuck to the filter housing before analysing the LDH. Finally the cells within the filter were also chemically lysed to try to account for the number of cells still residing within the filter post backflush. All samples were kept on ice during the period following the filtration and the start of the assay. Two controls were also set up; one containing medium only, the other containing a chemically lysed sample of the unprocessed cell control in order to calculate total LDH in the sample. All lysed samples were lysed by adding 10 μL of 9% v/v Triton®. The assay was carried out by loading 100 μL of each sample into a V-bottomed 96 well plate (Nalgene Nunc International, New York, USA). The plate was then centrifuged at 250 x g for 4 mins (Thermo, Strasbourg, France). 50 μL of the supernatant was then transferred to a flat bottomed 96 well plate (Nalgene Nunc International, New York, USA) along with 50 μl of the re-constituted substrate mix. The samples were then incubated at 21°C for 30 mins protected from light. The reaction was stopped using the stop solution provided and the absorbance at 490 nm was measured using a Tecan plate reader. Absorbance readings were normalised against the medium control and LDH release was calculated as a percentage of the unprocessed cell control. All samples were stored on ice prior to the assay.

2.6.3. Particle size distribution

Particle size distribution measurements were taken and analysed using a label free cell viability and cell sizing system (CASY® Model TTC, Roche, Indianapolis, USA). The CASY uses electric current exclusion as opposed to dye exclusion to determine the size and viability of a cell. Measurement is performed by firstly suspending the cells in an electrolyte (CASY TON). The cells are then aspirated through a precision measuring capillary at a constant flow rate. A pulsed low voltage field is applied to the measuring pore via two platinum electrodes; the electrolyte filled measuring pore now has a defined electrical resistance. Intact cells can generally be considered insulators and so as these cells pass through the pore they displace a proportion of the electrolyte equivalent to their volume; the subsequent change in resistance is relative to the cell volume and ultimately the cell diameter. The CASY is also able to distinguish between viable and non-viable cells (non-viable cells being defined as having lost membrane integrity). Once a cell loses its membrane integrity it is no longer an insulator. This means the electric field can pass through the membrane and this specific change in resistance allows the CASY to distinguish between viable and non-viable cells. By setting the gates for minimum and maximum cell size for a specific cell line the CASY is also able to give information on the levels of cell debris as well as cell aggregation.

When carrying out size distribution analysis on the CASY, 10 mL of CASY TON diluting agent was dispensed into a CASY cup and the cell suspension was added to give a final concentration of $\approx 50 \times 10^3$ cells mL⁻¹. A cap was placed on the cup and the cup was inverted twice to mix the sample. Results were measured in triplicate and the system underwent 5 wash cycles with CASY Clean before a new sample was loaded.

2.6.4. Cell morphology analysis

A MatLab script was developed by Nicholas Jaccard (Department of Biochemical Engineering, UCL) to re-analyse the images taken by the ViCell XR in order to categorise cells based on their morphology. Images used for the cell membrane integrity analysis were re-analysed by the software and the cells were classified into five categories; round viable, short elongated, long elongated, dead or debris. Figure 2.2 shows the decision process undertaken by the software in order to classify objects in the images into one of the five categories. Firstly any trypan blue positive object in the image is classed as a non-viable cell based on the pixel intensity. The next step is to distinguish between viable cells and debris (neither of which are stained by the trypan blue). Any object with a diameter of less than 8 μm is classed as cell debris; likewise any object above 11 μm is classed as a whole cell. Objects which fall in between this range (8-11 μm) are categorised based on the intensity of their borders, with objects which have an intense and defined border being classed as whole cells (Figure 2.2).

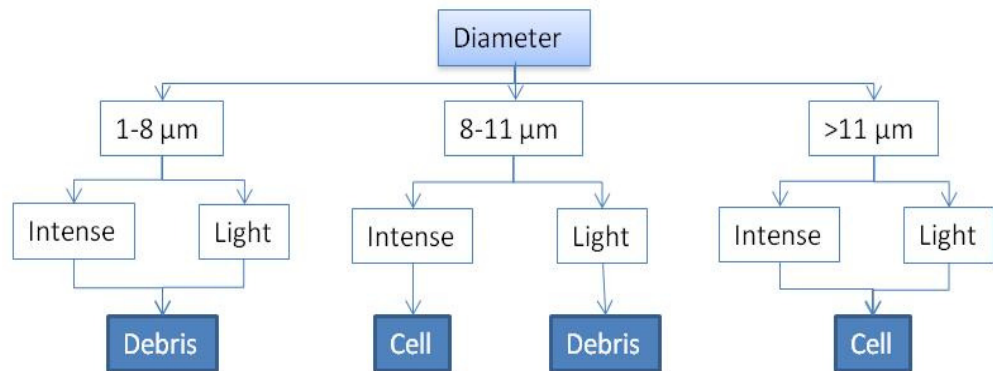
All objects classed as cells are then analysed based on their aspect ratio. Any cell at this stage with an aspect ratio of less than 2:1 is classed as having a round morphology, any cell with an aspect ratio greater than this is classed as being elongated. The severity of the elongation is further classified with cells that have an aspect ratio of greater than 3:1 being categorised as extremely or long elongated. Cells which fall in between these two aspect ratios (2:1 – 3:1) are classed as being partially or short elongated (Figure 2.2).

2.6.5. Cell death analysis

Cell death analysis was carried out using a fluorescence based assay to detect active caspases in cells undergoing apoptosis (CaspasTag pan-caspase in situ assay kit, MD Millipore Corporation, Billerica, MA, USA). Caspases are protease enzymes which play an essential role in apoptosis, necrosis and inflammation. The assay uses a

Stained cells categorised as non viable

Distinguish between viable cells and cell debris



Take forward only viable cells and categorise by shape (based on equivalent area but different aspect ratio)

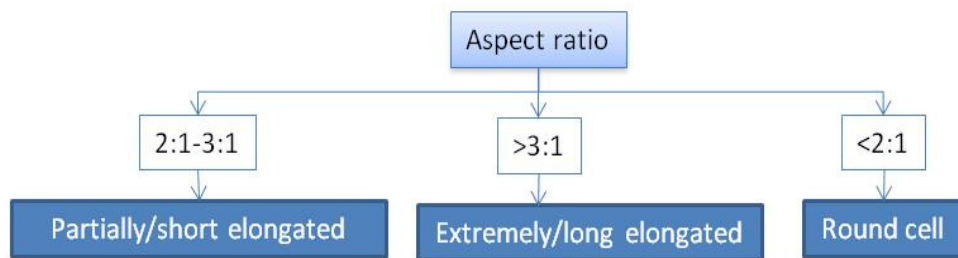


Figure 2.2 –Flow diagram detailing the categorisation process undertaken by the software when analysing objects within the images taken from the ViCell XR.

of Caspases (FLICA) which is cell permeable and non-cytotoxic. The FLICA is carboxyfluorescein-labelled meaning it produces a green fluorescence when it covalently binds to the cysteine residue of the active caspase enzyme. Any unbound FLICA is washed from the cell, meaning what's left is a direct measurement of the active caspase in the cell. In the cell death analysis, FLICA is combined with propidium iodide (PI) to identify apoptotic stages (early or late) and necrosis.

The FLICA reagent was reconstituted in 50 μL of DMSO and diluted 1:5 with PBS to make a concentrated solution. 1×10^6 cells in 300 μL of elution buffer were added to a 15 mL centrifuge tube along with 5 μL of the freshly prepared FLICA reagent. The tubes were then incubated for 1 hour at 37°C.

The wash buffer was prepared by diluting the 10X concentration stock 1:10 with deionised water (DI H₂O). Following incubation, 2 mL of wash buffer was added to each sample and the cells were centrifuged at 800 x g for 5 mins. The supernatant was then discarded and the cells were resuspended in 1 mL of wash buffer and the centrifugation process was repeated.

Finally the cells were resuspended in 400 μL of wash buffer. 2 μL of PI was then added before the cells were analysed using a flow cytometer (EPICS XL.MCL Flow Cytometer, Beckman Coulter, High Wycombe, UK). Before running samples for the first time, a series of control samples were set up to establish gating.

Two populations of cells were used, one set treated with 0.2% v/v Staurosporine (Sigma-Aldrich, Gillingham, UK) for 12 hours prior to harvest in order to induce apoptosis.

The other set was untreated. These samples all went through the staining protocol described above but with the following staining: -

- Unlabelled
- FLICA labelled only
- PI labelled only
- FLICA and PI labelled

These four controls were then used to set the four gates used for the analysis of all samples from all future experiments.

2.6.6. BCA total protein analysis

A total protein assay (BCA protein assay kit, Pierce protein biology products, Thermo Scientific, USA) was used to measure the total protein in recovered samples. The assay works by using bicinchoninic acid to detect the cuprous cation (Cu^{1+}) which is reduced from Cu^{2+} by proteins in alkaline solutions. A standard curve was set up each time using the bovine serum albumin standard (provided with the kit) diluted in the elution buffer. Samples were diluted 1:5 using the elution buffer. The assay was carried out in a 96 well plate with 200 μL of the BCA working reagent added to each well along with 25 μL of sample or protein standard. Samples were incubated for 30 mins at 37.5°C. Absorbance was measured at 562 nm using a fluorescent plate reader (Tecan Sapphire II, Tecan, Männedorf, Switzerland).

2.7. Microscopy

2.7.1. Fluorescent microscopy

Following processing, filters were cryosectioned in order to image any remaining trapped cells. The trapped cells were fixed overnight in 4% w/v paraformaldehyde

(PFA; VWR, Leicester, UK). The filters were then washed in DPBS in order to remove any traces of the PFA. Following washing, the filters were left in a solution containing 30% w/v sucrose solution in DPBS for 60 mins before they were set in an optimum cutting temperature resin (OCT, VWR, Leicester, UK). The filter was put into a plastic mould and the liquid OCT was poured on top. This was then incubated at -50°C for ~ 5-10 mins to set before being mounted onto the sectioning block. The filters were sectioned using a cryosectioner (Shandon Cryotome FE, Thermo Scientific, UK). The sectioning chamber was maintained at -26°C during sectioning and a sharpened blade was used to take 10 µm thick sections of the filter which were then mounted onto microscope slides (Microslide Superfrost Plus, VWR, Leicester, UK). Samples were stored at -80°C prior to staining. Cells were stained using 4',6-diamidino-2-phenylindole (DAPI, Life Technologies, Paisley, Scotland, UK) and were imaged with an inverted microscope (Ti-E, camera Fi-1, Nikon, UK).

2.7.2. Scanning electron microscopy

Scanning electron microscopy (SEM) was used to image cells trapped within the filter and those residing on the filter surface. Filter preparation and imaging was carried out by Mark Turmaine, Department of Biosciences, UCL.

2.7.2.1. Primary fixation

Following the filtration study, the filters were immersed in a fixative solution consisting of 2% w/v PFA and 1% glutaraldehyde in 0.1M sodium cacodylate buffer (pH 7.3) for 24 hours at 21°C. The filters were then washed twice in 0.1M sodium cacodylate buffer for 5 mins each time.

2.7.2.2. Freeze fracture of filters for SEM

Prior to imaging the filters containing the trapped cells were fractured in order to get a vertical cross section of the filter and image the cells residing within the filter matrix. The filters were cryoprotected for 2 hours in a solution of 25% w/v sucrose and 10% v/v glycerol in 0.05M phosphate buffer. The samples were then flash frozen in nitrogen slush and fractured using a razor blade at approximately -160°C. The samples were then placed back into the cryoprotectant and allowed to thaw at room temperature. Finally the samples were washed in 0.1M phosphate buffer (pH 7.4).

2.7.2.3. SEM protocol

Fractured filters were post fixed in a solution of 1% w/v osmium tetroxide (OsO₄) and 1.5% w/v potassium ferrocyanide (K₄[Fe(CN)₆] · 3H₂O) in 0.1M sodium cacodylate buffer (pH 7.3) for 1 hour in complete darkness at 3°C. Samples were then rinsed with DI H₂O before being dehydrated in a graded ethanol-water series up to 100% ethanol. The samples were then critical point dried using CO₂ (Polaron critical point dryer (CDP), Watford, UK).

For imaging, cells were mounted on aluminium stubs using sticky carbon tabs. The samples were mounted so as to present both the fractured surface and the filter surface to the beam. The samples were then coated with a thin layer (~2 nm) of gold and palladium using an ion beam coater (Gatan, California, USA). The samples were viewed and the images recorded using a scanning electron microscope (Jeol 7401 FEGSEM, Jeol, Massachusetts, USA).

Chapter 3: Development of an ultra scale-down filtration process for the recovery of human cells for therapy

3. Development of an ultra scale-down filtration process for the recovery of human cells for therapy

3.1. Introduction

The ability to carry out multiple experiments using a minimal amount of material is important for process development, allowing thorough process characterisation in the shortest possible time whilst keeping costs to a minimum. When working with whole cell therapies it is essential due to the previously discussed complexities associated with cell expansion (see section 1.3.1). Such complexities mean that producing significant quantities of material for focus studies can be time consuming.

3.2. Establishing and optimising operating conditions

The first target for this research was to establish an ultra scale-down filtration device and to optimise the operating conditions. In collaboration with both Pall Life Sciences and the UCL Rapid Design and Fabrication Facility a device was established which was able to load small volumes of homogenous cell suspension accurately. A method for recovering cells by backflushing the filter, i.e. by flow in the opposite direction to which the cells were loaded, was also devised.

3.2.1. Syringe hold time

In order to load reproducibly a known number of cells onto the filter it was essential to ensure that the cells expelled from the syringe remained at a consistent concentration throughout the filtration study. The mechanical stirrer (as described in section 2.4.1) was designed to maintain a homogenous single cell suspension within the syringe. To assess the functionality of the mechanical stirrer, the delivery of suspensions of HCA2 cells were studied. The cells were harvested and resuspended in cDMEM at a

concentration of 2×10^6 cells mL^{-1} . The cells were loaded into the syringe and maintained in suspension by the mechanical stirrer for 120 mins. 0.5 mL samples were collected from the syringe at a rate of 0.2 mL min^{-1} ($\equiv 150 \text{ LMH}$) at 15 min intervals and the concentration analysed. The cells in these samples were also analysed to test the effects of hydrodynamic shear stress and hold time on selected cell properties. A trypan blue exclusion test was used to analyse membrane integrity (section 2.6.1) and a cell death caspase assay (section 2.6.5) was used to look at levels of apoptosis and necrosis within the recovered cell populations. A control sample of fresh cells was taken from the harvested cells immediately before loading into the syringe ($<1 \text{ min}$) and kept on ice (lab temperature $20^\circ\text{C} \pm 1^\circ\text{C}$) until the cell death assay was carried out (maximum 150 mins). Figure 3.1 shows that when operated over a period of two hours there was no continuous increase or decrease in the concentration of the cell suspension. However there was a degree of fluctuation in cell concentration, with the average concentration of the cells collected varying $\pm 9\%$ on average with the main change occurring at the start. To accommodate this fluctuation, cells were given 30 mins in the syringe for the cell concentration to equilibrate before the start of the filtration study. Samples were also taken from the syringe before each filtration to get a more accurate concentration from which to calculate the number of cells loaded. The control samples on average showed a 5% increase in concentration following manual resuspension after being held on ice for the duration of the experiment.

The viability of the cells expelled from the syringe was also analysed. In each of the runs the proportion of viable cells in the collected samples did fluctuate ($\pm 1.5\%$) however overall there was no loss of viability of cells in the syringe after 120 mins. The control samples on average showed a 0.5% decrease in viability following manual resuspension after being held on ice for the duration of the experiment.

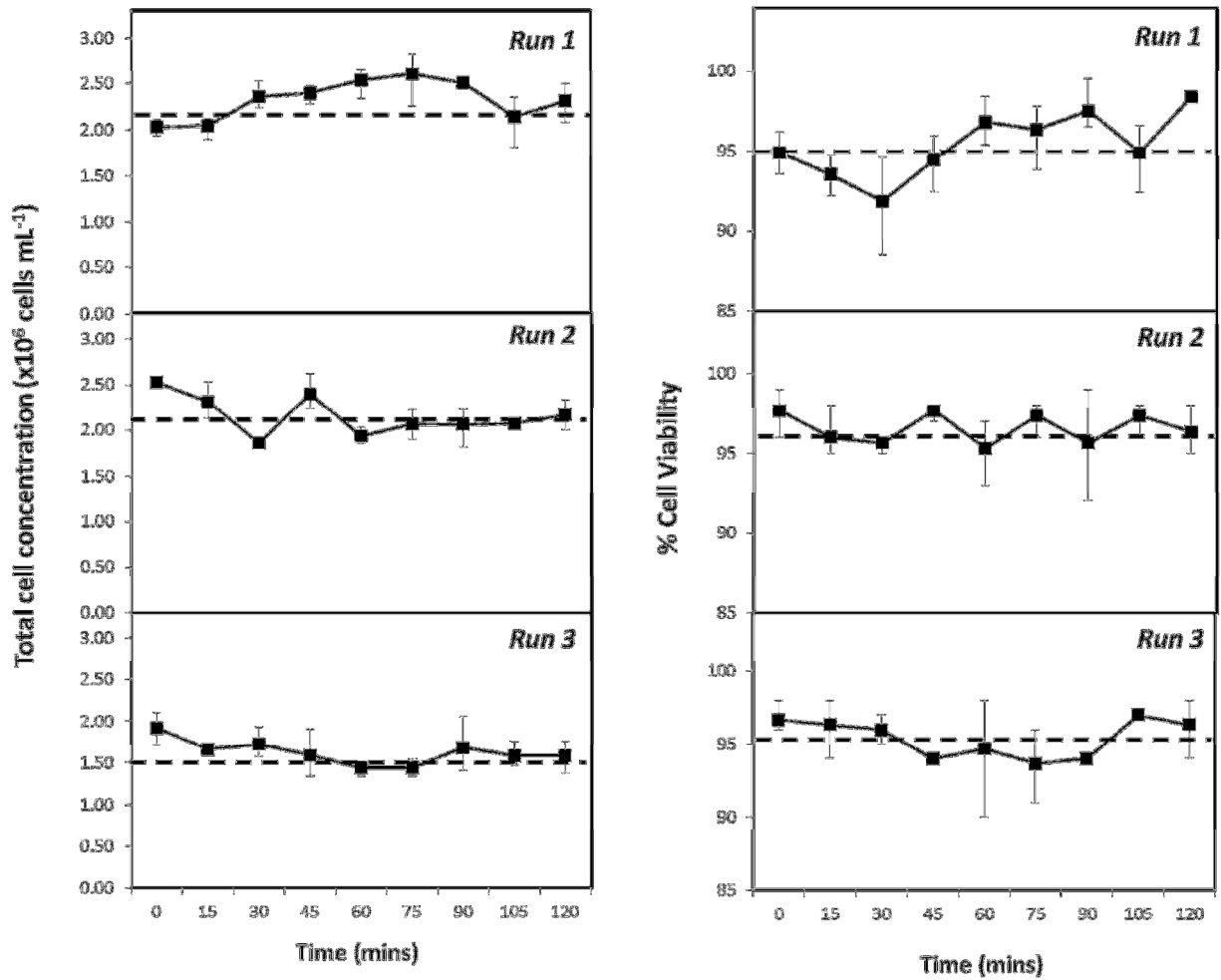


Figure 3.1 – Total cell concentration and viability of cells delivered by the syringe when maintained in suspension by the magnetic stirrer for three repeat tests.

Results show the mean average \pm the range for three separate experiemnts ($z=3, n=3$).

The quality of the cells expelled from the syringe was also analysed to assess whether there was any deterioration in cell quality over time, caused by the hydrodynamic shear forces produced by the mechanical stirrer. A cell death assay was carried out to determine whether or not the internal conditions of the syringe would cause an increase in the proportion of apoptotic cells which would not be picked up by the trypan blue membrane integrity test. Figure 3.2 shows the quality of the cells expelled from the syringe at the end of the 2 hour period, compared to those loaded initially into the syringe. The results show that the stirred syringe caused a significant increase in the proportion of necrotic cells ($p = 0.015$) in comparison to the control population of non-processed cells (maintained on ice for 120 mins). There was also a decrease in the proportion of viable cells and early apoptotic cells as well as an increase in the proportion of late apoptotic cells. However these changes were not deemed to be statistically significant ($p > 0.4$).

3.2.2. Backflush conditions

Arguably the most important part of the filtration process is the backflush step; both the number of cells recovered and the quality of those cells are dependent on this stage. Once the cells are loaded onto the filter they are recovered by passing an elution buffer through the filter in the opposite direction to which the cells were loaded. The volume of buffer used, the flow rate at which it passes through the filter and the viscosity of the elution buffer all need to be optimised.

The first conditions examined were the backflush flow rate and the backflush volume. The flow rate needs to be fast enough to drive the cells back out of the filter but at the same time not so fast that it would have a shearing effect which could potentially damage the cells.

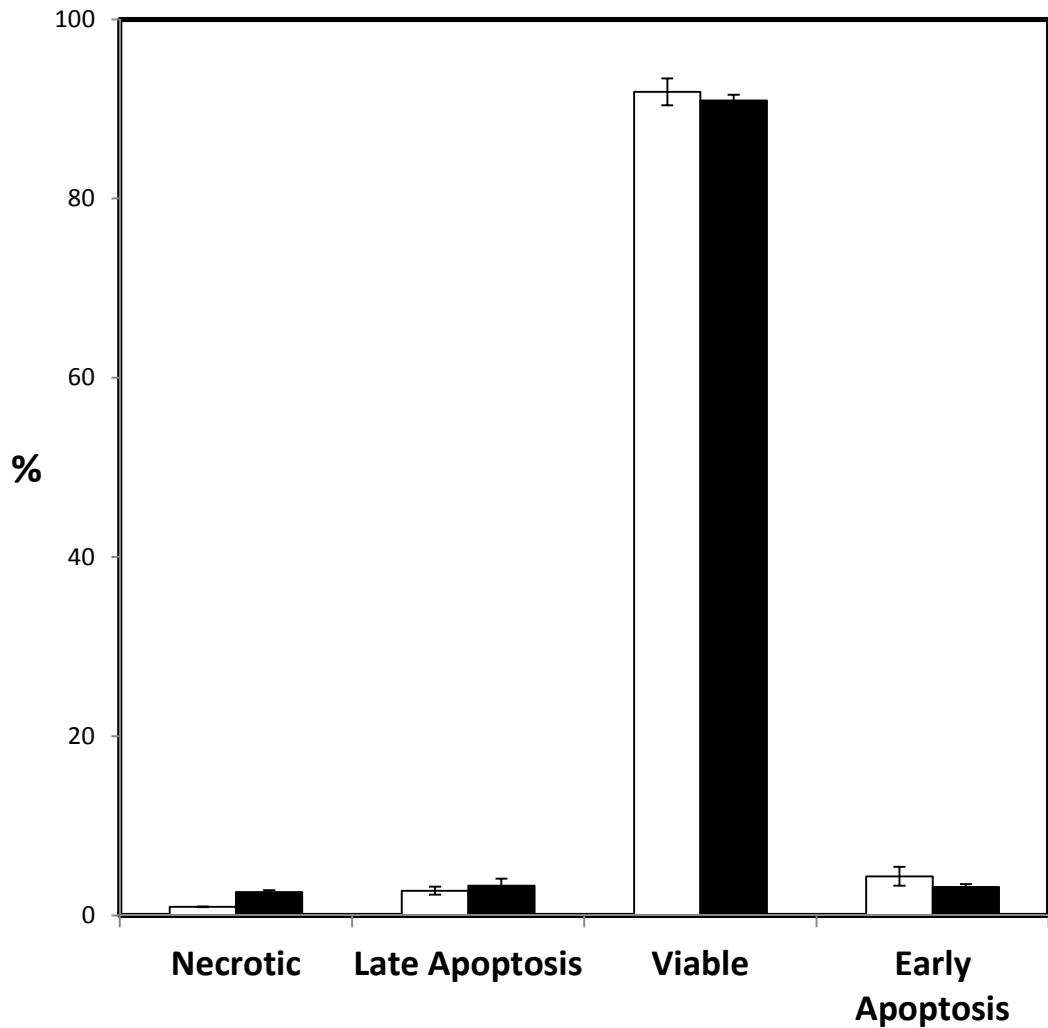


Figure 3.2 – Cell death analysis of cells maintained in suspension within the syringe barrel.

Results from caspase cell death assay combined with propidium iodide to analyse cell quality. Results are for fresh cells which had not been in the syringe barrel (but had been held for 120 mins on ice post-harvest) (□) and processed cells which had been stirred in the syringe barrel for 120 mins and then ejected by the syringe (■). The results showed that the syringe stirrer caused a significant increase in the proportion of necrotic cells ($p= 0.015$). Results show the mean values from three individual experiments \pm the range ($z=3, n=1$).

Three different flow rates were examined; 0.2 mL s^{-1} ($\equiv 9,000 \text{ LMH}$), 0.67 mL s^{-1} ($\equiv 31,500 \text{ LMH}$) and 1 mL s^{-1} ($\equiv 45,000 \text{ LMH}$). The flow rates were chosen to represent a wide range of flow rates utilising the full capacity of the pump (at the time the maximum flow rate the pump could achieve was 1 mL s^{-1} ($\equiv 45,000 \text{ LMH}$)). When the syringe pump was later upgraded to a newer model it was possible to recover the cells at flow rates of up to 2.1 mL s^{-1} ($\equiv 94,500 \text{ LMH}$).

HCA2 cells were harvested and resuspended in cDMEM at a total cell concentration of $2 \times 10^6 \text{ cells mL}^{-1}$. 0.6 mL ($\equiv 7.5 \text{ L m}^{-2}$) of cell suspension was loaded onto the filter at a constant flow rate of 0.2 mL min^{-1} ($\equiv 150 \text{ LMH}$). The cells were then recovered by backflushing the filter with elution buffer at 1 mL s^{-1} ($45,000 \text{ LMH}$). A total volume of 5 mL ($\equiv 62.5 \text{ L m}^{-2}$) of elution buffer was used and the backflush was continuous; $400 \mu\text{L}$ samples were collected for analysis after 0.4 mL , 0.8 mL , 1.2 mL , 1.6 mL , 2 mL and 5 mL backflush. The number of total cells and the viability of the cells at each stage of the backflush were compared to the total number of cells loaded and their viability. The total cells loaded will be referred to as total cells available for recovery at the start of the backflush (i.e. backflush volume = 0 mL) in the text and figures from here on in.

Figure 3.3 shows that the proportion of cells recovered by backflushing at 1 mL s^{-1} ($45,000 \text{ LMH}$) was significantly higher after a 5 mL ($\equiv 62.5 \text{ L m}^{-2}$) backflush than the proportion of cells recovered by backflushing at the lowest flux rate of 0.2 mL s^{-1} ($9,000 \text{ LMH}$; $p = 0.009$). On average $79.7\% \pm 5.9\%$ of cells were recovered when backflushing at 1 mL s^{-1} ($45,000 \text{ LMH}$) compared to $72.1\% \pm 3.8\%$ ($p = 0.13$) at 0.67 mL s^{-1} ($\equiv 31,500 \text{ LMH}$) which compares with $58.8\% \pm 7.1\%$ ($p = 0.02$) when backflushing at 0.2 mL s^{-1} ($9,000 \text{ LMH}$).

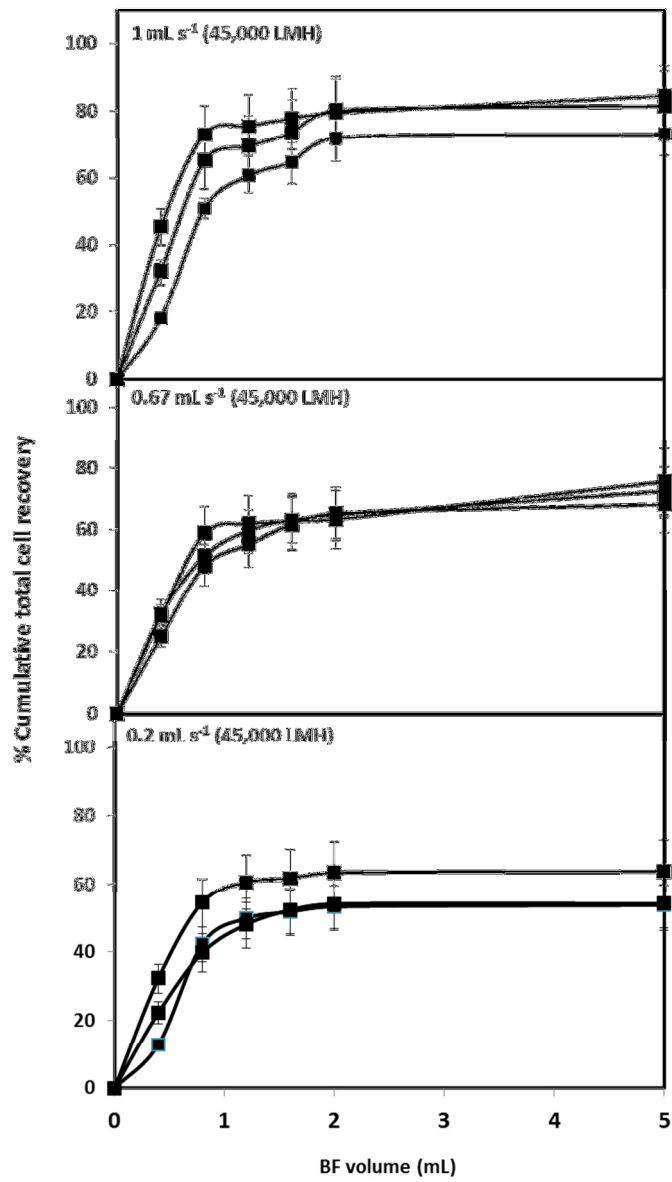


Figure 3.3 – Effect of backflush flow rate on total cell recovery.

Results show the mean values \pm the range from three individual experiments each measured in triplicate ($z=3$, $n=3$).

The ability to recover the cells using a high flow rate is beneficial as it reduces the overall processing time, however the quality of the cells is paramount and it is important that high flow rates do not expose the cells to excessive amounts of hydrodynamic shear stress which could potentially damage the cells. Figure 3.4 shows the effect of increased back flush flow rates on loss of cell viability as defined by the integrity of their membranes. Viability was measured by trypan blue exclusion using the ViCell XR and all of the viability measurements taken for the recovered samples were analysed against the initial viability measured in the load to assess the overall loss in viability post-processing. The results show that on average, when backflushing at the lowest flow rate to recover cells (0.2 mL s^{-1}) there was little or no drop in cell viability post-processing. This did increase slightly when recovering cells using the maximum backflush flux rate (45,000 LMH) however this change was deemed statistically insignificant ($p = 0.40$). There was a high degree of variability in the overall loss of viability for runs using the same backflush flow rate which made it difficult to identify any significant effects of backflush flow rate on cell viability.

Although it is not essential for a primary recovery step to concentrate the cells, it does increase the processing demands further downstream if the operation causes an increase in volume. The load volumes investigated within this research ranged from 0.6 mL (7.5 L m^{-2}) to 5 mL (62.5 L m^{-2}) of cell suspension at varying concentrations. With this in mind a backflush volume of 5 mL at best provides no change in concentration but in most cases will actually dilute the cells. Figure 3.5 shows the cumulative proportion of recovered cells (PT_R) which are recovered in each part of the backflush. The dashed line indicates when the volume of backflush buffer which has passed through the filter is equal to the volume of the filter housing (0.6 mL). It can be seen that although 5 mL of backflush buffer was used, around 80% of the cells which were recoverable, were

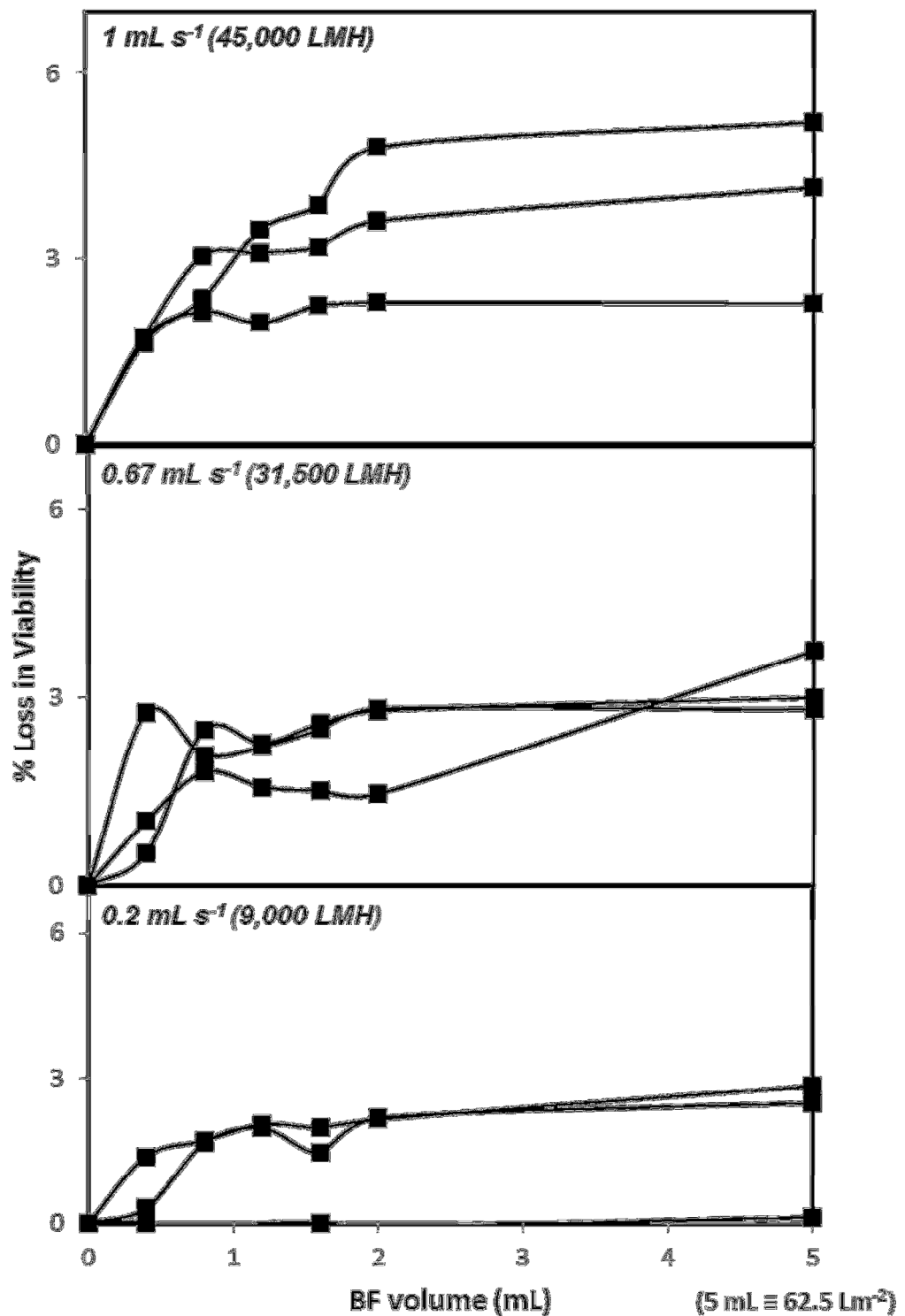


Figure 3.4 - Effect of backflush flow rate on the membrane integrity of recovered cells.

The backflush flow rate had no significant effect on the membrane integrity of recovered cells. Results show the mean values \pm the range from three individual experiments each measured in triplicate ($z=3, n=3$).

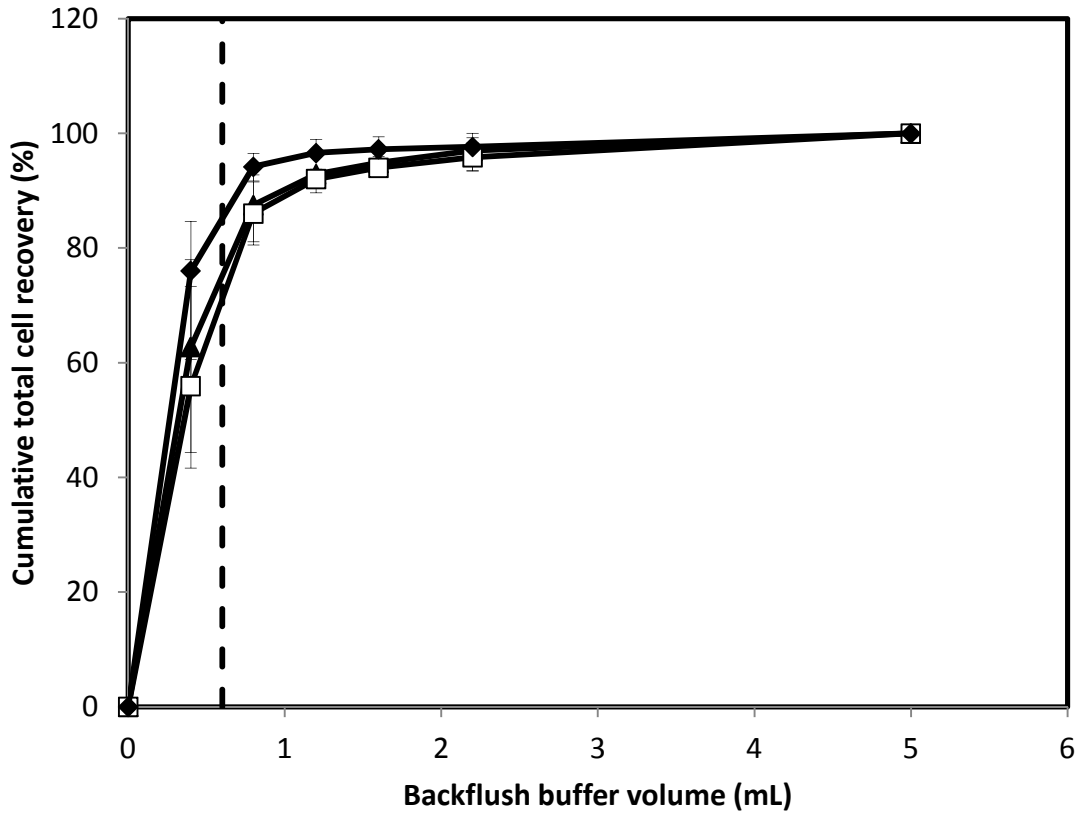


Figure 3.5 – Proportion of recoverable cells recovered in each section of the backflush buffer.

Results show the mean average \pm the range (z=3, n=3).

recovered within 0.6 mL of backflush buffer independent of backflush flow rate; i.e. as soon as the backflush buffer passes through the filter, it recovers the majority of the recoverable cells. This means that although the 5 mL backflush volume was maintained throughout in order to ensure that all of the recoverable cells were recovered, it may be possible to significantly decrease that volume (meaning the filtration step could potentially concentrate the cells), without significantly affecting the yield.

3.2.3. Backflush buffer

The elution buffer used to recover the cells back off the filter consisted of 10% dextran in DPBS. The dextran was added to increase the viscosity of the buffer in order to minimise the effects of changing resistance across the filter and ensure an even distribution of backflush buffer across the filter surface.

Figure 3.6 shows the shear stress versus the shear rate for the three concentrations. Each fluid follows a power law, relationship over the shear rate range studied:

$$\tau = K\gamma^n$$

Equation 3.1

where τ is shear stress, K is the consistency index, γ is the shear rate and n is the degree of non-Newtonian behaviour (Newtonian or constant viscosity fluids, $n = 1$). The values for K and n are shown in Table 3.1.

The dextran suspensions are slightly pseudoplastic or shear thinning. This means that for increased levels of shear stress the viscosity reduces but only slightly. The backflush buffer is designed to have a high viscosity to ensure even distribution of flow across the filter. In the filter housing before the buffer passes through the matrix of the filter, the shear rate is relatively low ($\approx 5 \text{ s}^{-1}$).

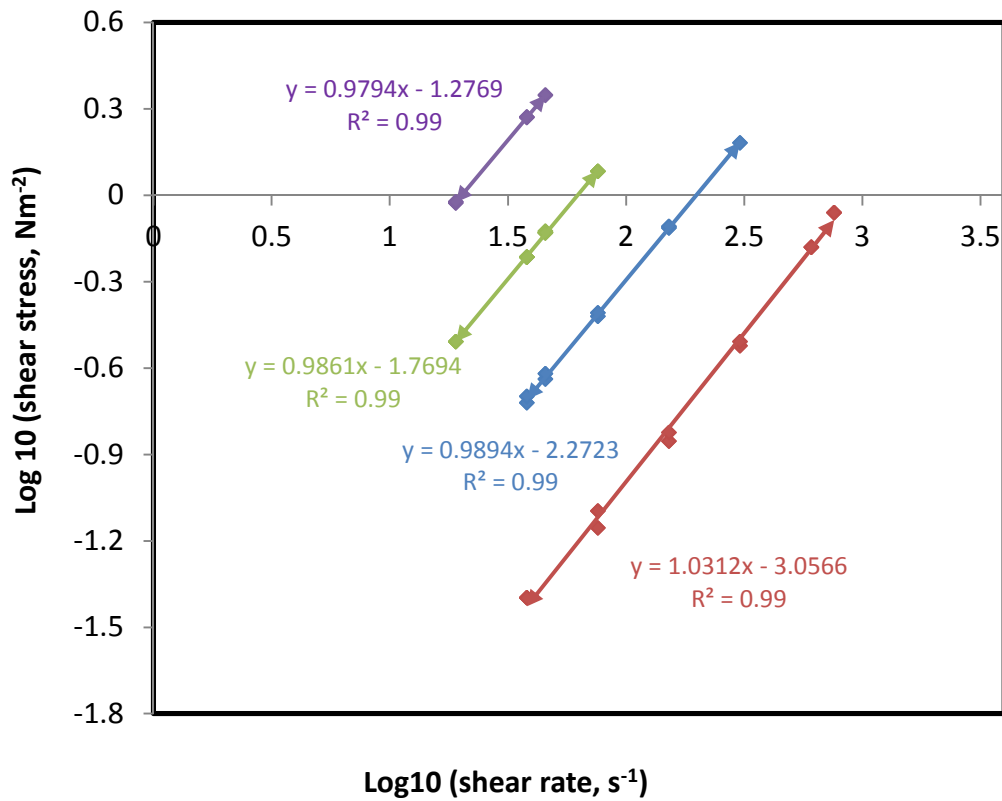


Figure 3.6 – Effect of dextran concentration on rheology of backflush buffer; 10% (◆), 20% (◆) and 30% (◆) dextran in DPBS.

Water was also measured as a control (◆). Each data curve shows the data points for both increasing and decreasing shear rate. The rheological properties are summarised in Table 3.1. The temperature was maintained at $21^{\circ}\text{C} \pm 1^{\circ}\text{C}$.

	n	K ($\text{N s}^n \text{m}^{-2}$)	Shear rate (s^{-1})
Water	1.031	0.00088	38-760
10%	0.989	0.0053	38-304
20%	0.986	0.0170	38-76
30%	0.979	0.0529	19-47

Table 3.1 – Rheological properties of dextran solutions using power law model, $\tau = k\gamma^n$

This means that the liquid will be more viscous and spread out evenly across the filter. However when the liquid is forced through the filter the shear rate increases ($\approx 1000 \text{ s}^{-1}$) and the viscosity will drop slightly allowing it to pass through the filter more easily. The level of pseudoplasticity is shown to increase with increasing concentrations of dextran and a 30% dextran solution is approximately 60 times more viscous than water. The rheological properties of all the solutions were fully reversible and any change in viscosity is rapid i.e. no hysteresis was observed.

There was no significant difference when recovering the cells using a 30% dextran solution compared to a 10 % dextran solution (results not shown here).

It was also important to ensure that the backflush buffer has no adverse effects on the cells. One major concern was that the rapid buffer change to which the cells are exposed during the backflush (from the complete growth media they are loaded in, to the elution buffer they are recovered in) could cause them to rupture, similar to the effects caused by osmotic shock.

To ensure that the dextran/DPBS backflush buffer did not have an adverse effect on the cells, cells recovered using the dextran buffer were compared to cells recovered using complete growth media (cDMEM ;i.e. the same buffer as that in which the cells were loaded) and DPBS (without dextran). As a negative control, water was also used to recover the cells from the filter.

HCA2 cells were harvested and 1 mL of cell suspension at a concentration of 2×10^6 cells mL^{-1} was loaded at a constant flow rate of 0.2 mL min^{-1} ($\equiv 150 \text{ LMH}$). The cells were then recovered via backflushing with 5 mL of the chosen elution buffer at a rate of 1 mL s^{-1} ($\equiv 45,000 \text{ LMH}$).

Viability measurements taken from trypan blue exclusion analysis of membrane integrity showed that there was no significant drop in viability for cells recovered using the dextran elution buffer compared to those recovered using cDMEM or DPBS. Water showed a greater drop in viability in comparison to the other three elution buffers (Figure 3.7). This was expected as the water induces osmotic shock within the recovered cells causing them to burst. However there was a wide range of viability results when backflushing with water compared to the other buffers, meaning that in some cases the extent of the damage caused by backflushing with water was in the same range as when using the other buffers. The total cell recovery on average was higher when using DPBS and DPBS/dextran ($21\% \pm 4.1\%$ and $21\% \pm 1.9\%$ respectively) compared to CGM and water. ($13\% \pm 6.1\%$ and $16\% \pm 7.1\%$ respectively). However the lack of reproducibility with these results made it difficult to identify any consistent trends.

Size distribution analysis was also carried out on the recovered samples using the CASY Model TTC (section 2.6.3). If the sudden change in buffer did cause the cells to burst open, it is likely that there would be an increase in cell debris. Debris is not picked up by the ViCell trypan blue exclusion analysis and therefore potentially any decrease in viability caused by the cells breaking up, would not be identified. The CASY was used to classify the particles in the recovered samples based on their size. Particles smaller than $8\ \mu\text{m}$ in diameter were classified as debris.

Figure 3.8 shows that the level of debris caused by backflushing with cDMEM, DPBS and the dextran elution buffer was consistent; using the dextran elution buffer did not appear to cause excess levels of cell debris. As predicted the osmotic shock caused by backflushing with water caused a significant increase in the level of debris.

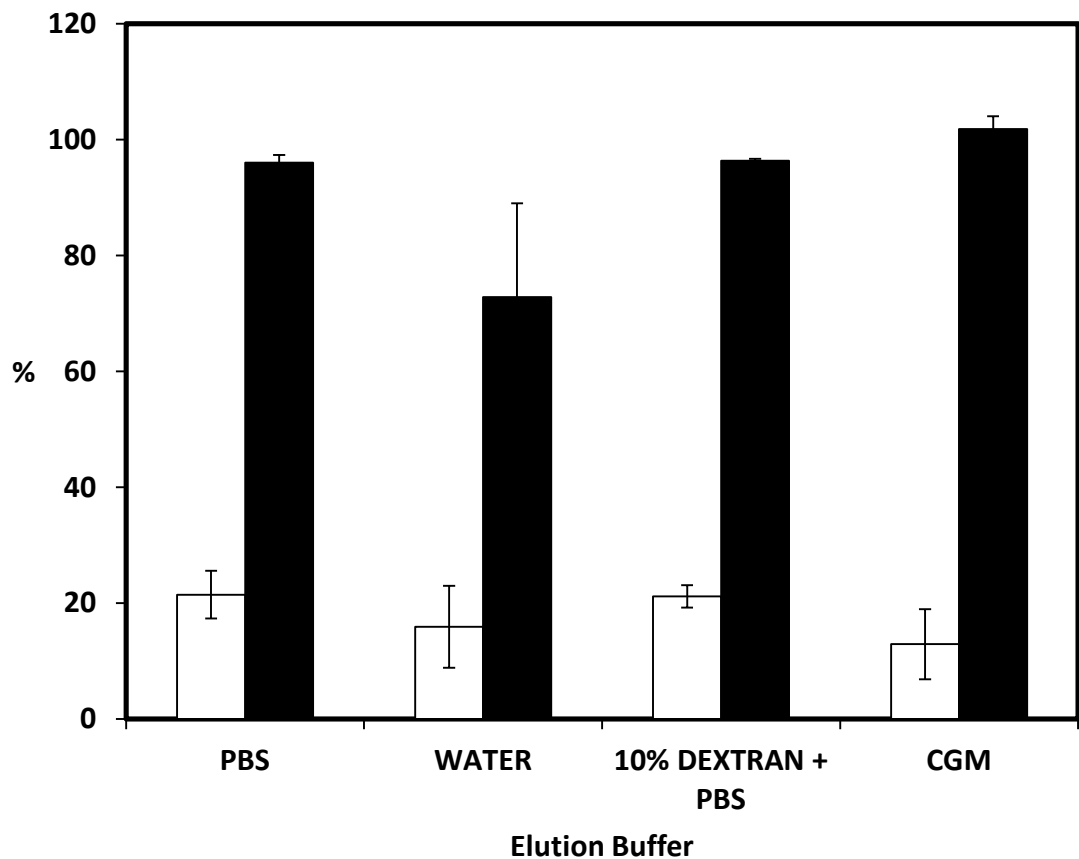


Figure 3.7 – Effect of elution buffer on total cell recovery and viability of recovered cells.

Results show the effect of four different elution buffers (DPBS, water, 10% dextran in DPBS and cDMEM) on the total cell recovery (□) as well as the viability of the recovered cells (■). Results show that the elution buffer had no significant effect on total cell recovery and only water caused a decrease in the viability of the recovered cells. Data shows the mean values and the range (z=3, n=2).

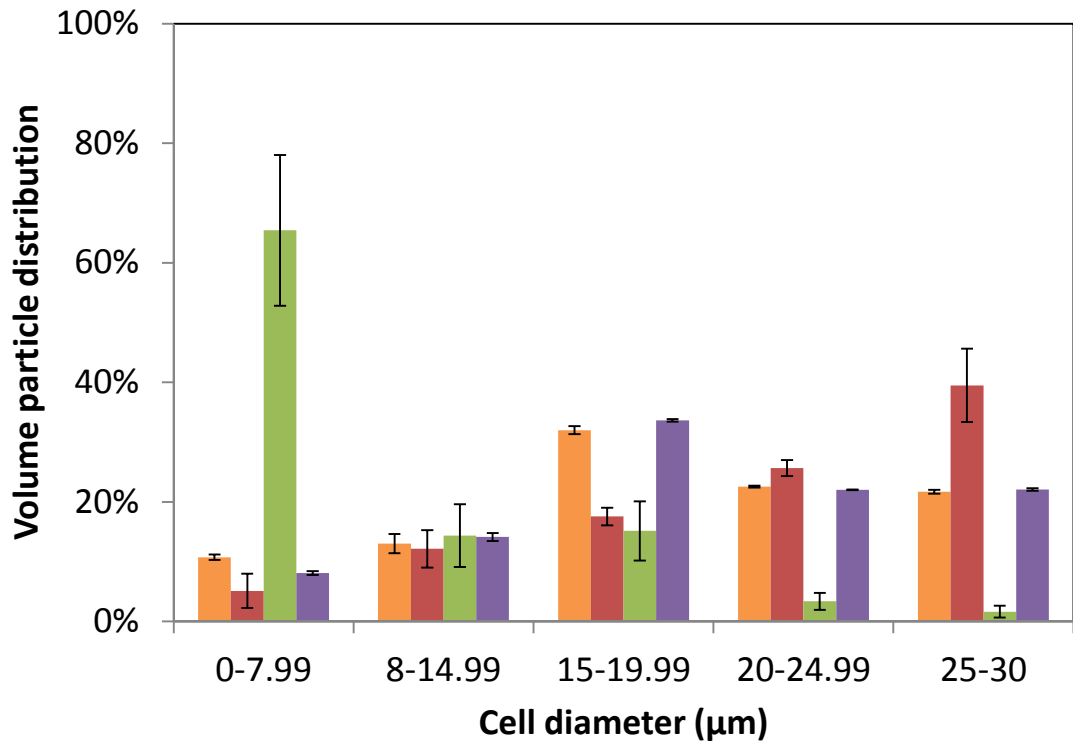


Figure 3.8 – Particle size analysis of recovered samples.

1.5 mL of cell suspension at a concentration of 2×10^6 cells mL^{-1} was loaded at 150 LMH. Cells were recovered by backflushing the filter with an elution buffer consisting of either PBS (■), CGM (■), water (■) or 10% dextran in PBS (■) at 45,000 LMH. Results showed that apart from water which caused a significant increase in cell debris compared to the other elution buffers, the remaining three elution buffers did not cause a significant increase in the level of debris. Data shows the mean average and the range ($z=2$, $n=1$).

3.2.4. Effect of loading conditions on recovery of HCA2 cells

3.2.4.1. Load cell number

In any filtration process it is important to know the capacity of the filter being used and the optimum load with which it will operate. Suspensions of HCA2 fibroblasts (adherent) and CHO cells (suspension) were loaded onto the filter at a controlled flow rate of 0.2 mL min^{-1} ($\equiv 150 \text{ LMH}$). The suspensions were varied in both volume and concentration to cover a wide range of load cell numbers. Once loaded, the cells were recovered by backflushing the filter with 5 mL ($\equiv 62.5 \text{ L m}^{-2}$) of 10% dextran in DPBS at 1 mL s^{-1} ($\equiv 45,000 \text{ LMH}$). Cells were then counted using the ViCell XR to calculate the number of cells recovered as well as to record the membrane integrity of the recovered cells.

Figure 3.9 shows that there is an approximately linear relationship between the number of cells loaded and the number of cells recovered ($R^2 = 0.7881$); the more cells that are loaded, the more cells are recovered (and likewise more cells are lost). It is also interesting to note that for the two different cell lines which were used, one adherent and one grown in suspension, the performance appears to be the same.

Figure 3.10 shows the same data as Figure 3.9; however this time the number of cells recovered are shown as a proportion of the cells loaded (Equation 3.2):

$$PT_R = \frac{T_R}{T_L - T_P} \times 100$$

Equation 3.2

Where PT_R is the percentage of total cells captured on or in the filter which are recovered, T_R is the number of total cells recovered in the backflush, T_L is the number of total cells loaded and T_P is the number of cells appearing in the permeate. Throughout the research the number of cells which passed through the filter and were

found in the permeate (T_P) were insignificant in comparison to the number of cells loaded (on average $2.00\% \pm 2.2\%$ of the total number of cells loaded; $n=24$). Figure 3.11 shows a possible increase in T_P with cells loaded with a maximum of 7% of the load recorded and it may be that cells are forced deeper into the filter as more cells are loaded behind them.. For the purpose of this study the focus will be on examining the recovery of cells retained on the filter.

Figure 3.10 shows that by increasing the number of cells loaded, the proportion of those cells which are recovered decreases significantly. When the number of cells loaded is less than 1×10^6 , then the recovery appears to be greater than for higher cell loadings. Recovery decreases significantly as the load number is increased, plateauing around 7×10^6 cells loaded.

It is interesting to note that the trend line in Figure 3.9 might not pass through zero. Based on this observation, it was hypothesised that there are a population of cells of constant number (independent of the number of cells loaded) which are fully recovered. If this population of cells were to reside on the surface of the filter and were fully recovered, it would only have a significant effect on the proportion of cells recovered when a low number of cells are loaded and be almost insignificant when a large number of cells are loaded.

A simple hypothesis for the filtration model is that the cells either enter the filter and are only partially recovered or the cells don't enter the filter and are fully recovered. These two populations of cells will be referred to as 'filtered' and 'surface' respectively from here on:

$$T_R = T_{SURF} + (T_{FILT} * x)$$

Equation 3.3

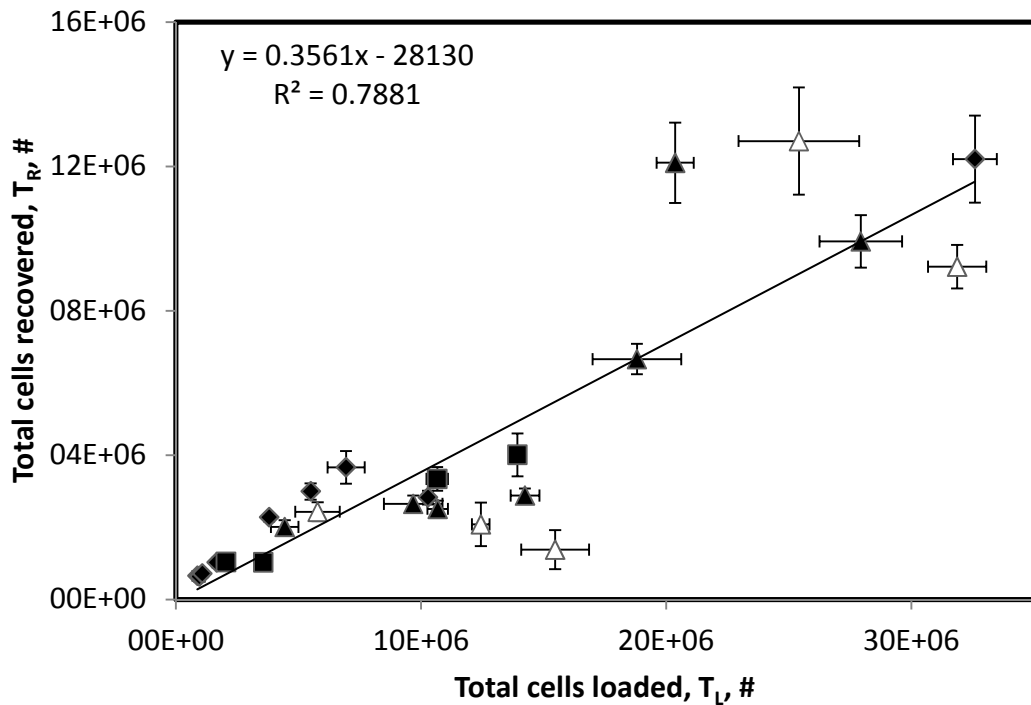


Figure 3.9 – Effect of number of total cells loaded on the number of total cells recovered.

Suspensions of HCA2 cells at a concentration of 1.5×10^6 cells mL⁻¹ (◆), HCA2 cells at a concentration of 3.0×10^6 cells mL⁻¹ (■), HCA2 cells at a concentration of 7.0×10^6 cells mL⁻¹ (▲) and CHO cells at a concentration of 7.0×10^6 cells mL⁻¹ (Δ) were loaded at a constant flow rate of 150 LMH. Cells were recovered via backflushing with 5mL (≈ 62.5 L m⁻²) of 10% dextran in DPBS at 45,000 LMH. Line of best fit (—), $R^2 = 0.7881$. All of the cell counts and associated calculations are based on total cells (i.e. viable and non-viable), however the processed cells showed no significant loss in cell viability. Average loss in cell viability was $3\% \pm 2\%$ (n=24), see later Figure 3.12. Each data point shows the mean average of triplicate inter-experimental measurements ± 1 sd.

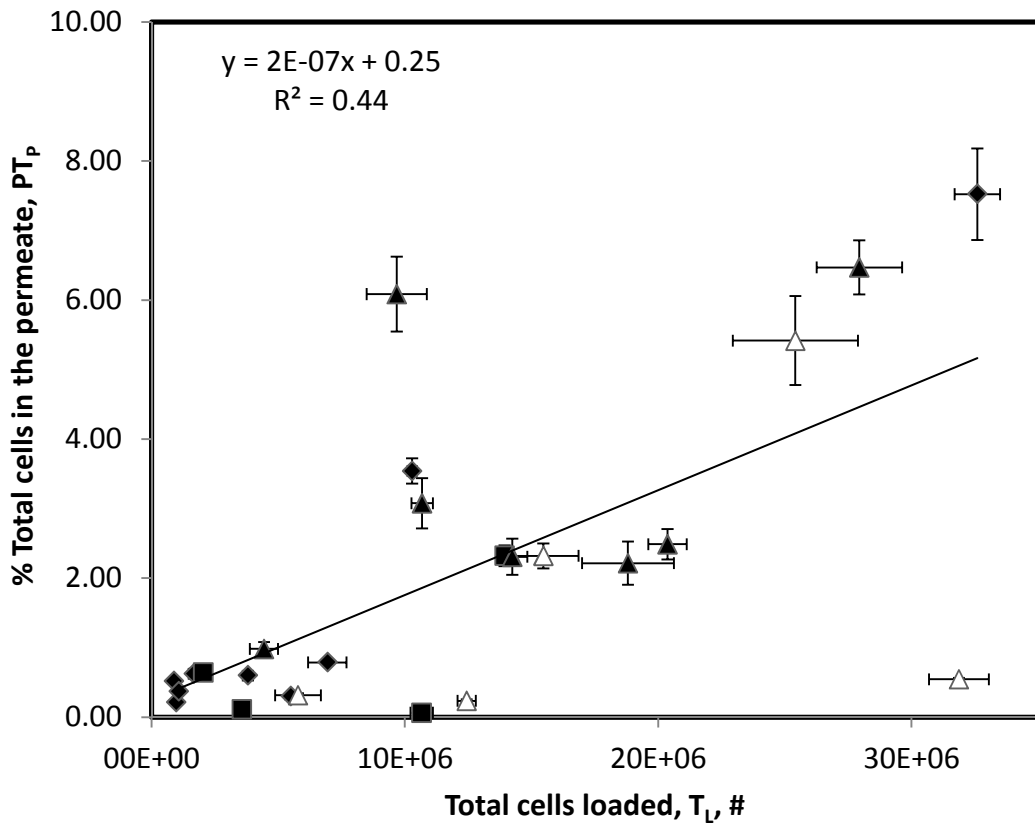


Figure 3.11 - Effect of number of load cell number on the proportion of cells in the permeate.

All processing details are the same as in Figure 3.9. A small proportion of cells did pass through the filter and were found in the permeate following filtration. On average over the 24 filtration runs, the average proportion of cells found in the permeate was $2\% \pm 2\%$ (1sd). Each data point shows the mean average of triplicate inter-experimental measurements ± 1 sd ($z=23$, $n=3$).

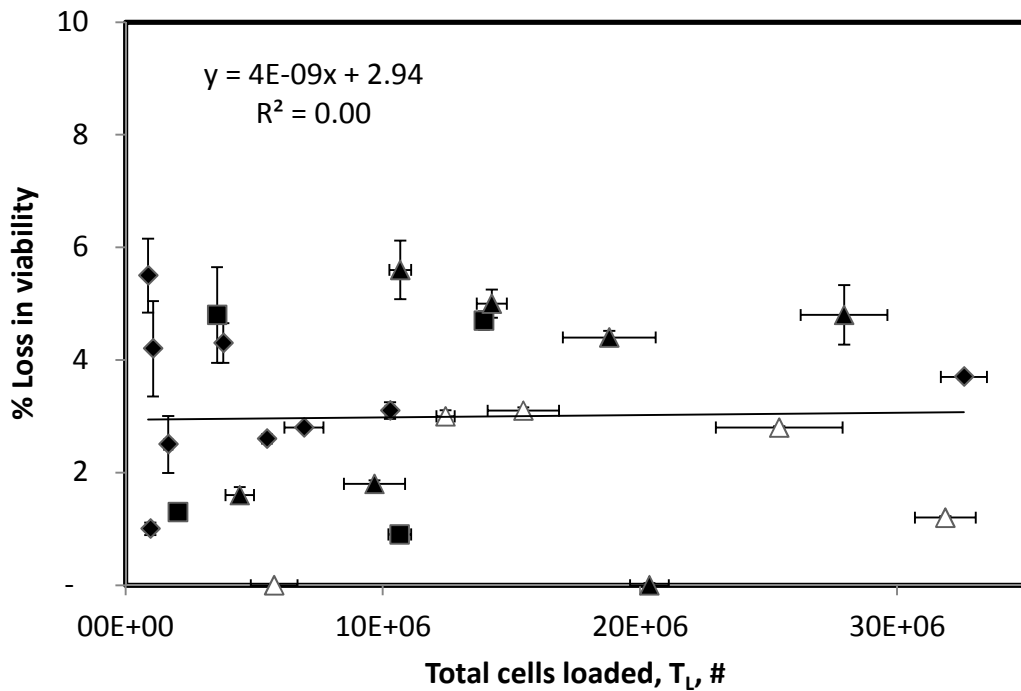


Figure 3.12 – Effect of load cell number on the viability of the recovered cells.

All processing details are the same as in Figure 3.9. Results show that the process did not cause a significant drop in cell viability regardless of the number of cells which were loaded onto the filter. Average loss in viability was 3 % ± 2% (1sd). Each data point show the mean average of triplicate inter-experimental measurements ±1sd (z=23, n=3).

where,

$$T_{\text{FILT}} = T_L - T_P - T_{\text{SURF}}$$

Equation 3.4

i.e. the number of total cells recovered (T_R) is equal to the number of cells which reside on the filter surface (T_{SURF}) plus the proportion (x) of filtered cells (T_{FILT}) which are recovered from within the filter matrix.

A trial and error method was used to establish a value for T_{SURF} . Figure 3.13 shows that when a surface population of 500,000 cells is subtracted from the number of cells recovered then the proportion of cells recovered for the majority of the filtrations fall into a similar range regardless of the number of cells loaded. The mean average recovery for all of these filtrations is now $35\% \pm 11\%$ (1sd), meaning the value of x (Equation 3.3) is 0.35.

The proportion of total filtered cells recovered by backflush (PT_R^*) is given by:

$$PT_R^* = \frac{T_R - T_{\text{SURF}}}{T_L - T_P - T_{\text{SURF}}} \times 100$$

Equation 3.5

A simple hypothesis to explain the size of the surface population would be that the surface residing cells (T_{SURF}) are a single layer which cover the majority of the filter surface area. The size of the surface cell population would then be given by: -

$$T_{\text{SURF}} = \frac{C}{100} \cdot \frac{A}{\pi d_c^2}$$

Equation 3.6

For a filter area (A) of $1.33 \times 10^{-4} \text{ m}^2$ and a T_{SURF} value of 500,000 cells (i.e. 3.73×10^9 cells m^{-2}), a confluency (C) of 70% is estimated for a mean cell size of (d_c) of 15 μm . Such a value might be expected for cells collected at a porous surface.

Using this information a model formula was derived.

For $T_L \geq 500,000$

$$T_R = 500,000 + 0.35 \cdot T_{\text{FILT}}$$

$$T_R = 500,000 + 0.35 * (T_L - T_P - 500,000)$$

$$T_R = 335,000 + 0.35 * (T_L - T_P)$$

For $T_L < 500,000$

$$T_R = T_L - T_P$$

Equation 3.7

Figure 3.14 shows how the model data compares to the actual data shown in the previous figures. The model data for load numbers greater than 500,000 cells fits closely with the actual results, there were no actual data points for load numbers less than 500,000 cells, therefore it is not possible to comment on how accurate that part of the model is.

3.2.4.2. Load cell volume

Primary recovery processes are often required to work with large volumes of material produced upstream which may only contain very low concentrations of the target molecule or cell. It is therefore essential that the system is able to achieve consistently high levels of cell recovery whilst processing large volumes of feed material.

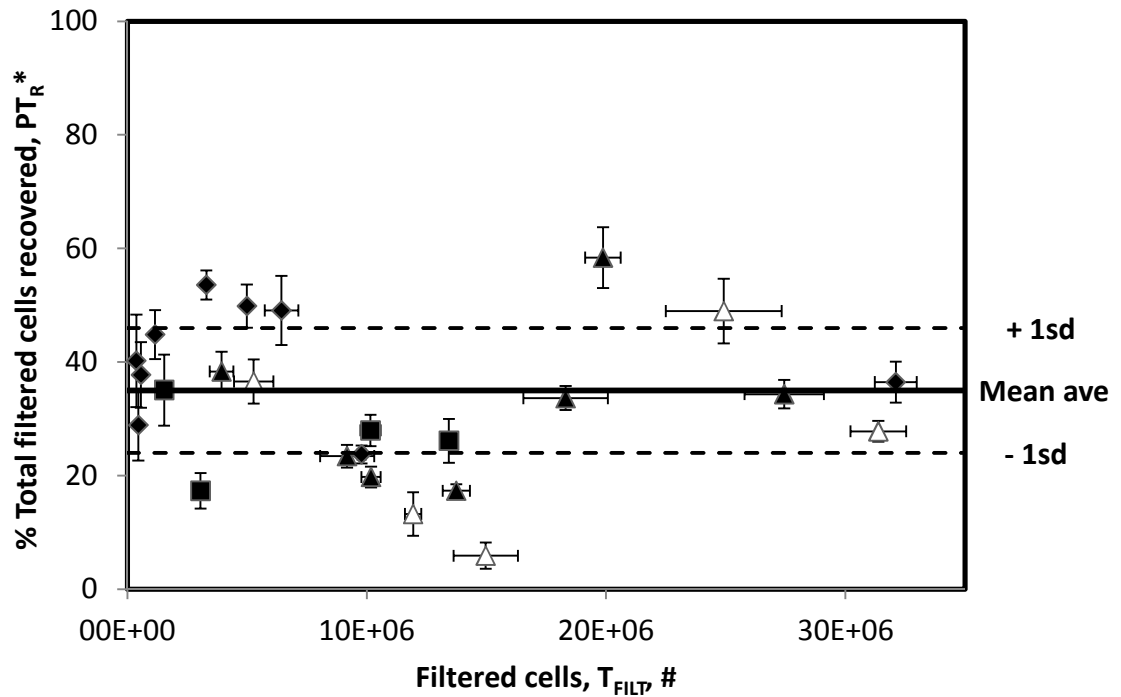


Figure 3.13 – Proportion of “filtered” cells which are recovered (see Equation 3.4 and Equation 3.5).

An estimated population of 500,000 “surface” cells was subtracted from the total cells loaded and the total cells recovered. All processing details are the same as in Figure 3.9. The mean average recovery for all of these filtrations was $35\% \pm 11\%$. Each data point shows the mean average of triplicate inter-experimental measurements $\pm 1sd$ ($z=23$, $n=3$).

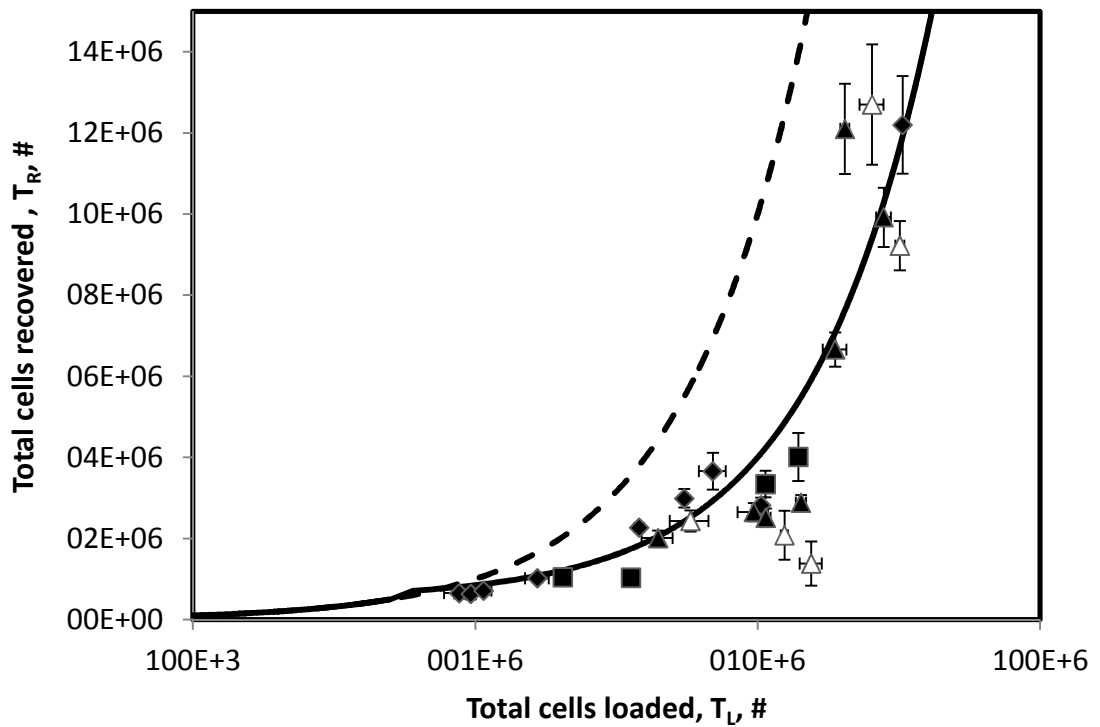


Figure 3.14 – Effect of the number of total cells loaded on the number of total cells recovered.

Figure shows the actual data vs the model described in Equation 3.7. All processing details are the same as in Figure 3.9. Figure shows the data produced using the model described in Equation 3.7 (—), where $x = 0.35$ and $T_{SURF} = 500,000$ cells. The parity line (----) indicates whereabouts the data points would lie if all of the cells which were loaded were fully recovered. Each actual data point shows the mean average of triplicate inter-experimental measurements ± 1 sd ($z=23$, $n=3$).

The data from the previous section (section 3.2.4.1) was reanalysed to investigate the effect that the volume of cell suspension loaded has on the performance of the process.

Figure 3.15 shows the data from Figure 3.13 with load volume as the main variable. The trend line does indicate a possible decrease in the recovery with increasing load volumes, however there is a large degree of variation ($R^2 = 0.03$). It is hypothesised that increased load volumes could force the cells further into the filter making the “filtered” cells (T_{FILT}) more difficult to recover (decreasing x) and possibly even reducing the proportion of cells which reside on the surface (T_{SURF}) which overall will decrease total cell recovery.

3.2.4.3. Load cell concentration

As previously discussed, downstream processing and in particularly primary recovery operations can often be required to deal with large volumes of low product concentration feed material. It is important to understand how the process will perform across a wide range of volumes and product concentrations. The data from section 3.2.4.1 was reanalysed to investigate the effect of cell concentration on the total cell recovery of the process.

Figure 3.16 shows the effect that the concentration of the cells in the feed stream, has on the proportion of “filtered” cells which are recovered. The concentration of cells in the load does not appear to have a significant effect on the proportion of “filtered” cells which are recovered.

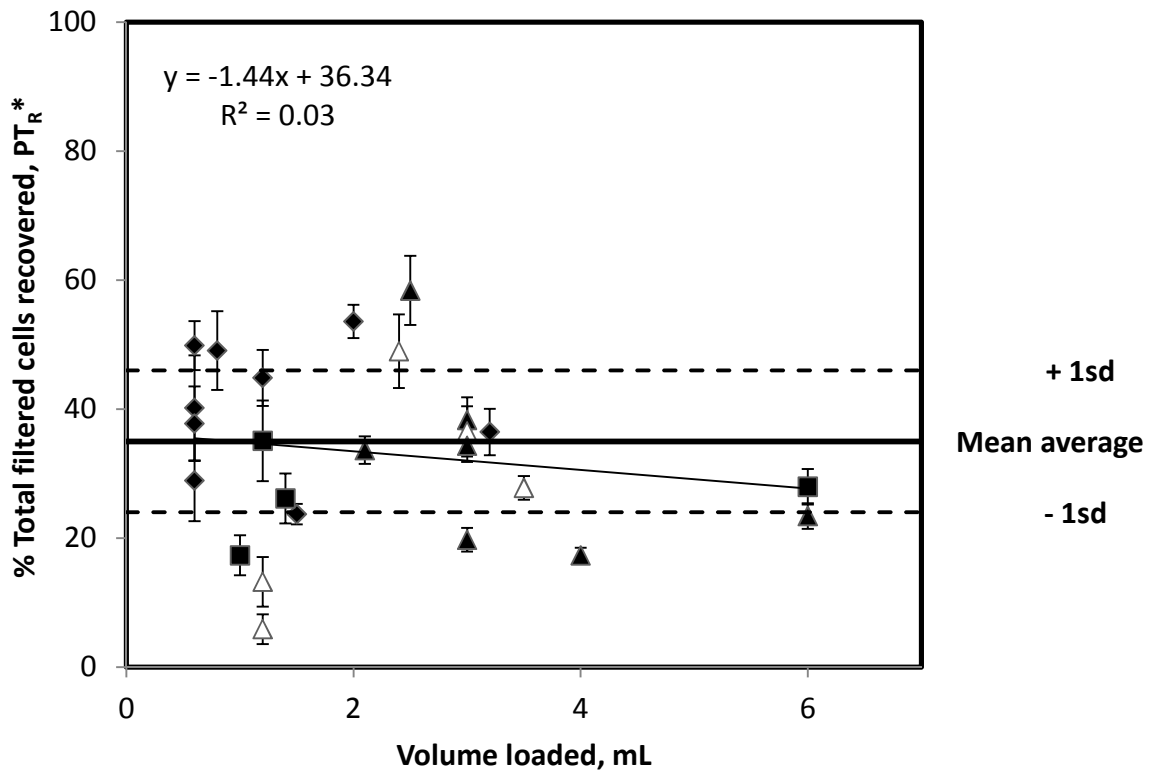


Figure 3.15 – Effect of volume of cell suspension loaded on recovery of “filtered” cells.

An estimated population of 500,000 “surface” cells was subtracted from the total cells loaded and the total cells recovered. All processing details are the same as in Figure 3.9. Results show a possible decrease in the recovery of filtered cells with increased load volumes. The mean average recovery for all of these filtrations was $35\% \pm 11\%$ (1sd). Each data point shows the mean average of triplicate inter-experimental measurements $\pm 1sd$ ($z=23$, $n=3$).

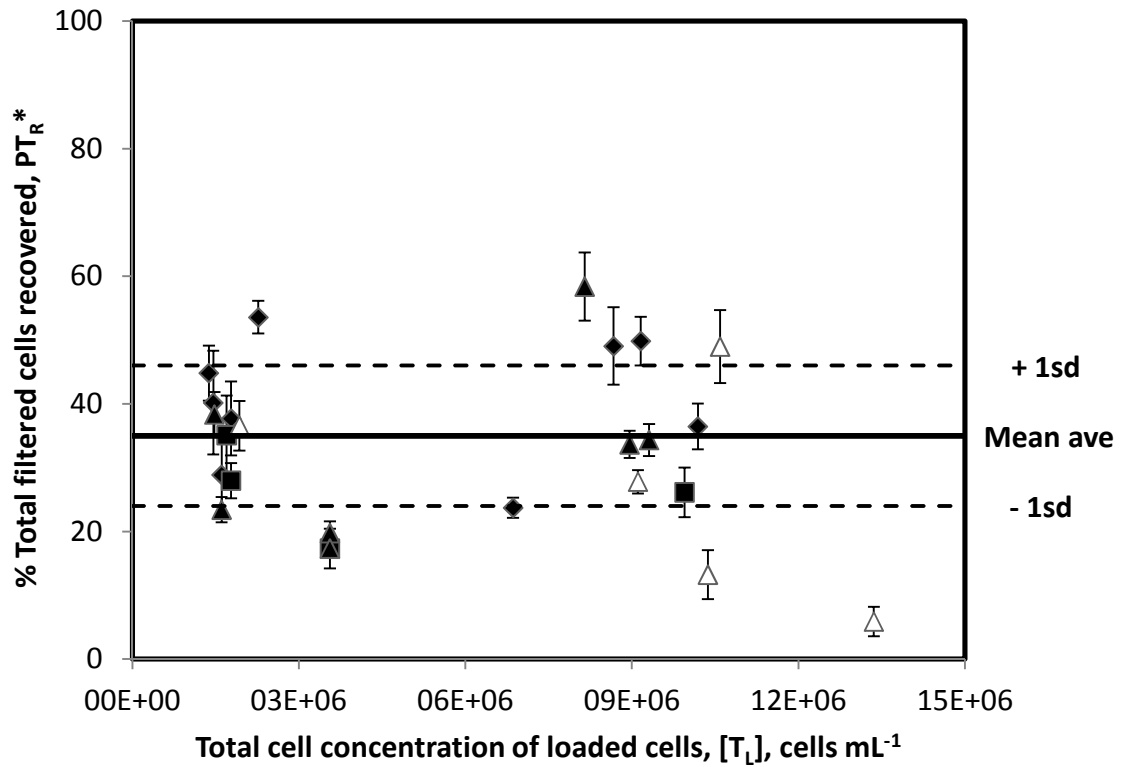


Figure 3.16 – Effect of cell concentration in the feed on the recovery of “filtered”

An estimated population of 500,000 “surface” cells was subtracted from the total cells loaded and the total cells recovered. All processing details are the same as in Figure 3.9. The mean average cell recovery was 35% ± 11% (1sd) regardless of feed concentration. Each data point shows the mean average of triplicate inter-experimental measurements ±1sd ($\bar{z}=23$, $n=3$).

3.3. Chapter Discussion

The development of ultra scale-down tools and devices is a key part of process development and has a potential role to play particularly in the development of whole cell therapeutics where only small volumes of sample are available at early development stages due to the costs and complexities associated with large scale processing.

Depth filtration has the capacity to provide a simple yet effective alternative to batch centrifugation. There is the potential for a single step, closed process eliminating the inherent risks of contamination and cell damage associated with batch centrifugation and tangential flow filtration (hydrodynamic shear forces associated with TFF have been shown to damage cells), if the challenges surrounding levels of recovery can be addressed.

An ultra scale-down filtration device has been developed to investigate the primary recovery of adherent cells for therapy. It has been demonstrated that the device (as shown in Figure 1.2) is capable of maintaining cells in a homogenous single cell suspension (although there was some fluctuation $\approx \pm 9\%$) and accurately delivering small volumes of the suspension to the filter over a range of flow rates. The cells maintained in the device did not show a significant drop in cell viability over time.

A method for recovering the cells by backflushing the filter in the opposite direction to which the cells are loaded was also established. The filter is backflushed with an elution buffer consisting of 10% dextran in PBS. The dextran is added to increase the viscosity in order to ensure an even flow distribution across the filter regardless of changing resistance due to areas of cells being cleared. The rate at which the cells were recovered from the filter had an effect on both the proportion of total cells recovered (PT_R) and the viability of the recovered cells. On average $79.7\% \pm 5.9\%$ of cells were recovered when

backflushing at 1 mL s^{-1} (45,000 LMH) compared to $58.8\% \pm 7.1\%$ ($p = 0.02$) when backflushing at 0.2 mL s^{-1} (9,000 LMH). However when backflushing at the lowest flow rate to recover cells (0.2 mL s^{-1}) there was little or no drop in cell viability post-processing, whereas using the maximum backflush flux rate (45,000 LMH) there was an increased drop in viability although this was not deemed statistically significant ($p = 0.40$). It is important to note that the high recoveries were only achievable at low levels of cell loading. When the number of cells loaded increased above 1×10^6 cells, the recoveries were significantly reduced.

The buffer used to recover the cells was examined to assess its effect on cell viability and total cell recovery. The dextran elution buffer was compared to DPBS and cDMEM. The total cell recovery on average was higher when using DPBS and the dextran based elution buffer ($21\% \pm 4.1\%$ and $21\% \pm 1.9\%$ respectively) compared to cDMEM ($13\% \pm 6.1\%$). There was no significant drop in viability for cells recovered using the dextran elution buffer compared to those recovered using cDMEM or DPBS.

Analysis and optimisation of the cell loading showed that the proportion of cells recovered was high when only a small number of cells were loaded ($< 1 \times 10^6$ cells), however when a larger number of cells were loaded the recoveries decreased significantly. A hypothesis for a model for the recovery of cells from the filter has been proposed and the model fits the actual data well. The hypothesis is that on loading the filter, cells fall into one of two populations. The first population of cells reside on the surface of the filter (“surface” cells) and are almost entirely recovered. The second population of cells are the cells which enter the filter (“filtered” cells) and these cells are difficult to recover. “Surface” cells are constant in number, regardless of the number of cells which are loaded. The size of this population has been estimated as 500,000 cells ($\equiv 67\%$) filter confluency. The fact that this population is constant in number

independent of the load means that when only a small number of cells are loaded the recovery is high as the recovered “surface” cells represent a large proportion of the cells loaded. In contrast when high numbers of cells are loaded the “surface” population of cells is almost insignificant in comparison and therefore the recoveries are low.

The “filtered” cells are the main reason behind the low recoveries at high load numbers. When a high number of cells are loaded onto the filter, the “filtered” cells are the major population of cells, the recovery of these “filtered” cells is low which means the overall recovery is low. When analysing the cell recoveries it was possible to focus solely on the “filtered” cells by discounting the “surface” cells from both the loaded and the recovered cells. By doing this it was observed that the recoveries all fell into a relatively tight range regardless of the number of cells loaded, the concentration at which they were loaded or the type of cells which were loaded (adherent or suspension). The average recovery was $35\% \pm 11\%$.

The only factor which seemed to have some effect on the recovery of cells which actually entered the filter (T_{FILT}) was the volume in which the cells were loaded. When a large volume of material was loaded there was some evidence to suggest that the overall filtered cell recovery is decreased (although the R^2 value = 0.1155 indicating only a slight trend). Drawing firm conclusions from the results in this section was problematic due to the significant degree of variation in the data (Figure 3.9 to Figure 3.16), in particular Figure 3.12 and Figure 3.15 showed significant variability with R^2 values of 0.00 and 0.03 respectively. This meant that whilst these results did go some way to supporting the hypothesised filtration model discussed previously in this chapter, it did make it difficult to identify the effect of any of the processing parameters on the number of cells recovered or the quality of those recovered cells.

It was hypothesised that large load volumes could potentially wash cells further into the filter which would make “filtered” cells more difficult to recover and could potentially reduce the number of “surface” cells.

Chapter 4: Mechanisms affecting the recovery of high quality adherent cells during filtration

4. Mechanisms affecting the recovery of high quality adherent cells during filtration

In the previous chapter a model for the primary recovery of cells using an ultra scale-down depth filtration device was proposed. Results indicated that post loading there are two distinct populations of cells; “surface” cells which reside on the filter surface and are fully recoverable and “filtered” cells which enter the filter matrix and which can only be partially recovered using the methods applied. Unless the number of cells loaded is very low ($>7.5 \times 10^5$ cells cm^{-2}) then the majority of the cells loaded are “filtered” cells. The results suggested that regardless of how many cells enter the filter (“filtered” cells) only around 35% of them are recovered. In order to improve the recovery of the process it is important to either increase the number of “surface” cells or increase the proportion of “filtered” cells which are recovered (x).

4.1. Locating and quantifying the unrecovered cells

In order to improve the recovery of “filtered” cells from the filter (x), it was first important to identify where they were getting trapped and then attempt to quantify the number of cells unrecovered in order to fully account for all the cells in the process. It was hypothesised that the cells were trapped within the filter matrix where they were unable to be recovered.

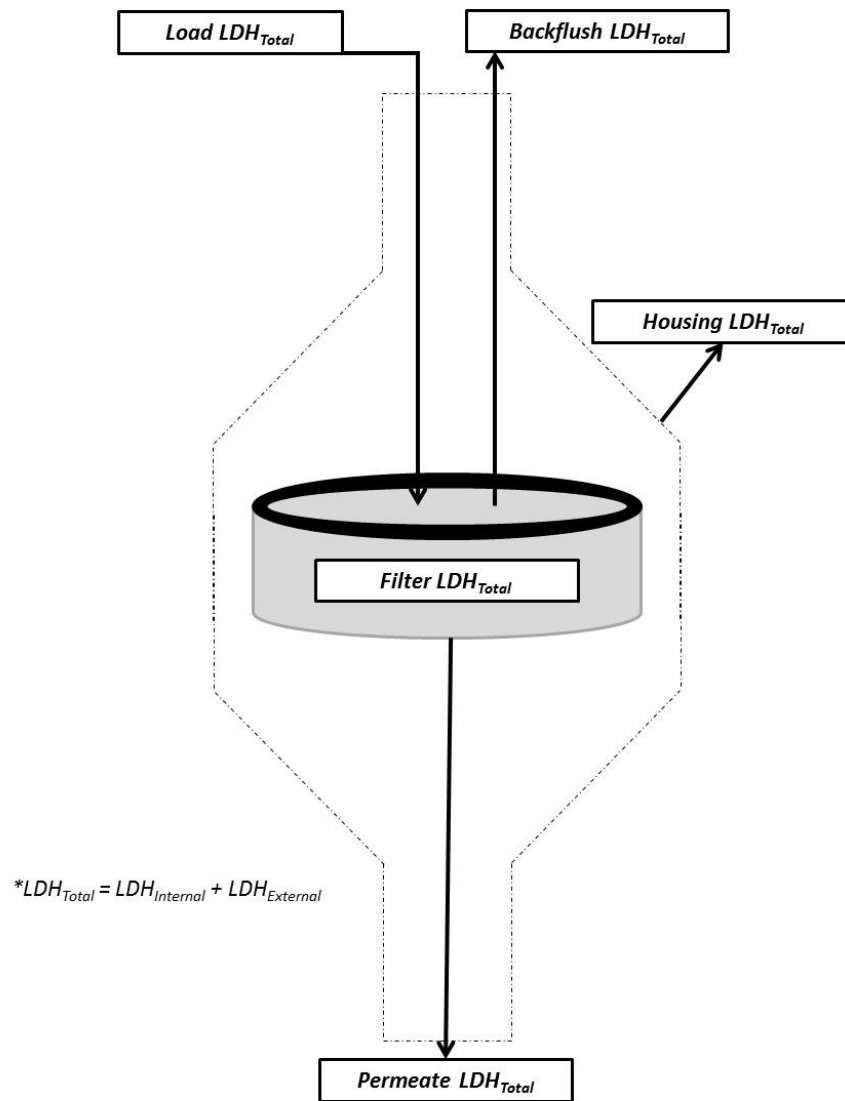
4.1.1. Lactate dehydrogenase

Lactate dehydrogenase (LDH) is an intracellular enzyme which is released when the cellular membrane is compromised. It is commonly used as a marker for cell damage during bioprocessing (Legrand et al., 1992, Danpure, 1984, Konjevic et al., 2001). The LDH assay was used to investigate cell damage but also to identify where within the

process the unrecovered cells were located. Figure 4.1 outlines the mass balance used to account for the total LDH entering and being recovered from the system. As well as the LDH released from damaged cells (LDH_{External}), the internal LDH (LDH_{Internal}) of intact cells was also measured by chemically lysing the cells in the samples to give a value for the total amount of LDH present (LDH_{Total}). Samples were collected from the load, the permeate and the backflush. The housing was also immersed in TrypLE™ Select in order to detach any cells stuck to the filter housing before analysing the LDH. Finally the cells within the filter were also chemically lysed to try to account for the number of cells still residing within the filter post backflush.

Figure 4.2 shows the results from a series of mass balance experiments which attempted to account for all of the cells within the system. Results showed that there were very few cells which passed through the filter and into the permeate (average permeate $LDH_{\text{Total}} = 4.7\% \pm 0.6\%$) and no cells were recovered from the filter housing through trypsinisation (housing LDH_{Total}). The majority of the LDH which was accounted for in all four runs, came from either cells recovered in the backflush (average backflush $LDH_{\text{Total}} = 17.7\% \pm 4.0\%$) or from the cells still unrecovered from the filter (average filter $LDH_{\text{Total}} = 23\% \pm 4.0\%$). The LDH assay proved to be reproducible with similar trends observed throughout the four filtration runs. However on average the LDH assay was only able to account for just under half of the cells ($\approx 45\%$). It was hypothesised that either the filter was having a protective effect on the cells trapped within it, which prevented them from being completely lysed, or once the cells were lysed the LDH was sticking to or becoming trapped within the filter.

A number of different methods were used to try to solve this issue including mechanical cell lysis using sonication (Li et al., 2012), flash freezing of the filter in liquid nitrogen



$$Load\ LDH_{Total} = Backflush\ LDH_{Total} + Filter\ LDH_{Total} + Housing\ LDH_{Total} + Permeate\ LDH_{Total}$$

Figure 4.1 – Schematic of LDH mass balance.

Samples were taken from the load, the permeate and the backflush. Cells attached to the filter housing were enzymatically detached and chemically lysed along with any unrecovered cells trapped within the filter. The LDH recovered from the backflush, permeate, housing and filter is compared to the total amount of LDH loaded to give a value for cell accountability.

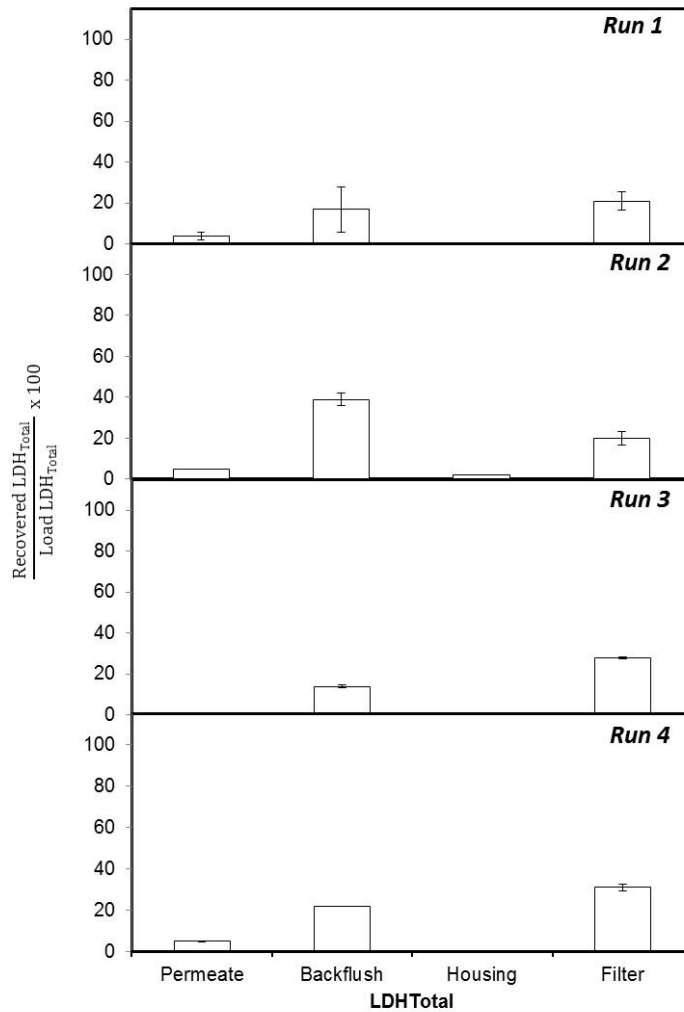


Figure 4.2 – LDH accountability.

Figure shows the proportion of LDH found in each part of the system. 1 mL of HCA2 cell suspension at a concentration of 2×10^6 cells mL^{-1} was loaded at a constant flow rate of 150 LMH. The cells were recovered by backflushing with 62.5 Lm^{-2} of elution buffer at 45,000 LMH. Samples were taken from the permeate and the backflush and chemically lysed to release LDH. Any cells attached to the housing were enzymatically detached and those remaining unrecovered from the filter were lysed and before the LDH flushed from the filter. The total LDH recovered from these samples was compared to the amount of LDH calculated in the load sample. Over 50% of the cells were still unaccounted for. Data shows mean average ± 1 sd from four separate filtrations, measured in triplicate ($z=4$, $n=3$).

in order to grind the filter into a fine powder to release the LDH and dissolution of the filter in a chemical solvent to release the trapped cells. The filter was also flushed extensively following lysis in order to recover the released LDH. None of the methods led to an improvement in LDH accountability.

4.1.2. Cryosectioning and fluorescent microscopy

In order to image any cells trapped within the filter, the filters were cryosectioned into 25 μm layers following the backflush (section 2.7.1). As a control, filters were loaded with complete growth medium (no cells) and backflushed in the same way before they were sectioned. The filters were stained with DAPI to identify any cells trapped within the sections (see section 2.7.1). Figure 4.3 shows that following backflushing of the filters there are still a considerable number of cells residing within the filter. However these images do not offer any form of quantitative analysis of the number of cells trapped there nor do they provide any detailed information as to why these cells are not recovered during backflushing of the filter.

4.1.3. Effect of filter geometry on cell recovery

A number of theories were developed to try to understand why only a small but constant proportion of cells are recovered from within the filter. It was hypothesised that dead areas caused by the geometry and design of the filter housings, could allow cells to

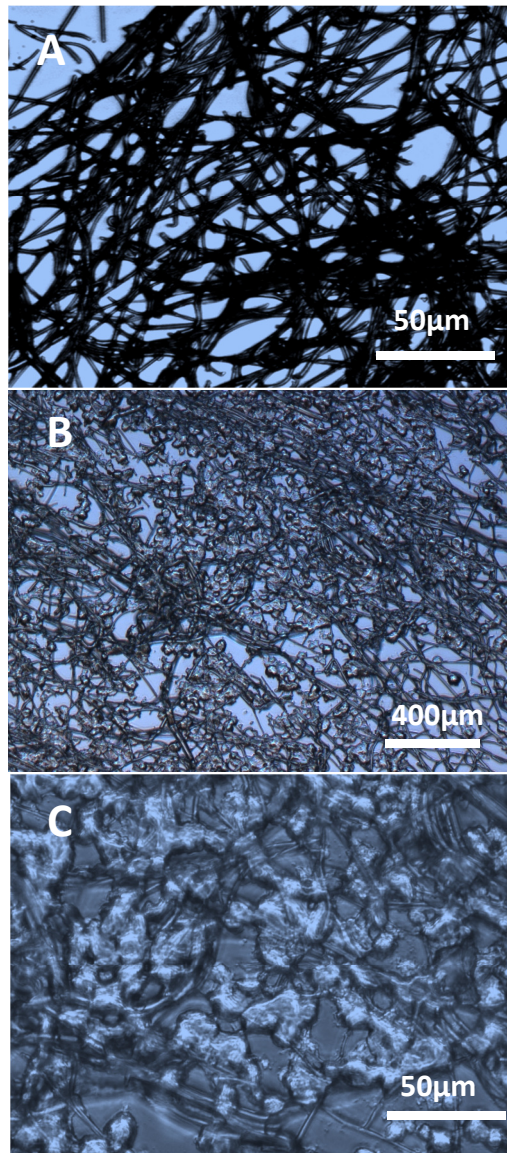


Figure 4.3 – Fluorescent microscopy images of cryosectioned filters.

1 mL of HCA2 cell suspension at a concentration of 2×10^6 cells mL^{-1} was loaded at a constant flow rate of 150 LMH. The cells were recovered by backflushing with 62.5 L m^{-2} of elution buffer at 45,000 LMH. Processed filters were then fixed in PFA and set in an OCT resin at -50°C before being sectioned into $10 \mu\text{m}$ layers. Individual layers were then stained with DAPI before imaging. Figure shows sectioned filter at 10x (B) and 40x (C) magnifications. The control (image A) is a filter processed identically to the other filters however only cDMEM was loaded (no cells), it is shown at 40x magnification. Unrecovered cells can be clearly seen trapped in the filter following backflushing.

enter parts of the filter which were then not accessible to the backflush buffer (Figure 4.4).

The filter housing consists of two main sections which screw together either side of the filter. There is a back support for the filter to rest on in one part of the housing and an O-ring which sits on top of the filter to create a seal. It is possible that cells enter the filter and flow both outwards and down through the filter as there is similar resistance to flow in both directions. Hence cells come to rest in the areas of the filter below the O-ring. When the filter is backflushed these cells may not be exposed to the elution buffer due to the higher resistance to flow in those sections of filter caused by the O-ring at the top (Figure 4.4) i.e. compared with parts of the filter which the cells are recovered from.

In order to reduce the effect of these dead zones as well to prove their existence, filters were 'pre-loaded' with cells prior to filtration in order to prevent the freshly loaded cells becoming trapped in any of the 'dead zones'.

Figure 4.5 shows the increase in the proportion of total cells recovered when the filter is pre-blinded with cells (load 1 to load 2). Results show that, on average, blinding the filter with cells prior to loading increased the total cell recovery by almost 50% to $0.35 \pm 0.1\%$. This method did not have a significant effect on the quality of the cells recovered from load 2 compared to load 1. The results suggest that the dead zones do have a negative impact on recovery; however their presence does not fully explain the extent of the cell loss.

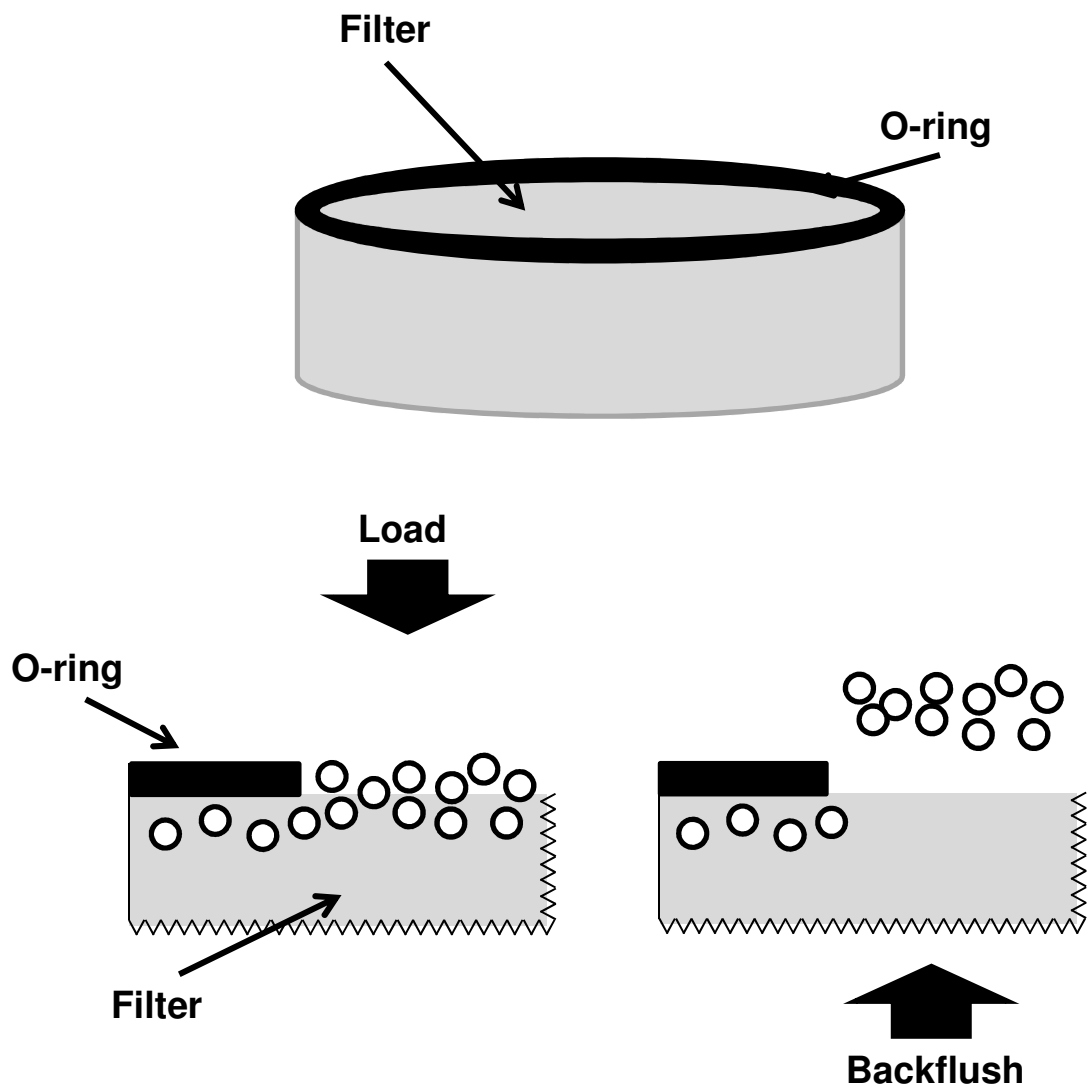


Figure 4.4 – Schematic drawing of the hypothesised mechanism which causes cells to become trapped within ‘dead zones’ in the filter.

The o-ring on the surface of the filter creates a zone beneath which cells can enter, however the resistance caused by the o-ring prevents the elution buffer from passing through these zones and recovering the cells residing within them.

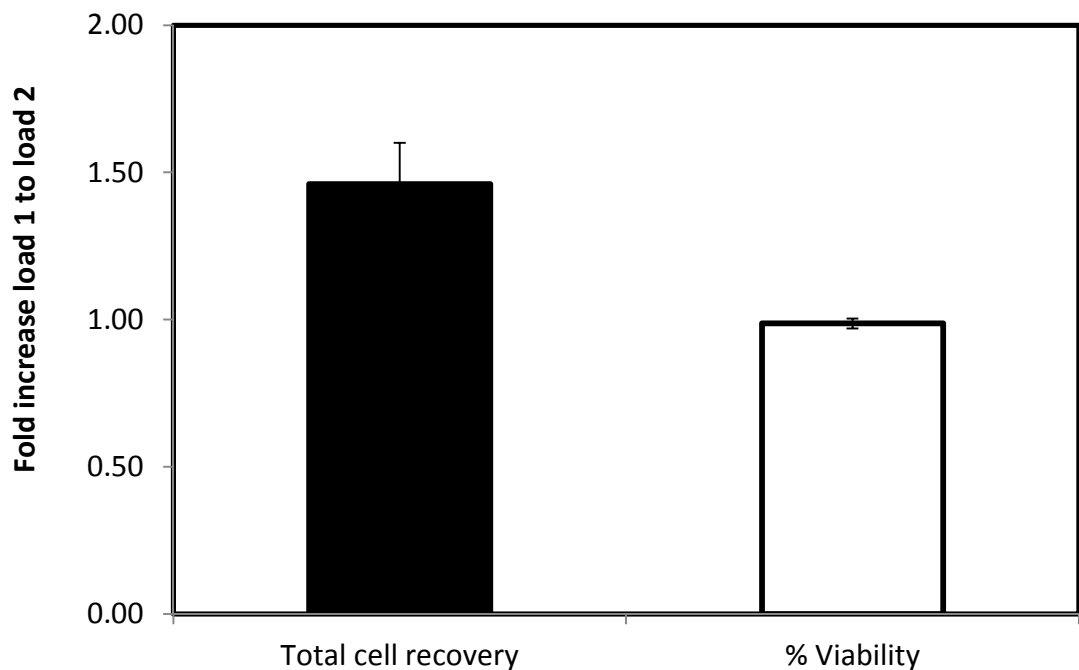


Figure 4.5 – Effect of reuse of filter on increase in total cell recovery.

2 mL of HCA2 cell suspension at a concentration of 2×10^6 cells mL^{-1} (load 1) was loaded at a constant flow rate of 150 LMH. The filter was then backflushed with 62.5 Lm^{-2} of elution buffer at 45,000 LMH in order to recover any of the cells which were not residing in the ‘dead zones’ of the filter. A further 2 mL of cell suspension at the same concentration was then loaded and recovered in the same way (load 2). Results show the mean average \pm the range from two separate filtrations each measured in triplicate ($z=2$, $n=3$).

In order to minimise the effect that the ‘dead zones’ had on the proportion of cells recovered during processing, a number of different filter geometries were analysed. The aim of altering the geometry of the filters and the filter housings was to minimise the proportion of ‘dead space’ there was within the system. A 25 mm filter housing of the same geometry was tested. The idea was that by using a larger filter housing which had a similar diameter O-ring, the O-ring would take up a smaller proportion of the available filtration surface area therefore reduce the size of the ‘dead zones’.

A 50 mm pre-loaded filter was also tested. The filters were supplied by Pall and consisted of a 50 mm diameter disc of filter material (the same cell capture material was used throughout the research) which had been ‘ultrasonically welded’ between two sides of the filter housing. This meant that the filter is sealed into the housing with no need for any seal or O-ring which could potentially cause ‘dead zones’ as previously observed.

It was important that when moving between the different filter sizes and geometries that the processing conditions were scaled accordingly. Table 4.1 shows the processing conditions which were used for each of the different filter set ups. 6.25×10^{10} cells m^{-2} were loaded at a concentration of 2×10^6 cells mL^{-1} .

Once the cells were on the filter they were recovered via backflushing with $62.5 mL m^{-2}$ of elution buffer (5 mL, 21 mL and 123 mL for 13, 25 and 50 mm diameter filters respectively) at a constant flow rate of $1 mL s^{-1}$ (this was the maximum capacity of the pump and so could not be scaled up any further).

Experiments using the 13 mm and the 25 mm diameter filters were carried out using adherent HCA2 cells. However due to the cell culture demands it was not feasible to run the 50 mm filters with this cell line and so CHO cells, grown in suspension were used

	13mm Swinnex	25mm Swinnex	50mm clamped filter
<i>Diameter (m)</i>	0.013	0.025	0.050
<i>Surface Area (m²)</i>	0.000080	0.00034	0.0020
<i>Flow rate @150LMH (mL min⁻¹)</i>	0.20	0.85	4.91
<i>Cells loaded</i>	5.00E+06	2.13E+07	1.23E+08
<i>Cells m⁻²</i>	6.25E+10	6.25E+10	6.25E+10
<i>Vol Loaded at 2x10⁶ cells mL⁻¹ (mL)</i>	2.5	10.6	61.4
<i>Loading time (mins)</i>	12.5	12.5	12.5
<i>BF Volume (mL)</i>	5	21	123
<i>BF Volume (Lm²)</i>	62.5	62.5	62.5
<i>Backflush flow rate (mL s⁻¹)</i>	1	1	1
(LMH)	45,000	10,500	1,800

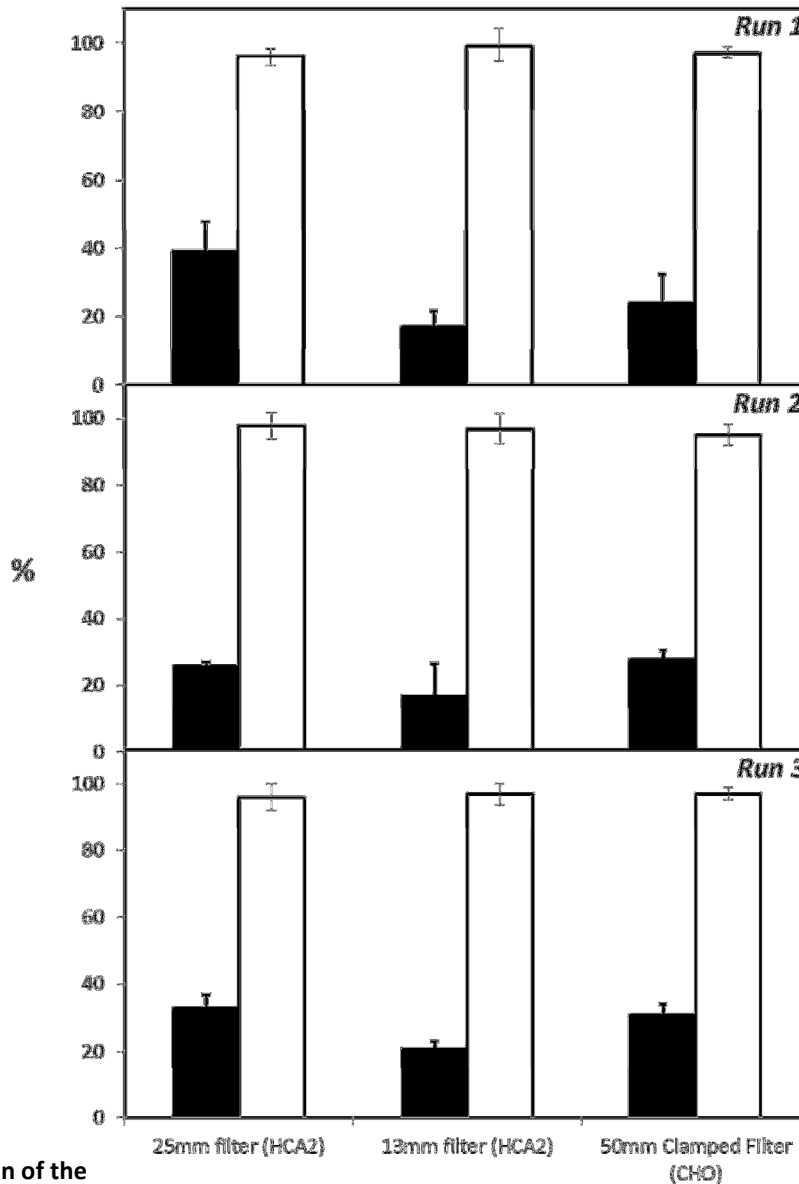
Table 4.1- Scale up of processing conditions for different filter housing geometries.

instead. Work documented in a previous chapter has already shown the CHO cells to behave in a similar way to the HCA2 fibroblasts during processing.

Figure 4.6 shows the effect of changing the filter geometry (and hence the proportion of the filter surface area masked by the seal) on both the proportion of cells recovered as well as the viability of those cells as determined by trypan blue. In all three runs the results showed an increase in the proportion of cells recovered for both the 25 mm Swinnex (2% of the filter masked by the seal) and the 50 mm pre-clamped filter housings (0% of the filter masked by the seal) when compared to the original 13 mm Swinnex filter housing (49% of the filter masked by the seal).

As with the pre-blinding experiments (Figure 4.5) this indicates that there are potentially dead zones within the filter housings. By increasing the diameter of the filter and the filter housing used (13mm to 25 mm), the proportion of the filter masked by the seal was reduced and the levels of recovery increased two fold ($14\% \pm 3\%$ to $32.5\% \pm 7\%$; $p = 0.12$). A smaller improvement was also seen when using the 50 mm clamped filters with a total cell recovery of $26\% \pm 2\%$ (compared to $14\% \pm 3\%$; $p=0.080$).

These results indicate that the filter geometry does have an effect on the total cell recovery and that 'dead zones' within the filter do have a negative impact on the proportion of cells recovered. However this does not explain the full extent of the cell loss. The recovered cells from all 3 filters maintained a high proportion of viable cells ($98\% \pm 1.73\%$). The results were reproducible with similar trends being observed for all three runs.



Proportion of the filter masked by the o-ring

2%

49%

0%

Figure 4.6 – Effect of filter housing geometry on total cell recovery.

Three different filter housings were tested with filter diameters ranging from 13 mm to 50 mm. Processing conditions were scaled up based on filter area. 6.25×10^{10} cells m^{-2} were loaded by loading accurate volumes of HCA2 cell suspension at a concentration of 2×10^6 cells mL^{-1} at a constant flux rate of 150LMH. Cells were recovered by backflushing with $62.5 Lm^{-2}$ of elution buffer at $1 mL s^{-1}$. ViCell XR counts were taken to calculate the cell recovery (■) as well as the viability (□) of the cells after each load. Results show mean values \pm the range from three separate runs measured in triplicate ($z=3, n=3$).

4.1.4. Scanning electron microscopy

Fluorescent microscopy of thinly sectioned filters had previously identified populations of cells residing within the filter even after backflushing (Figure 4.3). However the detail shown and the information that was possible to derive from these images was limited. The images proved the existence of the cells but the reasons as to why they were difficult to recover were not clear. Scanning electron microscopy was used to further investigate the reasons why a large proportion of cells were still unrecoverable and to identify the mechanisms which result in their loss.

Working in collaboration with Mark Turmaine at the UCL Department of Biosciences, filters were prepared and imaged. Two different control filters were also set up; a 'no cells' control filter and a non-backflushed control filter. The non-processed control filter was processed in exactly the same way as described above, however it was loaded with cDMEM only (no cells). The non-backflushed control filter was used to assess the filters after loading in order to observe the differences in the filter and the cells trapped within it pre and post backflush. Once the filters were prepared they were fixed overnight in 2% w/v PFA and 1% glutaraldehyde in 0.1M sodium cacodylate buffer (pH 7.3) at 21°C. The cells were then sent to the Department of Biosciences where they were fractured and imaged. The filters were freeze fractured in such a way as to present a cross-sectional surface showing the entire depth of the filter.

Figure 4.7 shows a cross sectional view of the filter. The filter is comprised of 4 individual layers of cell capture filter material which are laminated together to form the

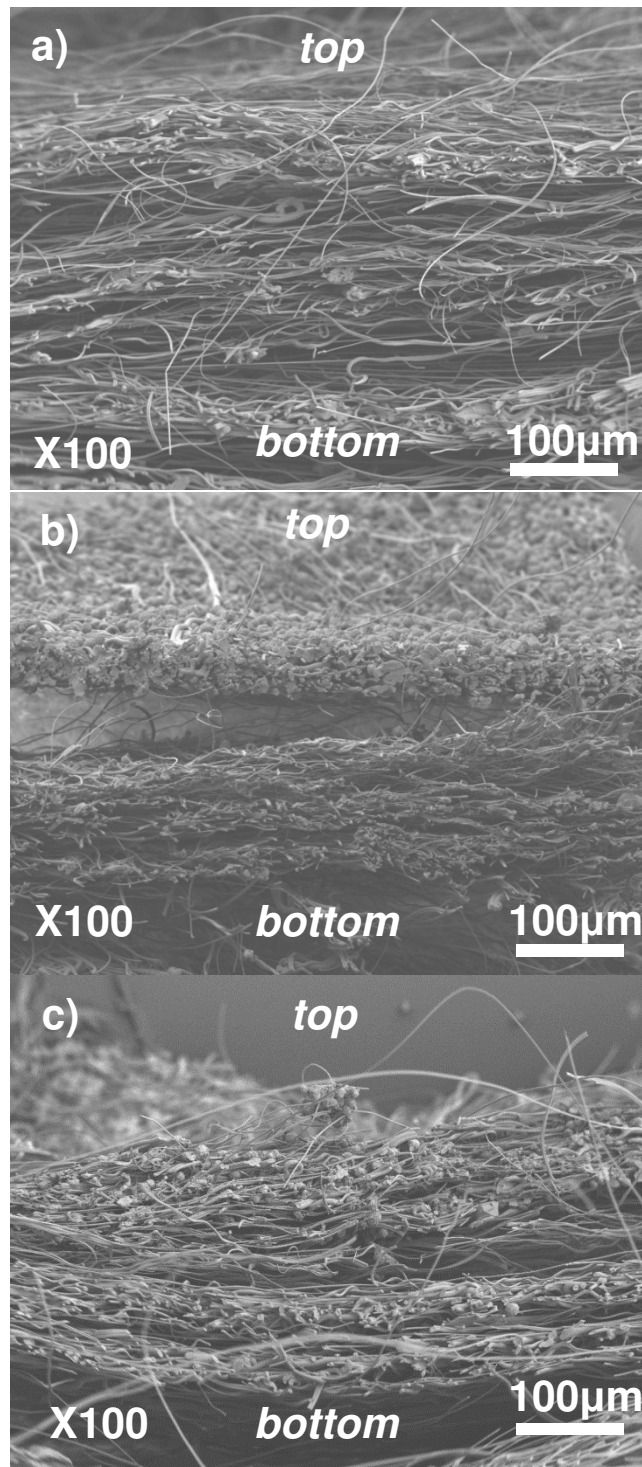


Figure 4.7 – Scanning electron microscopy of filter cross sections.

The fixing process has undone the lamination process revealing the four distinct filter layers. A control filter (a) which had been processed using CDMEM only (no cells), a processed filter pre backflush (b) and a processed filter post backflush (c) were imaged. The processed filters were loaded with 10×10^6 HCA2 cells at 150 LMH and backflushed at 45,000 LMH with 62.5 Lm^{-2} of elution buffer.

filter. The filter was loaded top to bottom (as indicated on image 'b') and the first thing to notice is that the majority of the cells seem to reside within the top layer and the other layers appear to be clear of cells. The top layer appears tightly packed with cells, whereas there does not appear to be any cells in the bottom 3 layers indicating that the cells do not permeate deep into the filter. Even after the backflush (image C), cells appear to be tightly packed into the top section of the filter. This can be seen again in Figure 4.8 with a view of the surface of the filter.

Figure 4.8 shows the surface of the filter post backflush. Image 'a' is a control which has been processed using cDMEM only and has therefore not come into contact with cells. Image 'b' has been loaded with cells under the conditions already described but has not been backflushed. Image 'b' again shows a large number of cells packed into the top layer of the filter, visible just below the surface of the filter. There are also a population of HCA2 cells in the top left corner of the image (image 'b') which appear to be slightly raised up from the other HCA2 cells. Whereas the majority of HCA2 cells seem to be residing just below the surface, these cells appear to rest on top of the filter surface. Image 'c' shows that following the backflush the sub-population of HCA2 cells that appeared to be raised up and residing on top of the other HCA2 cells are no longer visible. The cells appear to be more uniform in terms of depth and seem to all reside below the filter surface. It could be that the raised sub-population of HCA2 cells

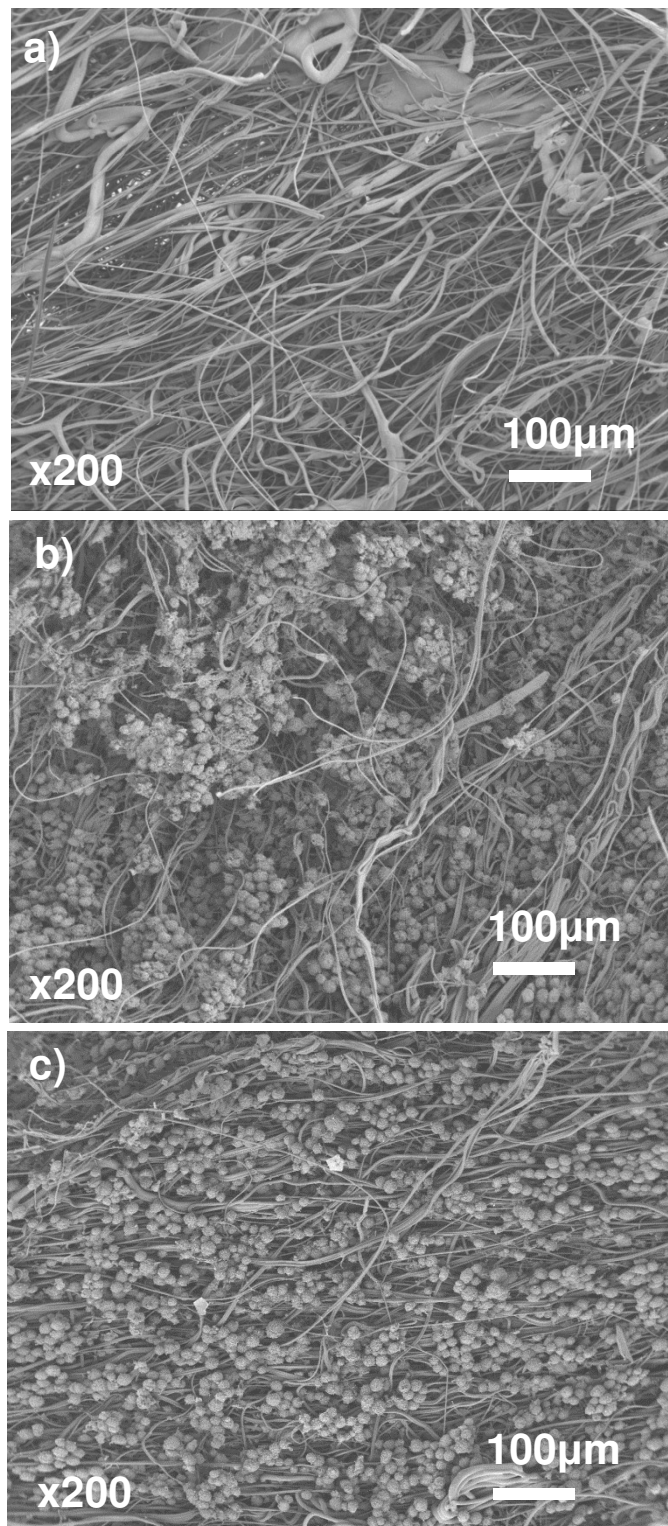


Figure 4.8 - Scanning electron microscopy of filter surface.

The control filter (a) has not come into contact with cells, the processed filters are shown pre (b) and post (c) backflush. The processed filters were loaded with 10×10^6 HCA2 cells at 150 LMH and backflushed at 45,000 LMH with 5 mL of elution buffer.

seen in image 'b' have been recovered in the backflush. It was hypothesised that these cells were the 'surface' cells discussed previously (section 3.2.4).

Figure 4.9 shows the reasons why the cells trapped within the filter are difficult to recover. Image 'a' shows the surface of the filter, whereas image 'b' shows a cross section of the filter. The cells which enter the filter appear to project cellular protrusions which wrap around the individual filter fibres. The cells become entangled within the filter matrix making them difficult to dislodge and recover during backflushing.

4.2. Impact of processing on the quality of recovered cells

Previous results have shown that the viability of the recovered cells as determined by membrane integrity is high. However it is possible for a cell to be damaged or stressed whilst still having an intact membrane. When cells are stressed they can enter apoptosis which is a phase of programmed cell death. Despite the fact that these cells have been damaged by the processing conditions and are dying, the cell membrane does not lose its integrity, therefore basic tests such as trypan blue or propidium iodide would recognise these cells as viable.

A cell death assay was used to look more closely at the effects of processing conditions on the remaining cells i.e. those that are not fragmented. The cell death assay (section 2.6.5) classifies apoptotic cells based on caspase activity within the cell.

Figure 4.10 shows the levels of apoptosis caused by processing of the cells. The results showed that, on average, the filtration process caused a significant reduction ($p = 0.065$) in the proportion of viable cells compared to the unprocessed control. The drop in the proportion of viable cells post processing was due to an increase in the proportion of late apoptotic and necrotic cells following filtration. However it was interesting to note that the proportion of early apoptotic cells actually decreased post processing.

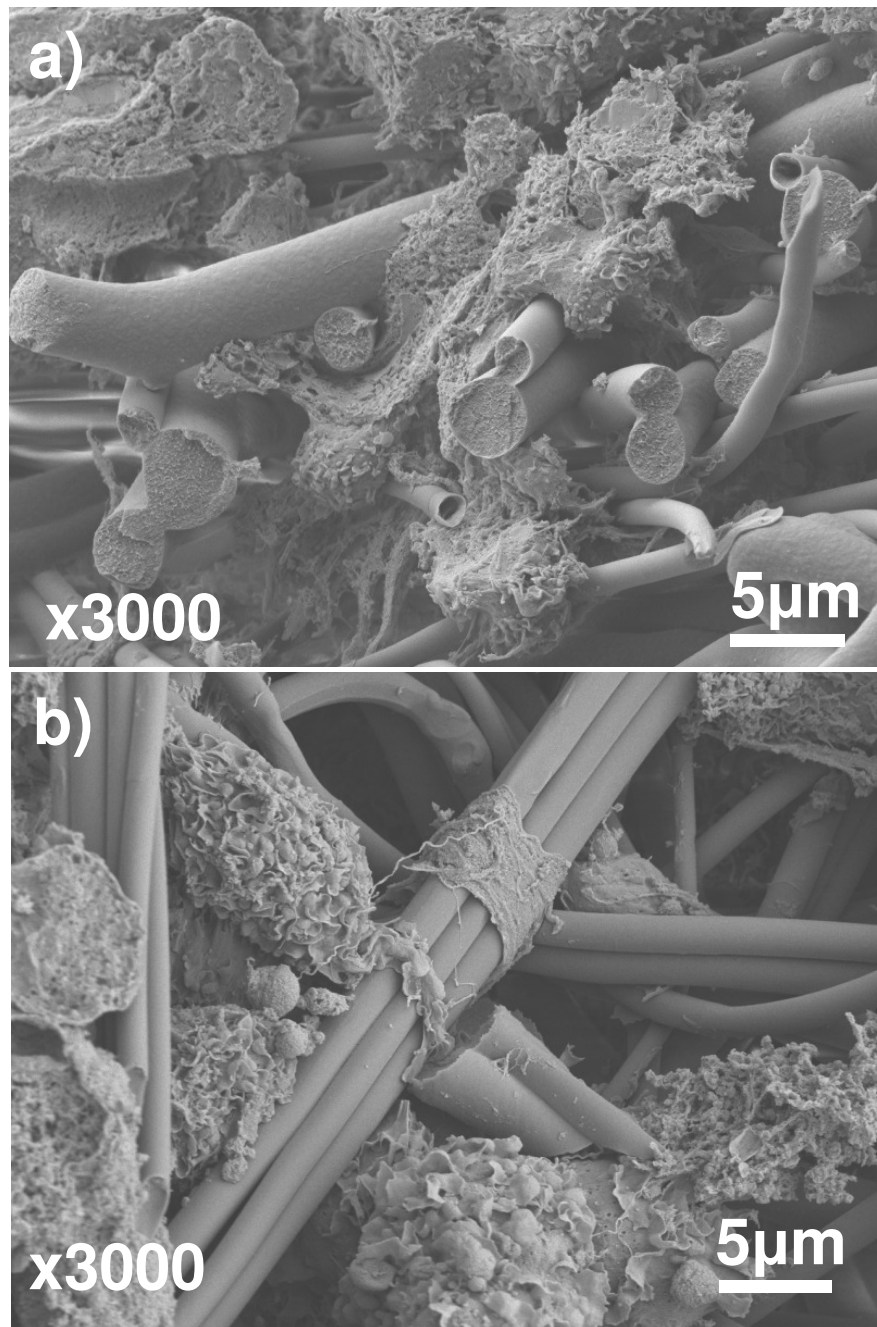


Figure 4.9 – Cellular interaction with filter fibres.

Image shows how the cells interact with the filter both at the surface (a) as well as within the filter matrix (b). The HCA2 cells project protrusions which wrap around the individual filter fibres making them difficult to recover.

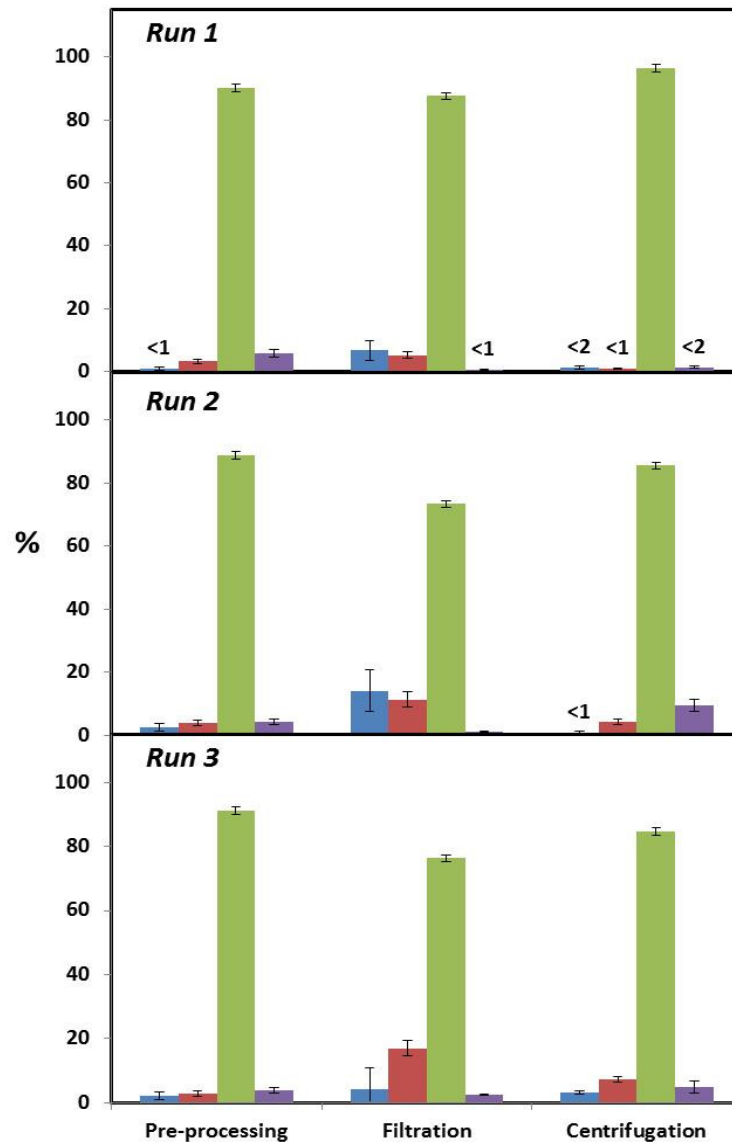


Figure 4.10 – Cell death caspase assay results for the effect of processing on the quality of recovered cells.

Cell death assay results showing the proportion of necrotic (■), late apoptotic (■), viable (■) and early apoptotic (■) HCA2 cells post processing. Filtered cells were loaded at a concentration of 2×10^6 cells mL^{-1} at a controlled flow rate of 150 LMH. Cells were then recovered by backflushing the filters with 10 mL of elution buffer at 45,000 LMH. Centrifuged cells were spun at 800 x g for 5 minutes and resuspended in 10 mL of elution buffer. Results were compared to an unprocessed bench top control. Results show the mean average values ± 1 sd from three separate runs each measured once ($z=3$, $n=1$). Error bars are ± 1 sd and are derived from typical standard deviations for previous runs using the same method. 124

This is most likely due to the cells which were already in an early state of apoptosis pre-processing progressing to late apoptosis or even necrosis following filtration.

On average over the three runs, the cell death assay results also indicated a significant decrease in the proportion of viable cells within the cells recovered using filtration in comparison to those recovered via centrifugation.

As a proof of concept experiment the filtration device was used to process a population of CTX0E03 cells. CTX0E03 are a multipotent neuronal stem cell known to be more susceptible to stress during processing (private communication). However although the results did show an increase in the proportion of necrotic cells post processing, the proportion of viable cells post processing was higher than both the pre-processing control and the HCA2 filtration. This was most likely due to apoptotic cells being pushed toward necrosis by the processing and necrotic cells breaking down during processing (Figure 4.11). It is however important to note that due to the complex culture protocols and the slow growth rates of the CTX0E03 cells, it was only possible to do a single filtration, meaning it is difficult to draw any significant conclusions. The proportion of CTX0E03 cells recovered was the same as the recovery observed with the HCA2 cells (both at 19%).

The centrifugation process appeared to have less of an effect on the quality of the cells compared to the filtration process, however due to the lack of reproducibility with the results it was difficult to make any firm conclusions.

Scanning electron microscopy has previously been used to image cells which remained unrecovered following the backflush; the imaging helped to understand the reasons why some of the cells could not be recovered. The same technique was used to image individual cells post processing in order to look at the extent of the damage caused by the filtration.

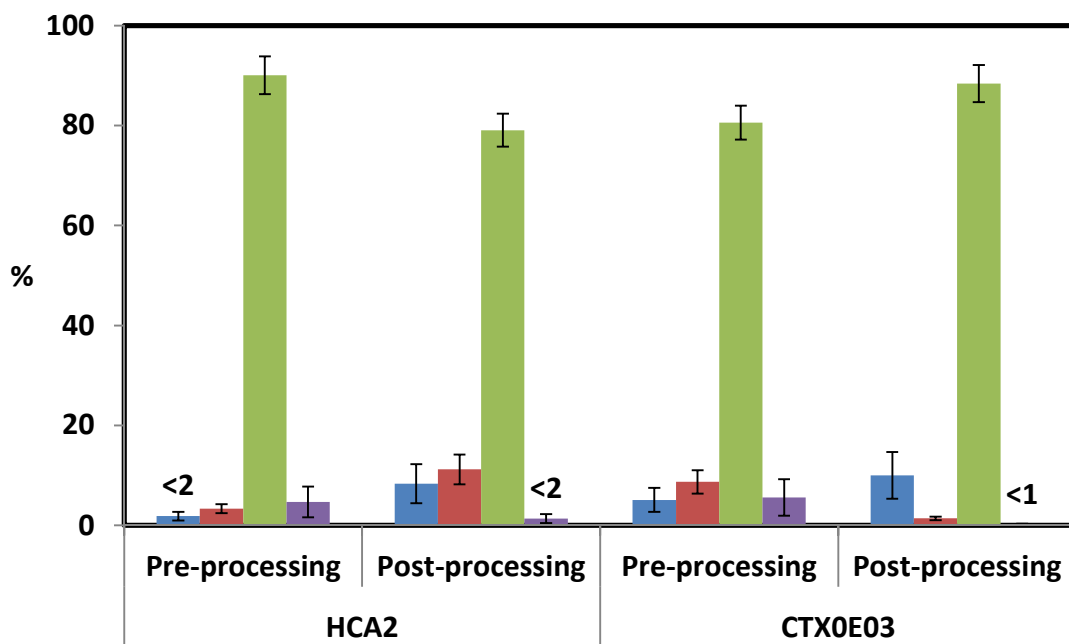


Figure 4.11 - Cell death caspase assay results for the effect of processing on HCA2 and CTX0E03 cells

Cell death assay results showing the proportion of necrotic (■), late apoptotic (■), viable (■) and early apoptotic (■) cells post processing. Cells were loaded at a concentration of 2×10^6 cells mL^{-1} at a controlled flow rate of 150 LMH. Cells were then recovered by backflushing the filters with 10 mL of elution buffer at 45,000 LMH. Results are from a single filtration run with each cell type measured once ($z=1$, $n=1$). Error bars are ± 1 sd and are derived from typical standard deviations for previous runs using the same method.

The cells were processed as described in Figure 4.11 and a control was set up using unprocessed cells. The cells were centrifuged at 500 x g for 3 minutes and the elution buffer was removed, before the cells were gently resuspended in the fixative (2% w/v PFA and 1% glutaraldehyde in 0.1M sodium cacodylate buffer).

Figure 4.12 shows both (a) the unprocessed cells and (b) the processed cells. Image 'a' shows a number of large rounded cells with a small amount of debris. However the processed cells show a substantial amount of debris indicating that the filtration and elution have caused some cells to rupture and breakdown into cell debris.

The possibility that these images showed blebbing of the cells as opposed to cell debris was considered. It has been shown that when cells are exposed to damaging levels of shear stress, protrusions through the cell membrane known as blebbing can occur (Elmore, 2007). Blebbing is a characteristic of the apoptosis pathway in cells and is a key indicator of cell damage. Throughout the research light microscopy imaging showed no signs of 'blebby' cells, therefore it was decided that the images showed an increased level of cell debris post processing as opposed to cell blebbing.

4.2.1. Continuous culture of processed cells

The ability of processed cells to continue to grow and proliferate following filtration is a good measure of the level of stress and damage inflicted on the cells during processing. During cell growth, the growth might be expected to follow a first order relationship:

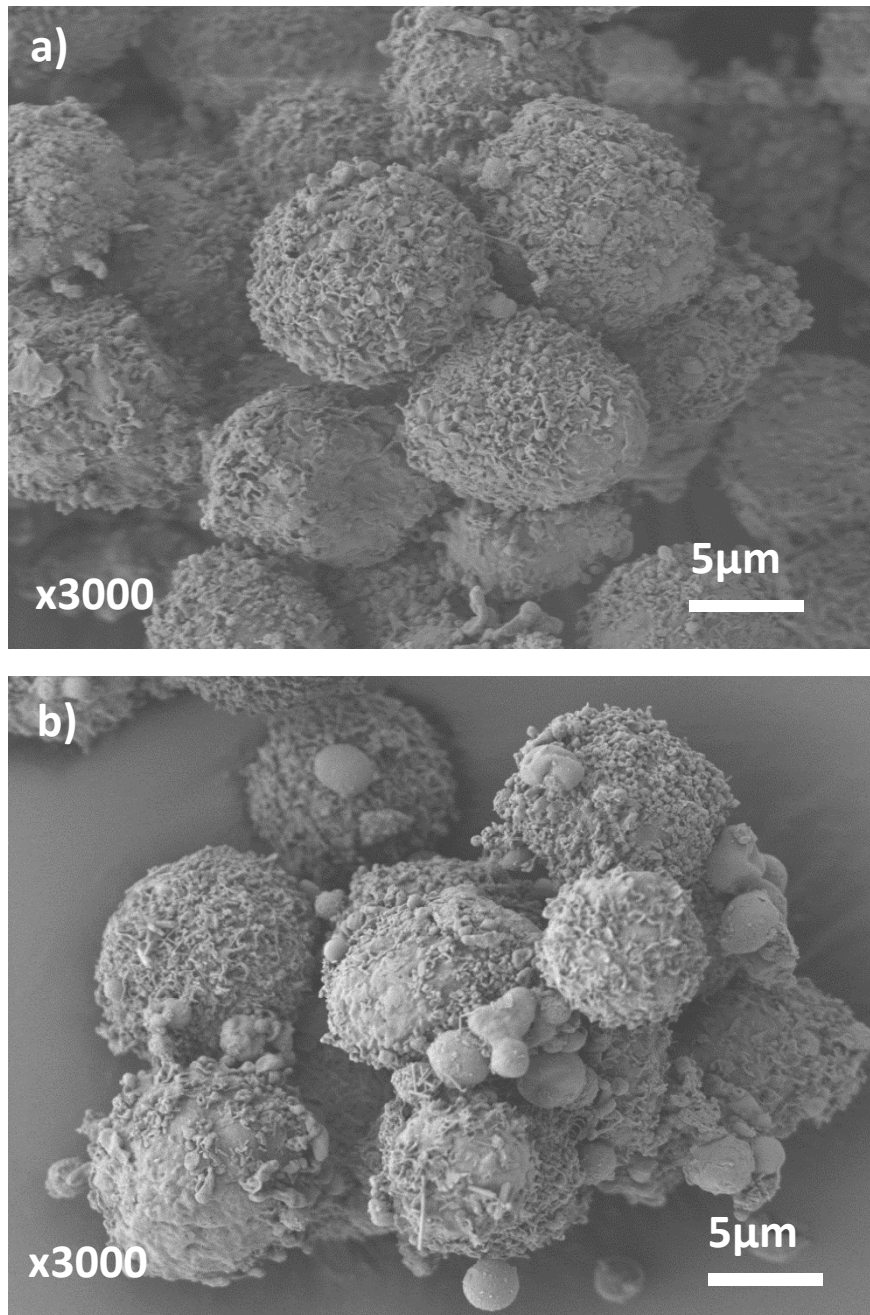


Figure 4.12 – Effect of processing on the quality of recovered cells

Scanning electron microscopy images of HCA2 cells pre and post processing. The processed cells (b) were loaded at 150 LMH and backflushed at 45,000 LMH with 62.5 Lm^{-2} of elution buffer. The unprocessed cells (a) were kept on the bench for the duration of the experiment. Both populations of cells were then centrifuged at $500 \times g$ for 3 minutes and resuspended in fixative before imaging.

$$\frac{dN_{vc}(t)}{dt} = kN_{vc}(t)$$

Equation 4.1

where $N_{vc}(t)$ is the number of viable cells at time t and k is the specific growth constant (h^{-1}). Integrating between the limits of $N_{vc}(t_1)$, which is the number of viable cells at t_1 and t_2 gives:

$$k = \frac{2.303}{t_2 - t_1} \times \log_{10} \left(\frac{N_{vc}(t_2)}{N_{vc}(t_1)} \right)$$

Figure 4.13 shows the growth curves for each of the three runs and the control. It also compares the specific growth constants of the four runs. Results show that there was up to a 38% decline in cell numbers over the initial 24 hours after seeding for the three processed runs in comparison to the control. This could be due to stresses induced by the processing causing cells to enter an apoptotic phase. The counts were done by trypan blue exclusion and so if a cell was dying but still had an intact membrane it would still be counted as a viable cell. The surviving cells after 24 hours gave similar specific growth rate constants for processed and unprocessed cells.

4.2.2. Effects of process hold times

One of the main complications which is often overlooked when scaling up laboratory scale experiments to full scale manufacturing is the length of time cells can be held during processing. In the laboratory there is often a rapid progression from cell harvest to cell processing to final analysis. At larger scales the time taken to harvest and process adherent cells often results in batches of cells being held in vessels for long periods (e.g.

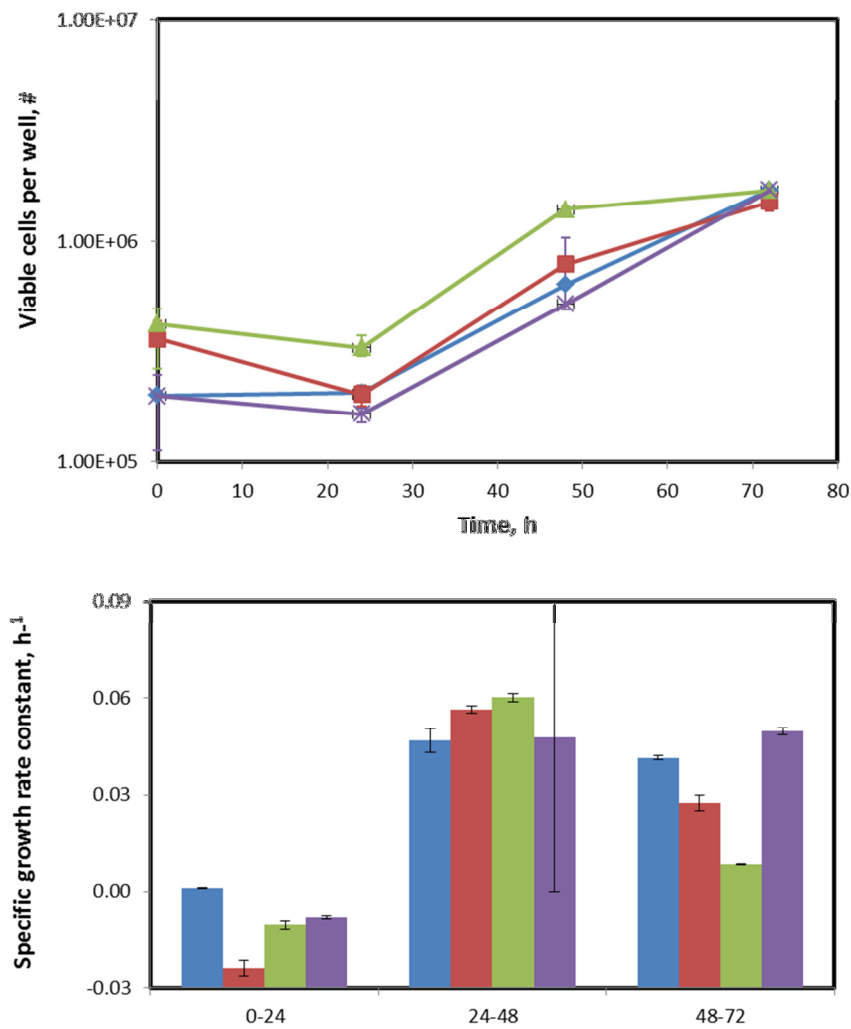


Figure 4.13 –Growth curves and specific growth constants for processed HCA2 cells.

Results show the growth curves and the specific growth constants for the unprocessed control (■), as well as the three processed samples (run 1 (■), run 2 (■) and run 3 (■)). 5mL of HCA2 cells at a concentration of 2×10^6 cells mL^{-1} were loaded at a rate of 150 LMH. The cells were recovered by backflushing the filters with 5mL of elution buffer at a flow rate of 45,000 LMH. Following filtration the cells were gently spun down at 500 x g for 3 minutes and resuspended in cDMEM. 3×10^4 cells cm^{-2} viable cells were loaded into each well of a 6 well plate. Cells were cultured for 72 hours with light microscopy images and cell counts were taken every 24 hours. A control unprocessed population of cells which were harvested and left on the bench for the duration of the experiment were also seeded in the same manner. The results showed that the processing caused a drop in the number of viable cells over the first 24 hours. Data shows the mean average \pm the range from three separate filtration runs each measured in triplicate ($z=3$, $n=3$).

up to 6 hours; private communication). It is important to understand the effect of processing cells which have been held for a period of time on the cell quality.

A population of HCA2 cells was harvested 24 hours prior to processing. The cells were then held in cDMEM for 24 hours at 21°C. A 24 hour hold period was selected in order to investigate the effect of holding the cells in the most extreme of circumstances; it is unlikely that cells would be held for this length of time during large scale manufacturing.

Figure 4.14 shows the effect of the 24 hour hold on both the quality and the recovery of the cells. The results show that there is a significant drop (p value = 0.0036) in the proportion of viable cells recovered following a 24 hour hold period in comparison to the control. The viability measurement was carried out using trypan blue exclusion to determine membrane integrity. The mean viability of the 'fresh cells' $97\% \pm 3\%$ in comparison to $81\% \pm 3\%$ for the cells which had been held prior to processing.

Caspase analysis of recovered cells showed that there was no significant difference in the level of apoptosis in the control population compared to the 'held' cells. There was only a very small population of early apoptotic cells in both the held and fresh cells ($<2\%$). The proportion of cells which were deemed late apoptotic (stained positive for both PI and FLICA, see section 2.6.5) was also significantly higher ($p = 0.0257$), however there was no significant difference between the fresh and held cells.

The main differences highlighted by the cell death caspase assay were the necrotic and viable cell populations. This was expected as cells which are deemed non-viable (or necrotic) by trypan blue exclusion are likely to also stain positive for PI and therefore be classed as necrotic.

One other interesting result was that the total cell recovery was higher for the cells which had been held ($32\% \pm 5\%$ compared with $19\% \pm 4\%$ ($n=3$)). Scanning electron

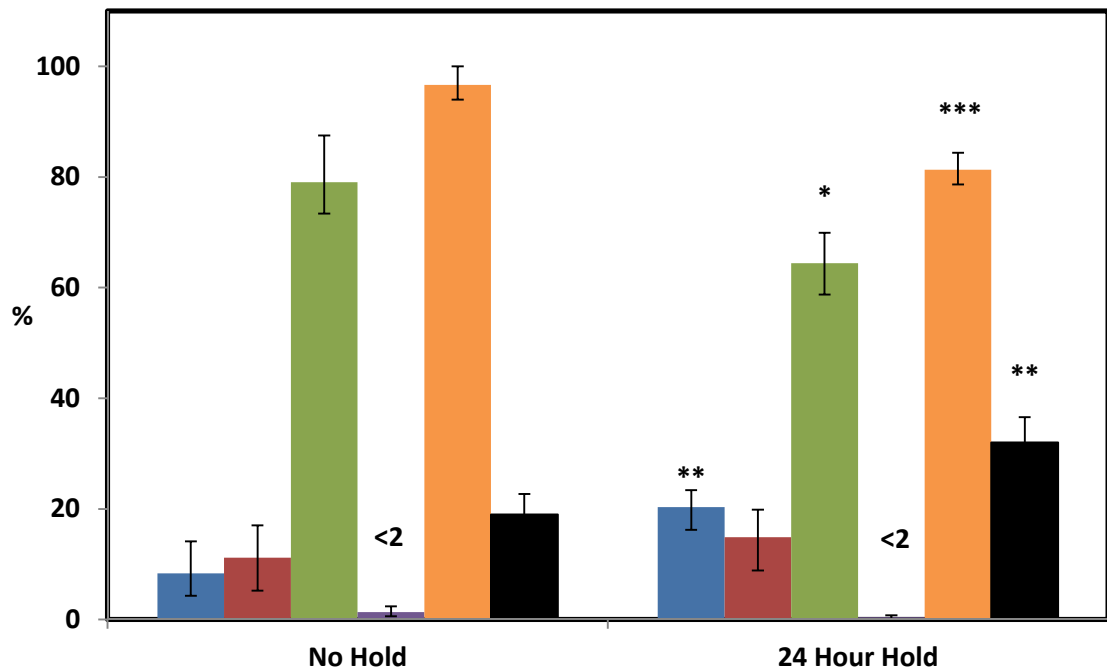


Figure 4.14 – Effect of a 24 hour hold time on the quality of recovered HCA2 cells.

Cell death assay results showing the quality of recovered cells following a 24 hour hold. Figure show the proportion of necrotic (■), late apoptotic (■), viable (■) and early apoptotic (■) cells. The % viability (■) and total cell recovery (■) is also shown. 5mL of HCA2 cells at a concentration of 2×10^6 cells mL^{-1} were loaded at a rate of 150 LMH. The cells were recovered by backflushing the filters with 5mL of elution buffer at a flow rate of 45,000 LMH. A control was set up using a population of freshly harvested HCA2 cells processed in the same way. Data shows the mean average \pm 1sd from three separate filtrations each measured once ($z=3$, $n=1$).

microscopy has already shown that cells lodged within the filter put out structures which wrap around the filter fibres making recovery difficult (section 4.1.4). The higher recoveries achieved using the cells which had been held, could be explained by the higher proportion of necrotic cells within this population. Necrotic cells will be unable to put out such structures and effectively cling to the filter so may be easier to recover. If this is the case then this would indicate that the cells are already dead before they are backflushed meaning that it is either the loading or the time in the syringe that causes damage to the cells weakened by the hold time.

The reduced quality of the cells recovered post processing following a hold period could be an issue when producing commercial products. Necrotic cells produce cytotoxins and if large numbers of necrotic cells are injected into a patient it can cause an unwanted immune response. However as previously mentioned 24 hours is an extreme hold time and in reality the hold time is likely to be no more than a few hours which may or may not have a less significant impact on the cell quality (see Chapter 6: Future Work). Still it is important that hold times are carefully controlled during processing to ensure the quality of the cells is not affected. Hold times throughout this research were kept to a minimum however when a large number of filtrations were carried out in a single session, cells were held for up to 6 hours. The order in which experiments were carried out was changed for every repeat to ensure the length of time that the cells were held for did not affect the overall result.

4.2.1. Removal of protein during processing

As well as recovering a large proportion of good quality cells, it is also important that the filtration process removes protein which exists in the form of the FCS used in the culture media during cell expansion. Whilst essential for the growth of the cells it is

usual to reduce FCS levels before cells are administered to a patient in order maintain a “known” process with which the manufacturer knows exactly what constitutes the final product.

The filters were set up as previously described and loaded with 5 mL of cell suspension at a concentration of 2×10^6 cells mL^{-1} . A BCA total protein assay was used to analyse the amount of protein in the recovered cell samples and compare them to a sample of cells taken immediately prior to loading in order to assess the amount of protein removed. Figure 4.15 shows that the filtration process removes a significant proportion of the protein present in the cell suspension pre-processing ($p=0.065$). On average the process removed around $92\% \pm 3\%$ of the total protein. The protein removed per cells recovered is $\sim 70\%$ when accounting for cell loss. The results in terms of the proportion of protein removed were consistent across the three runs however there was variation in the protein concentration of the cellular suspensions prior to processing. This is important to note when looking to reduce protein concentration below a certain level, as the proportion of protein removed is fairly constant. This means that cellular suspensions which have a higher protein concentration pre-processing, are likely to have greater levels of protein post-processing than cell suspensions which had a lower concentration of protein to begin with. The upstream processing and cell culture would need to be further investigated and tightly controlled to ensure a more predictable protein concentration.

One means for increasing the amount of protein removed is to add a forward wash step. Increasing volumes of wash buffer were used to look at whether increasing the volume of wash buffer increased the amount of protein which was removed.

Figure 4.15 shows that washing the filter prior to the backflush step further decreased the amount of protein remaining post processing. In all three of the filtration runs

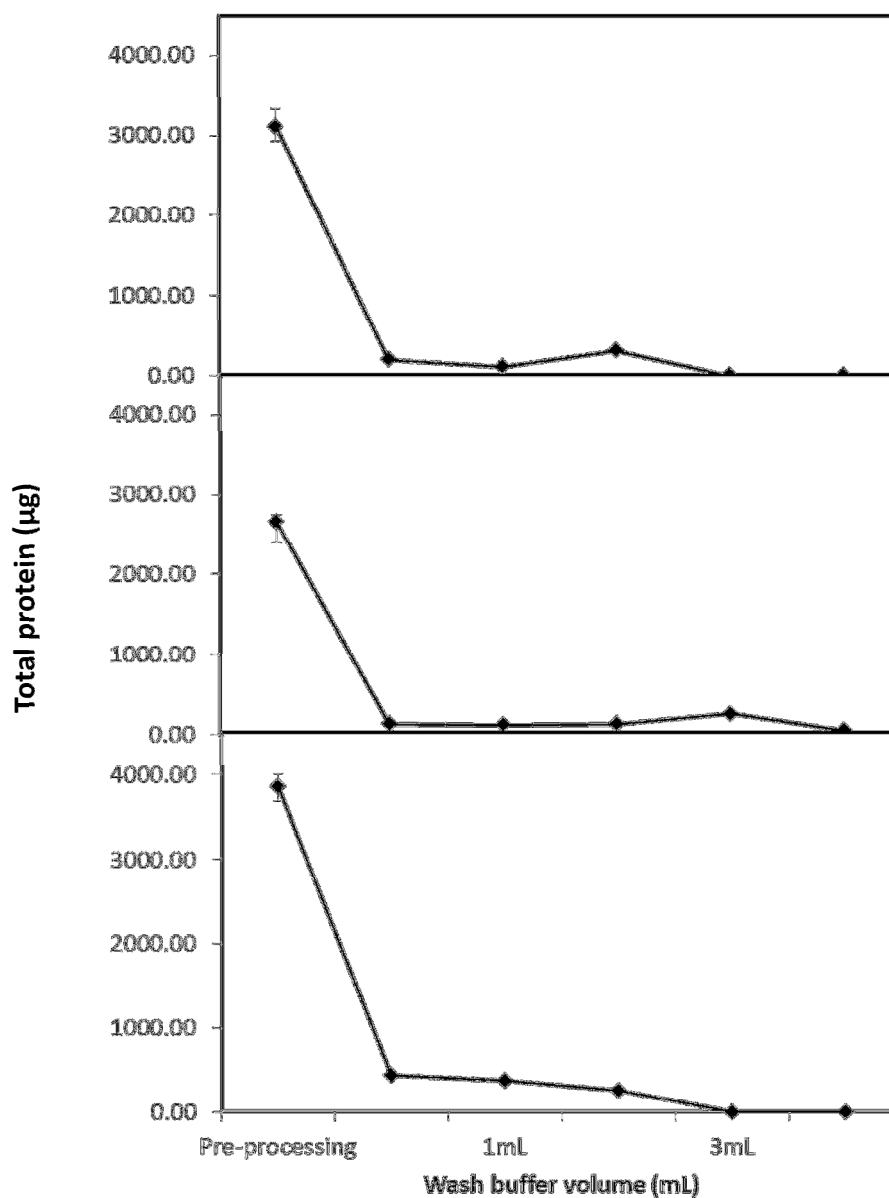


Figure 4.15 – Effect of a pre-backflush forward wash step on protein removal. 5 mL of HCA2 cell suspension at a concentration of 2×10^6 cells mL^{-1} . Cells were loaded at a constant flow rate of 150 LMH and recovered via backflushing with elution buffer at 45,000 LMH. Prior to the backflush the HCA2 cells on the filter were gently forward washed at 150 LMH with increasing volumes of DPBS. A BCA total protein assay was used to analyse the amount of protein in the recovered cell samples. Results show the mean average \pm the range from three separate filtration runs ($z=3$, $n=3$).

shown, a 5 mL wash step led to a 99% removal of total protein. Run 3 shows a continuing decrease in protein levels with increasing wash buffer volume, however on average there did not appear to be any significant increase of protein removal with increasing volumes of wash buffer.

The amount of protein remaining following processing without a wash step may have been so small that the assay was not sensitive enough to measure any changes in it; this would explain why the effect was more noticeable in run 3 as the initial amount of protein present was significantly higher than in the first two filtration runs.

Figure 4.16 show that overall the performance of the two methods was very comparable (although the lack of reproducibility between the filtration runs did make it difficult to draw any firm conclusions). However on average, by adding the wash step during the filtration step a significantly higher level of protein removal was achieved (p-value = 0.00080). It was interesting to note that the amount of protein removed by the centrifugation process decreased with the addition of a 5 mL wash step in all three runs. It was not fully understood why this was. It is also important to note however that on average the proportion of cells (and hence the number of cells) recovered was significantly higher using centrifugation compared to filtration ($94\% \pm 6\%$ compared to $16\% \pm 3\%$).

Figure 4.17 shows that including a wash step did not have a significant impact on the total cell recovery. Increasing the volume of the backflush step also had no significant impact on the yield.

A number of analytical techniques were carried out to assess the impact of the prolonged wash step on the overall quality of the recovered cells. Initial indications showed that the wash step had no impact on the viability of the cells in terms of the membrane integrity and the cells' ability to exclude trypan blue.

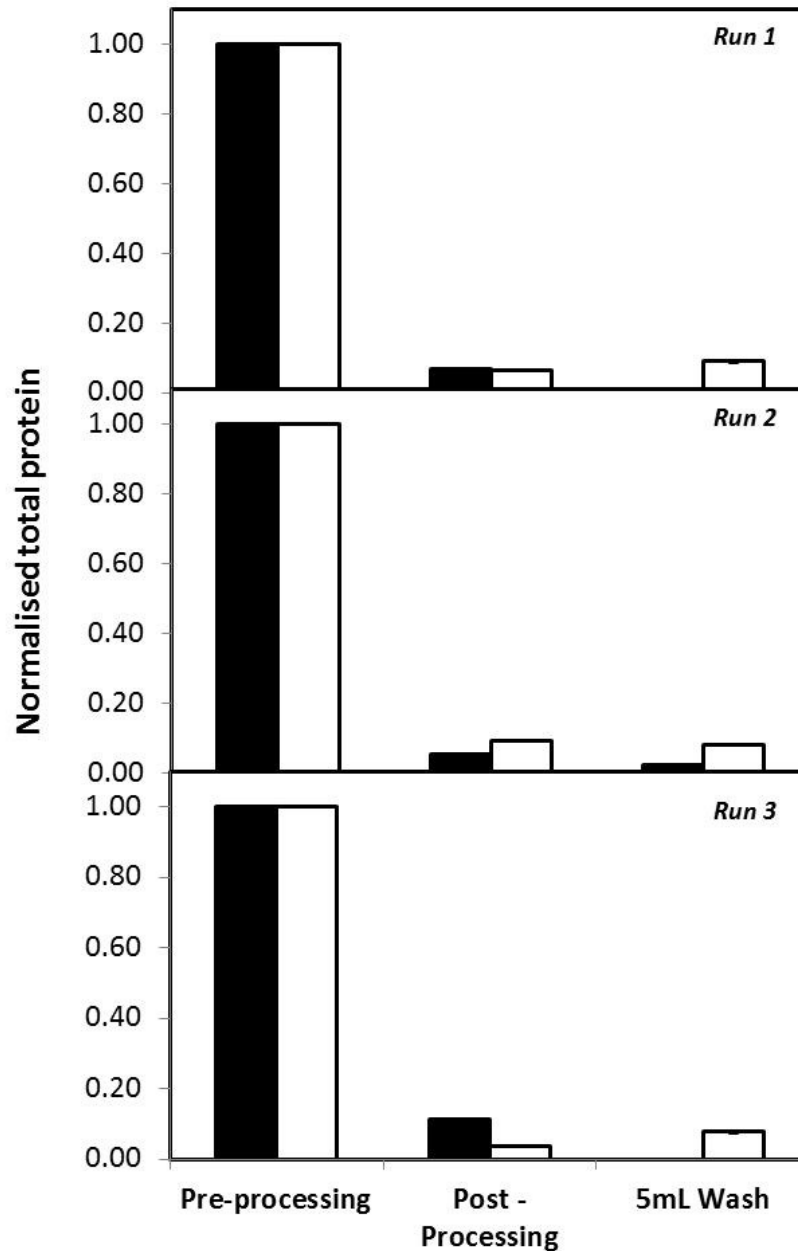


Figure 4.16 – Protein removal: filtration vs centrifugation.

Comparison of protein removal for filtration (■) and centrifugation (□). Filtration was carried out as described in Figure 4.15. For centrifugation experiments 5 mL of HCA2 cell suspension at a concentration of 2×10^6 cells mL^{-1} was centrifuged at $800 \times g$ for 5 mins and then resuspended in 5mL of the elution buffer. Cells were washed by removing the supernatant following the first spin, then resuspending in 5mL of PBS before centrifuging for a further 5 mins at $800g$ and resuspending in the elution buffer. Results show the mean average \pm the range from three separate filtrations ($z=3$, $n=3$).

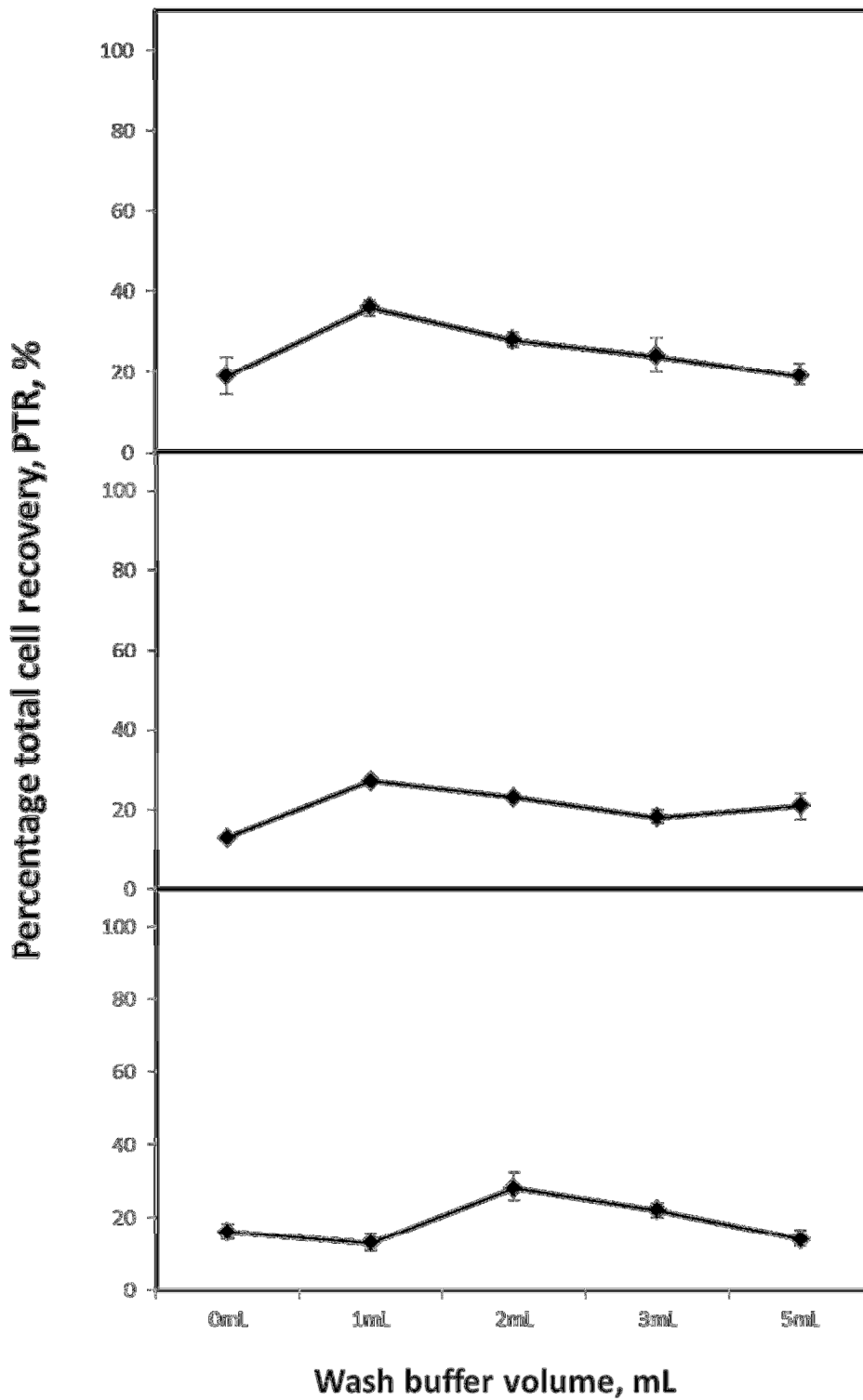


Figure 4.17 – Effect of wash buffer volume on total cell recovery

Filtration was carried out as described in Figure 4.15. Data shows the mean average \pm the range from three separate filtrations ($z=3$, $n=3$).

As well as chemical changes within the cells, stress caused during processing can impact the cells morphology. Changes in cell shape can be a sign of necrosis or apoptosis and so a MatLab script was developed in-house to re-analyse the images taken by the ViCell XR in order to categorise cells based on their morphology.

Image analysis of the processed cells also showed little change in the morphology of the cells pre to post processing or with an extensive wash step (Figure 4.18). Hydrodynamic shear can cause the cells to become elongated or blebby which is a sign of damage. However it appears that the forward wash step does not affect the morphology of the cells.

Cell death analysis using the CaspaTag™ Pan-Caspase *in situ* assay kit was used to see whether or not the increased wash step caused some cells to become apoptotic. Figure 4.19 results indicate a decrease in the proportion of viable recovered cells post processing (no wash), which can be seen in all three runs (more so in runs 2 and 3) and a more significant decrease post processing with a 5mL forward wash (runs 1 and 3).

On average the results also showed that there is a possible decrease in the proportion of viable cells with increased 'forward wash' buffer volume. However this is of low statistical significance ($p = 0.11$).

The proportion of cells which are early apoptotic show a potential decrease following processing and with increasing wash buffer volumes. This could be due to the shear exerted during processing pushing them further towards necrosis. It also means that any viable cells affected during processing are pushed rapidly towards late apoptosis and ultimately necrosis.

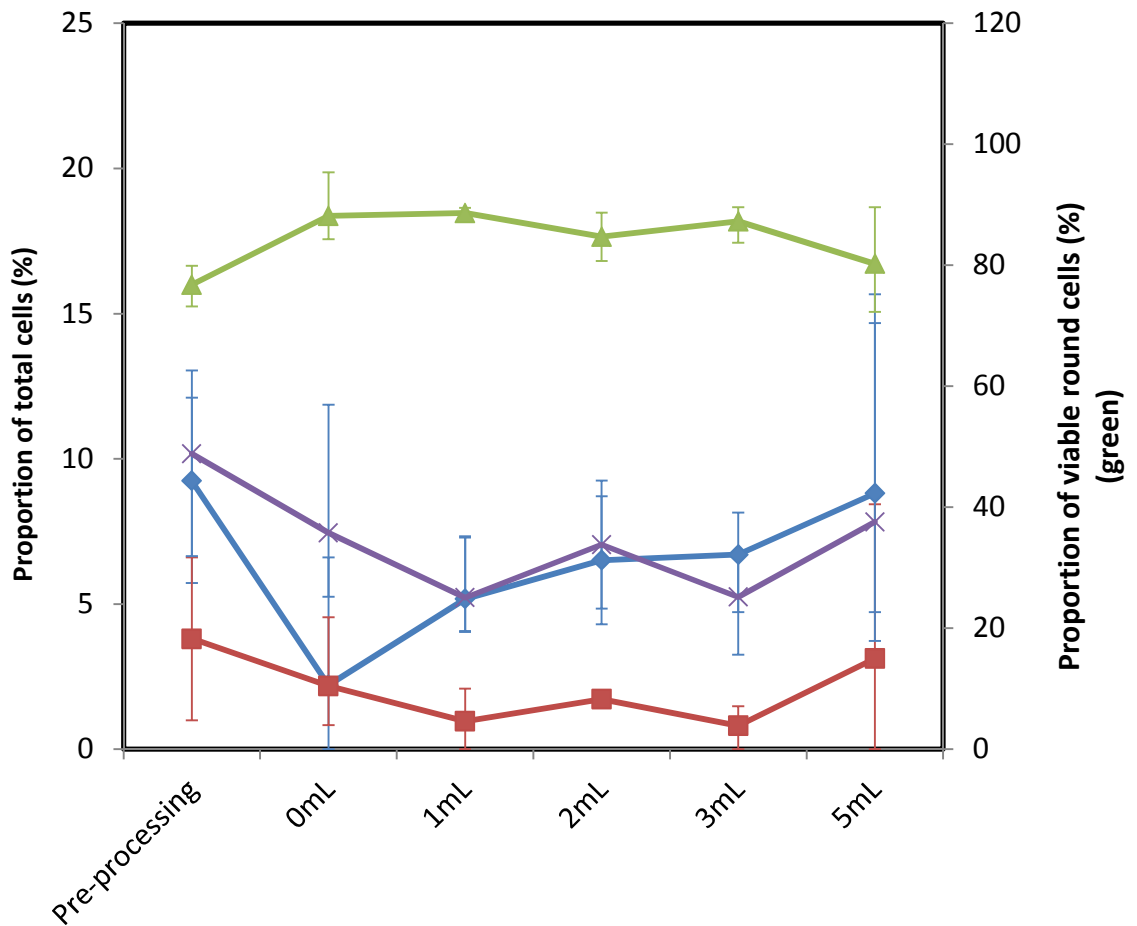


Figure 4.18 –Effect of a forward wash step on cell morphology

Categorisation of recovered cells based on cell morphology. A MatLab script was used to reanalyse ViCell images and classify HCA2 cells as either short elongated (■), long elongated (■), viable round (■) or non-viable (■). Filtration was carried out as described in Figure 4.15. Washing the cells prior to recovery did not have a significant effect on cell morphology. Data shows the mean average \pm the range from three separate filtrations measured once ($z=3$, $n=2$).

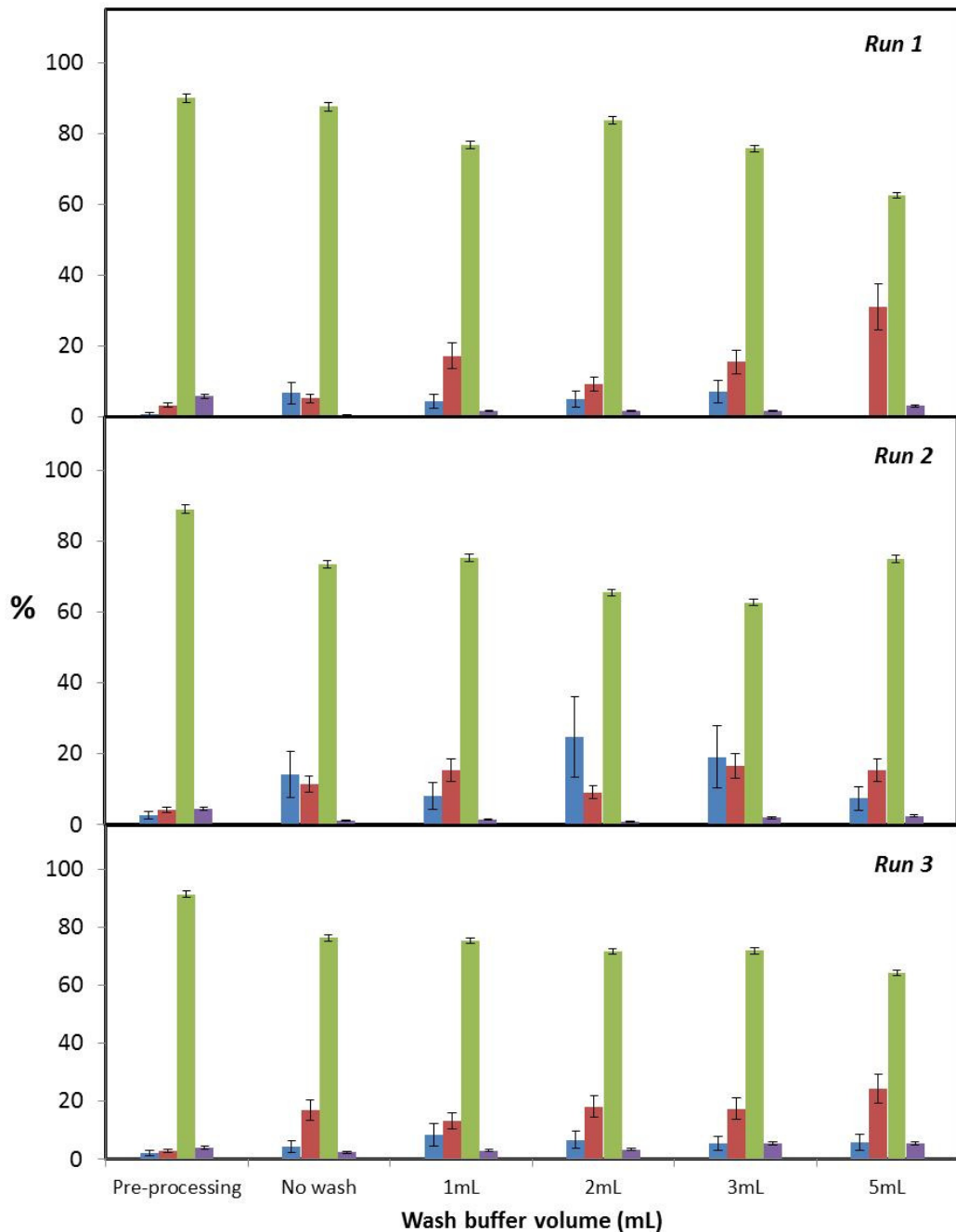


Figure 4.19 – Effect of forward washing on the quality of recovered cells

Cell death assay was used to identify necrotic (■), late apoptotic (■), viable (■) and early apoptotic (■) HCA2 cells. Filtration was carried out as described in Figure 4.15. Washing the cells prior to recovery did not have a significant effect on cell morphology. Data shows the mean average \pm 1sd from three separate filtration runs each measured once ($z=3$, $n=1$). Error bars are \pm 1sd and are derived from typical standard deviations for previous runs using the same method.

4.1. Chapter Discussion

In Chapter 3 a model was proposed for the primary recovery of cells using ultra scale-down filtration. The model is based on the presence of two distinct populations of cells post loading; “surface” cells which reside on the filter surface and are almost entirely recoverable and “filtered” cells which enter the filter matrix and are difficult to recover. Unless the number of cells loaded onto the filter is low ($<1 \times 10^6$ cells) then the majority of the cells enter the filter (“filtered” cells) and the recovery is low.

Scanning electron microscopy in this chapter (section 4.1.4) provided further evidence to support this model. Figure 4.8 appeared to show a population of cells which reside on the surface of the filter following loading but were no longer present post backflush. It was hypothesised that these were the “surface” cells described in chapter 3.

The first half of this chapter aimed to identify the mechanisms behind this model and explain why the cells which enter the filter are difficult to recover. A key part of building this understanding was to identify where the cells were becoming trapped and to understand why cells which enter the filter (“filtered” cells) are so difficult to recover.

Lactate dehydrogenase (LDH) was used to try and account for the number of cells not recovered after filtration in order to fully balance the process. Results showed that the majority of cells found were in the backflush ($\approx 18\%$) and the filter ($\approx 23\%$) with a small amount passing through into the permeate ($\approx 5\%$). However a large proportion of the cells ($\approx 54\%$) were not accounted for. It was hypothesised that the remaining cells were trapped in the filter and the filter was preventing the LDH being fully accounted for by somehow protecting entrapped cells from further LDH release.

Although the LDH was not able to fully account for the cells in the filter, it did confirm that some of the cells still resided there following the backflush. This was further

substantiated by fluorescent microscopy of cross sections of the filter. Cryosectioning was used to produce 25 μm thick cross sections of the filter. DAPI staining revealed a large number of cells trapped within the filter following the recovery.

It was not possible to quantify the number of cells trapped in the filter or to fully account for all of the cells in the system. This meant that despite evidence to suggest that the unrecovered cells were residing in the filter, it was not possible to prove that some cells were not being lost elsewhere, such as in the tubes and connections which made up the device.

Despite not being able to quantify the number of cells trapped within the filter post recovery, scanning electron microscopy of the cells residing within the filter did help to explain some of the mechanisms which cause them to become trapped. Figure 4.9 showed that the cells trapped within the filter had put out cellular protrusions which wrap around the individual filter fibres, entangling the cells within the filter matrix and making them difficult to recover.

The second half of the chapter looked at the quality of the cells recovered by the filtration process. A caspase assay was used to analyse the levels of apoptosis caused by filtering the cells. Figure 4.10 showed that the filtration process caused a significant reduction ($p = 0.065$) in the proportion of viable cells compared to the unprocessed control. The drop in the proportion of viable cells post processing was due to an increase in the proportion of early and late apoptotic cells following filtration. Results also appeared to show that filtering the cells was more damaging than centrifugation, however the lack of reproducibility made it difficult to draw any significant conclusions.

The damaging effect of processing on the cells was further demonstrated when the processed cells were cultured post filtration (Figure 4.13). Processed cells showed a

significant decline in the number of viable cells over the first 24 hours of culture. It was hypothesised that this was due to the filtration inducing apoptosis in the cells. The damaging effect of the filtration was exacerbated when cells were held in suspension for 24 hours prior to being processed. There was a significant drop in the viability of recovered cells which had been held for 24 hours pre-processing compared to the fresh cells. In large scale processing, cells are often held in suspension in large holding tanks for extended periods of time whilst other parts of the process are being carried out. This means that the increased levels of damage caused by the filtration for cells which have been held prior to processing could be a problem if the process was ever to be scaled-up. That being said, 24 hours is an extreme hold time and it may be that a hold time of only a few hours could have less of an impact on the quality of the cells.

As well as looking at the quality of the cells, it is also important to assess the overall quality of the suspension as it is this suspension of cells which could potentially be administered to patients as a whole cell therapeutic. As a primary recovery step it is desirable that the filtration not only recovers a large proportion of high quality cells, but also removes a significant amount of the protein present in the loaded cell suspension. On average the process removed approximately 90% of the total protein present (Figure 4.15), which increased to 99% with a 5 mL forward wash prior to backflushing the filter. The filtration process alone performed comparably with centrifugation in terms of protein removal, however when the wash step was used, the filtration process removed significantly more protein than centrifugation (Figure 4.16).

Results showed that the ultra scale-down filtration process does not recover a significant proportion of the cells and it is hypothesised that this is due to cells becoming trapped and entangled within the filter matrix, however it was not possible to quantify the number of cells trapped there. The cells which are recovered do show significant signs

of damage which is worsened if the cells are held in suspension for long periods of time prior to recovery. The process does however remove significant amounts of total protein and the protein removal improves when the cells are forward washed on the filter before they are recovered in the backflush.

Chapter 5: Improving the recovery and quality of an ultra scale-down depth filtration process

5. Maximising cell recovery

An ultra scale-down filtration tool has been developed which is capable of processing small volumes of human cell suspension. However the proportion of cells recovered from the filtration process is low and the quality is reduced. This chapter will discuss approaches to retain the advantages of a filtration whilst improving cell recovery. These approaches are based on the understanding gained in earlier chapters.

5.1. Membrane filtration

It was hypothesised that by using a membrane, cells would not be able to enter and entangle themselves within the fibres of the material making them easier to recover and improving the overall process yield. The membranes used were Pall ‘MMM’ asymmetric super-micron membranes with a 5µm diameter pore. The pore size was chosen based on conversations with experts at Pall Life Sciences and the work they had previously done in the area. These membranes have an asymmetric pore structure and are designed specifically to be low binding on the retentate side to prevent cells and proteins from sticking to the membrane.

Figure 5.1 shows the process yields for membrane filtration in comparison to cells processed under the same conditions using a depth filter. The figure indicates that the total cell recovery is higher when using a membrane (26%) in comparison to a depth filter (14%) however this is of low statistical significance ($p = 0.40$). There is no significant difference in the cell viability.

*Research carried out within thesis in collaboration and supervision of Kinza Islam as part of her MSc research project studies.

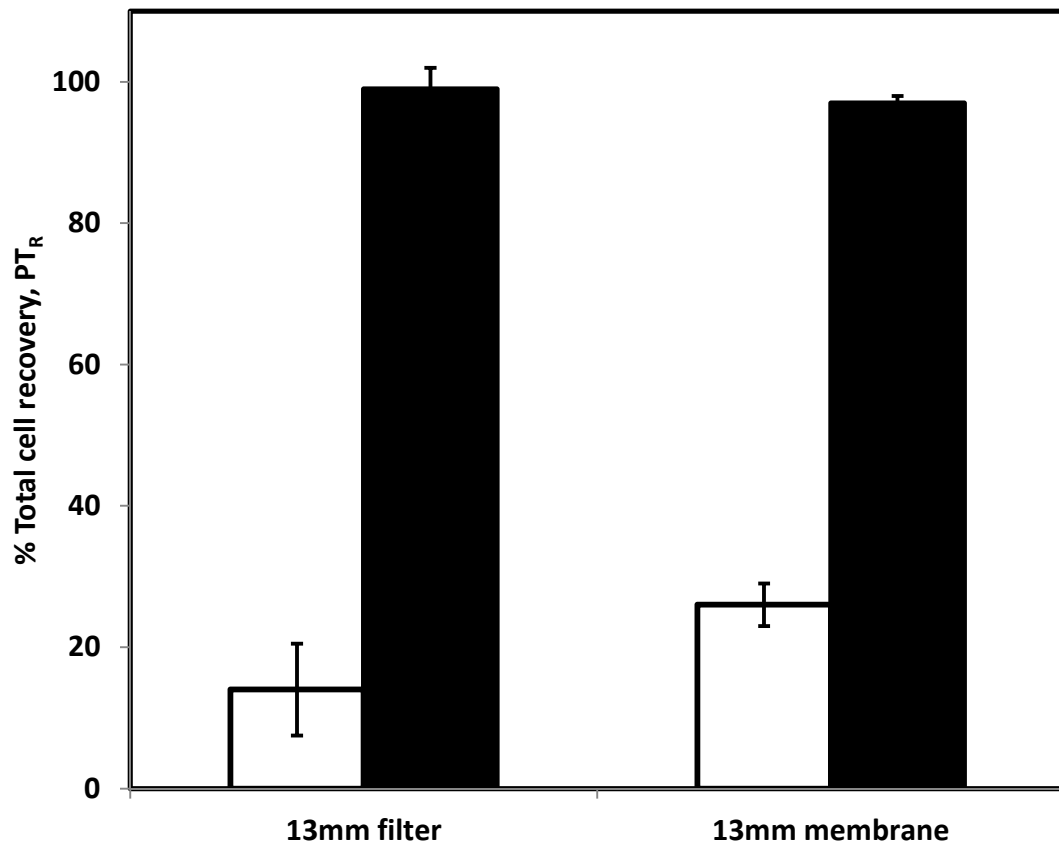


Figure 5.1 - Membrane vs depth filtration

13 mm diameter filters were loaded with 2.5 mL of cell suspension at a concentration at 2×10^6 cells mL^{-1} at a constant flow rate of 150 LMH and then recovered by backflushing the filters with 5 mL of elution buffer at 45,000 LMH. The total cell recoveries (□) and cell viabilities (■) were compared for cells processed using depth filters and cells filtered with membranes. Data shows the mean values \pm the range from three separate filtrations ($z=3$, $n=3$).

Figure 5.2 shows the effect of increasing the volume of cell suspension loaded (thereby increasing loading from $\approx 1.5 \times 10^6$ cells to 6×10^6 cells) on the proportion of cells recovered and the viability of the recovered cells. The results show that independent of the number of cells loaded a significant proportion of the cells were unrecovered following the backflush. Unlike the depth filter, the filter matrix is less open and therefore it is more difficult for the cells to enter and become trapped within the filter. However it could be that cells either adhere to the membrane or as with the depth filters, the cellular protrusions hook on and become tangled in the membrane pores.

Increasing the number of cells loaded did appear to have a negative impact on the cell recoveries, however this was not significant ($p = 0.19$). A large proportion of the recovered cells were viable and this appeared to also be independent of the number of cells loaded. Following these initial experiments it was determined that the issues with cell recovery observed with the depth filters would not be solved by solely replacing the depth filters with membranes.

5.2. Gravity settling as a method of loading to increase cell recovery

Based on the filtration model discussed in section 3.2.4 and some of the subsequent findings already discussed in this chapter, it was hypothesised that a possible way to increase the levels of recovery would be to increase the size of the 'surface' cell population (T_{SURF}). The dead zones in the filter (section 4.1.3) and the way in which the cells entangle themselves by wrapping around individual filter fibres (Figure 4.9) make cells which enter the filter (T_{FILT}) extremely difficult to recover.

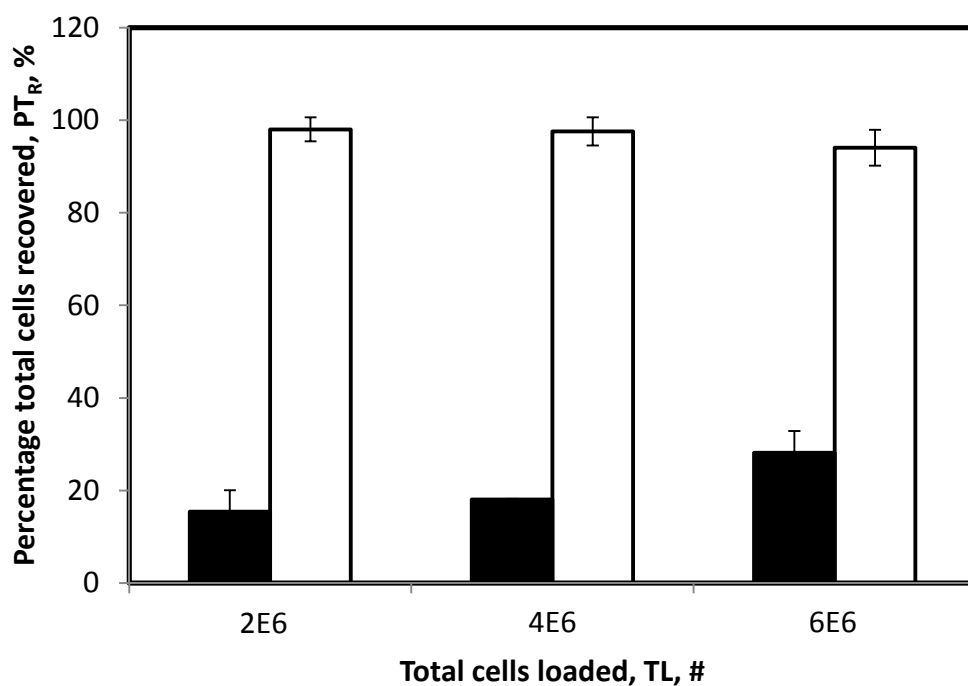


Figure 5.2 – Effect of load cell number on the total cell recovery

Increasing volumes of cell suspension at a concentration of 2×10^6 cells mL^{-1} were loaded at a constant flow rate of 150 LMH and were then recovered by backflushing the filters with 5 mL of elution buffer at 45000 LMH. The proportion of total cells recovered (■) in the backflush and the viability of the recovered cells (□) was calculated. Data shows the mean average values \pm 1sd from three separate filtrations ($z=3$, $n=3$).

It was thought that by allowing cells to gravity settle onto the surface of the filter before allowing any filtrate to pass through the filter; it may be possible to create a build-up of cells on the filter surface which act almost like a pre-filter. When the filtrate is allowed to pass through the filter, it might pass through the layers of cells before it permeates through the filter without the majority of cells entering the filter itself. The cells could then be recovered from the surface of the filter via backflushing or manual resuspension of the cells.

The settling time (t_{SET}) is a crucial factor within the gravity settling process; if cells are not given enough time to fully settle then they may be pulled through into the filter when the permeate is released. However if the cells are left to settle for too long then it may result in cell loss due to cells adhering to the filter housings or to the filter medium. It may also cause the cells within the pre-filter layer to form strong bonds between one and other which could cause the cells to become damaged on detachment.

In order to investigate this part of the process cells were allowed to settle onto a filter for increased lengths of time before being manually resuspended to see if they remain recoverable and of good quality; no liquid was allowed to pass through the filter. Depth filters with an effective filtration area of 0.28 cm^2 were punched out of a larger sheet using a specially designed filter punch created in collaboration with the UCL Rapid Design and Fabrication Facility. The experimental set up is shown in Figure 5.3. The filters were loaded into the USD depth filtration housings (Jackson et al., 2006, Kong et al., 2010) and then wetted with 1 mL (35.7 Lm^{-2}) of DPBS. The permeate outlet was blocked using a pinch valve and the housing was filled with 2 mL (71.4 Lm^{-2}) of DPBS. 1 mL of cell suspension at a concentration of $1.5 \times 10^6 \text{ cells mL}^{-1}$ ($5.35 \times 10^{11} \text{ cells m}^{-2}$) was manually loaded into the housing using a Gilson pipette. The cells were allowed to settle for up to 60 minutes before they were recovered via manual resuspension of the

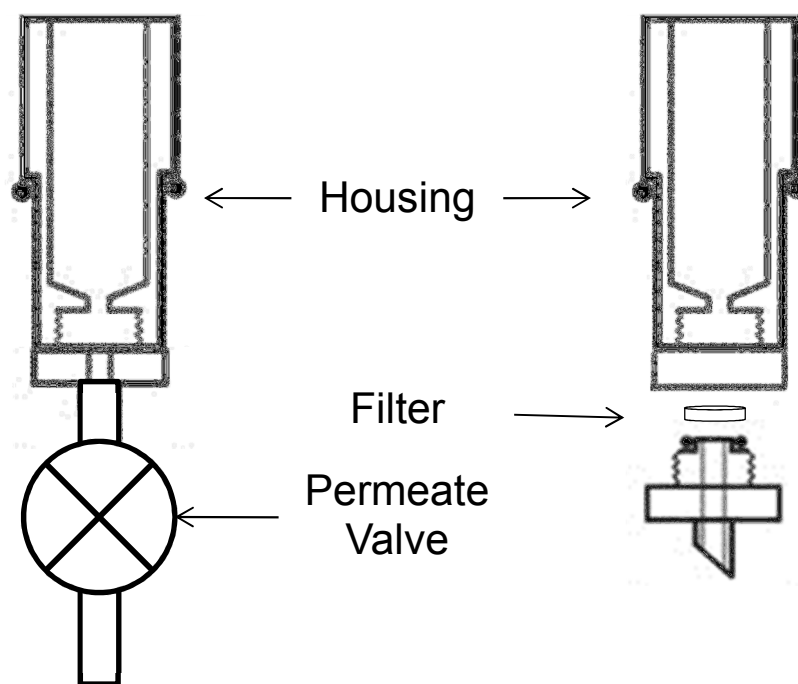


Figure 5.3 – Schematic drawing of gravity settling filtration set up

Figure shows the apparatus set up used during the gravity settling experiments. Small scale depth filtration filter housings (Jackson et al., 2006) were adapted in house at the UCL Rapid Design and Fabrication Facility. A pinch valve was used to control the rate of filtration by restricting filtrate flow through the permeate exit.

retentate with a pipette. As a control the filter was replaced with an impermeable disk which the cells could not enter or pass through. Cells were left to settle for 30 minutes before they were recovered.

Figure 5.4 shows that on average around 80% of the cells were recovered regardless of the settling time. 20% of the cells were lost which is approximately equivalent to a double layer of 100% confluent cells on the filter surface. It was presumed that these cells either entered or adhered to the filter and were difficult to recover. When using the impermeable disk, 100% of the cells were recovered. The settling time did not appear to have an effect on the cell viability with 93% of the recovered cells being deemed viable.

Having demonstrated that the cells can be allowed to fully settle onto a filter and the majority of the cells can then be successfully recovered, the next step was to allow the permeate to pass through the filter without dragging the cells into the filter and making them difficult to recover.

The permeate outlet was blocked using a pinch valve and the housing was filled with DPBS before the cells were loaded and allowed to settle for 30 minutes before being filtered. The cells were then resuspended in the DPBS to recover them. In subsequent runs the permeate valve was used to restrict and slow the flow of liquid through the filter in an attempt to try and improve the recoveries.

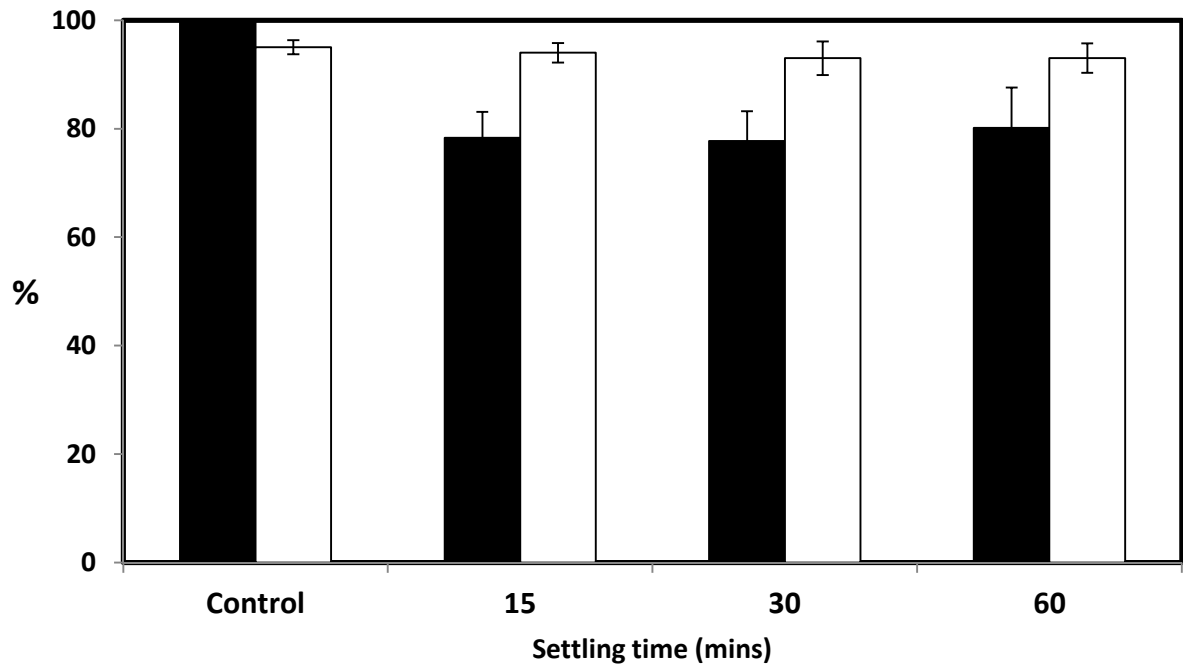


Figure 5.4 – Effect of settling times on the recovery of cells from the filter

A 0.28 cm² filter was loaded into the USD depth filtration housing and 35.7 Lm⁻² of cell suspension at a concentration of 1.5x10⁶ cells mL⁻¹ was manually loaded into the housing using a Gilson pipette. The cells were allowed to settle for up to 60 minutes before they were recovered via manual resuspension of the retentate with a pipette. As a control the filter was replaced with an impermeable disk which the cells could not enter or pass through. Cells were left to settle for 30 minutes before they were recovered. Data shows the mean values ± the range for total cell recovery (□) and cell viability (■) from two separate filtrations (z=2, n=3).

Figure 5.5 shows that allowing the permeate to pass through the filter, meant that the recoveries were significantly decreased when compared to the gravity settling filtrations with no flow through. Using the pinch valve to restrict the flow (run 2), the rate of flux was reduced 10 fold (280 LMH, ~10 mins for all of the filtrate to pass through the filter). The proportion of total cells recovered did appear to increase when the flow was restricted however there was a large degree of variability making it difficult to draw any firm conclusions and the cell loss was still significant. Two controls were used, the first used an impermeable disk in place of the filter (no permeate flow through) as previously described and the second was a centrifugation control were 1 mL of cell suspension at a concentration of 1.5×10^6 cells mL^{-1} was spun down at 500 x g for 5 mins. All of the cells were recovered in the first control and around 80% of the cells were recovered using the centrifugation control.

5.3. Using glass beads to prevent cell loss during filtration

Previous experiments had shown that if cells are drawn into contact with the filter medium under the influence of flow, then a large proportion of these cells are unrecoverable. If the cell recoveries were to be improved it was hypothesised that when filtration liquor passes through the filter, the cells are prevented from coming into contact with the filter medium.

One method studied here was to use layers of glass beads gravity settled onto the filter surface prior to loading, creating a pre-filter layer between the cells and the filter media.

Commercially available glass beads (Sigma Aldrich, Ayrshire, UK) were used to create a pre-filter layer between the cells and the filter.

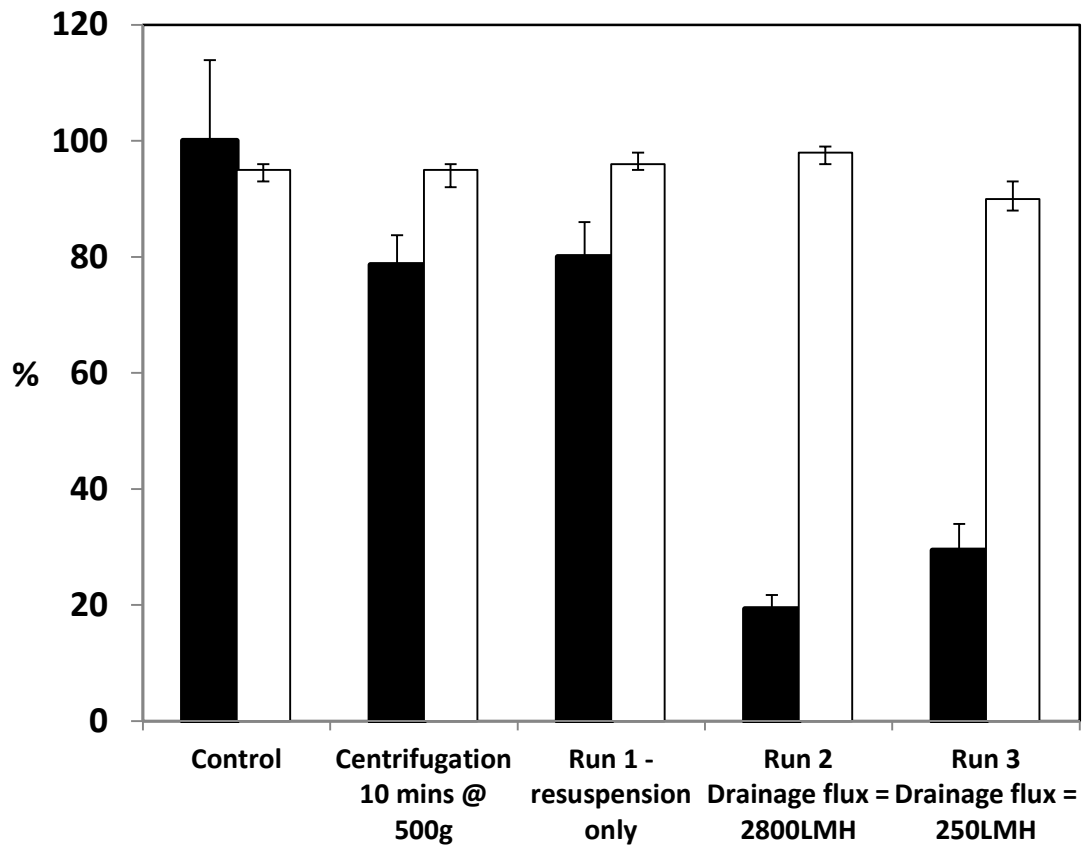


Figure 5.5 – Overview of gravity settling filtration experiments

Figure shows total cell recovery (■) and cell viability (□) for each of the gravity settling experiments. There is a filtration control using an impermeable disk in place of the filter, cells were allowed to settle onto the disk and 100% of the cells were recovered after 30 minutes settling time. A centrifugation control was also used. Data point shows the mean average of triplicate inter-experimental measurements ± 1 the range ($z=1$, $n=3$).

The beads were sized using the Mastersizer 2000 (Malvern, Worcestershire, UK) particle sizer (Figure 5.6). The beads were found to have an average diameter of 74 μm with particles ranging from 25 μm to 197 μm in diameter.

Initial experiments were developed to use 5 layers of beads. It was estimated that 5 layers of beads would be sufficient to prevent cells getting through and coming into contact with the filter. A bed of 5 layers of beads would have M_{Bead} ,

$$M_{\text{Bead}} = 5 \cdot A_{\text{Filt}} \cdot d_{\text{Bead}} \cdot \rho_{\text{Bead}}$$

Equation 5.1

Where d_{Bead} is the diameter (or height of the bead assuming they are perfectly spherical) and ρ_{Bead} is the density of the beads (ρ_{Bead} was $2.8 \times 10^6 \text{ g m}^{-3}$),

Due to the heterogeneous nature of the beads it was assumed that the packing within the bed would $\approx 100\%$. For a filter area of $2.8 \times 10^{-5} \text{ m}^2$ and a bead density of $2.8 \times 10^6 \text{ g m}^{-3}$ the mass of beads required was estimated to be 0.029 g.

5.4. Effect of glass bead ‘pre-filter’ on total cell recovery

The 0.28 cm^2 depth filters were loaded into the USD depth filtration housings (Jackson et al., 2006, Kong et al., 2010) and then wetted with 1 mL of DPBS. The permeate valve was closed and the beads were added in 1 mL of DPBS. As with the gravity settling filtrations (section 5.2) 1 mL of cell suspension at a concentration of $1.5 \times 10^6 \text{ cells mL}^{-1}$ was manually loaded into the housing using a Gilson pipette. The cells were allowed to settle for 30 minutes before permeate valve was opened fully and the liquid was allowed to pass through the filter. Once all of the liquid had drained through the filter, the cells were recovered by backflushing the filter at 1 mL s^{-1} with 10 mL of DPBS. Figure 5.7

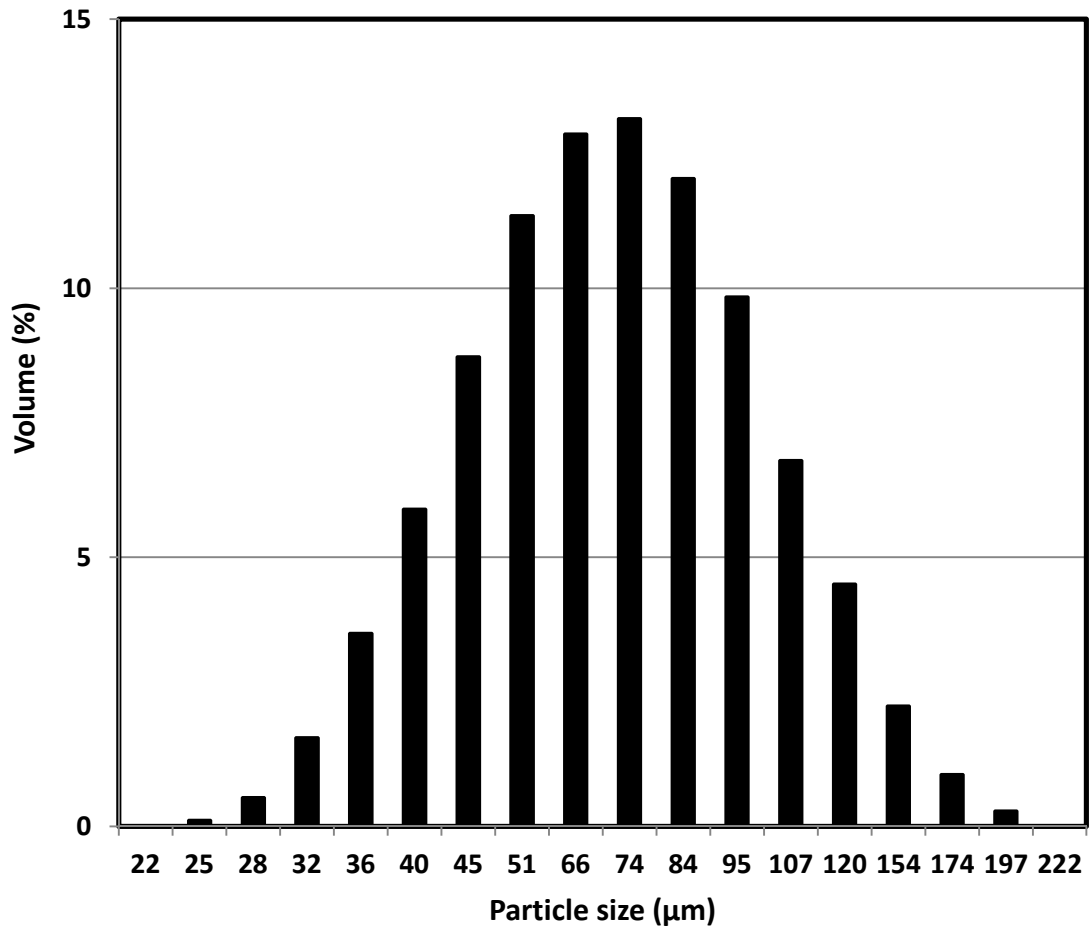


Figure 5.6 – Mastersizer 2000 particle size data distribution profile for the glass beads.

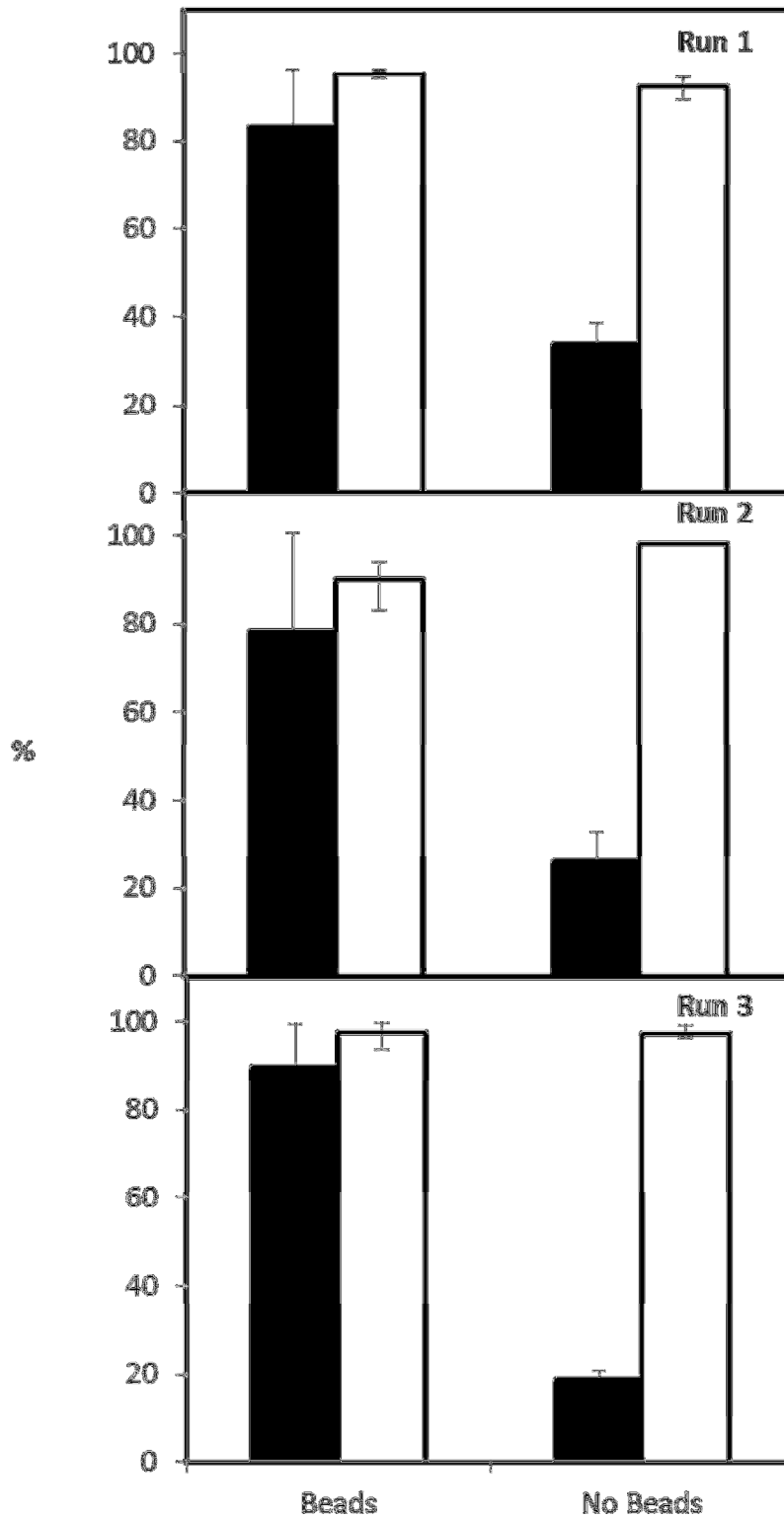


Figure 5.7 – Impact of glass bead pre-filter layer on the recovery of total cells.

Results show the effect of the glass beads on the proportion of cells recovered (□) as well as the viability of the recovered cells (■). Using the glass beads as a pre-filter layer between the cells and the filter led to a 3-fold increase in the proportion of cells recovered. Results show the mean values \pm the range from three separate filtrations ($z=3$, $n=3$).

shows that by filtering cells with the pre-filter layer of beads caused a significant increase in the recovery for all three runs. ($p = 0.0002$).

On average over the three runs a large proportion of the cells were recovered ($84\% \pm 6\%$) and the viability of the recovered cells was also high (94%). It appears that beads do prevent the cells from coming into contact with the filter which makes them easier to recover.

5.5. Why do the beads work?

It is hypothesised that the beads work by forming a permeable bed on which the cells settle, whilst the filtration liquor passes through when the permeate valve is opened. Assuming an average diameter of $74 \mu\text{m}$ (radius of $37 \mu\text{m}$) it is possible to estimate the size of the pores which could be created within this permeable bed.

Figure 5.8 provides a schematic of how the beads may form in a layer. The equivalent pore area, A_p , is extracted using

$$A_p = rh - \frac{\pi r^2}{2}$$

$$A_p = r(3r^2)^{\frac{1}{2}} - \frac{\pi r^2}{2}$$

$$A_p = 3^{\frac{1}{2}} \cdot r^2 - \frac{\pi}{2} r^2$$

Equation 5.2

Where the first term is the area of the triangle given in Figure 5.8, and the remaining two the area of the three segments S1, S2 and S3. The equivalent pore diameter is given by

$$d_p = \left(\frac{4A_p}{\pi} \right)^{\frac{1}{2}}$$

$$d_p = \left(\frac{4.3}{\pi} \cdot r^2 - 2r^2 \right)^{\frac{1}{2}}$$

Equation 5.3

For a bead radius of 37 μm , the equivalent pore diameter is 17 μm .

5.6. Effect of flux on the recovery of cells during glass bead filtration

The USD filter housings were adapted by the UCL Rapid Design and Fabrication Facility to make them air tight above the filter. A top was attached to the open filter housings which contained a female luer lock fitting (Figure 5.9). This meant that the rate of flux could be accurately controlled by creating a head pressure by forcing air on top of the filter liquor at a constant flow rate. This would cause the liquor to permeate through the permeable layers of cells and glass beads and through the filter itself at the same rate as the air was being pumped into the housing. Previously the liquid had been allowed to naturally permeate through the filter however the flow did eventually drop almost to the point of stopping due to the resistance caused by the beads and cells blocking the membrane; this adaption allowed for constant controlled flux rates through the filter.

The filters were inserted into the housings and wetted with 1 mL of DPBS. The permeate valve was closed and the beads were added in 1 mL of DPBS. 1 mL of cell suspension at a concentration of 1.5×10^6 cells mL^{-1} was manually loaded into the housing using a Gilson pipette.

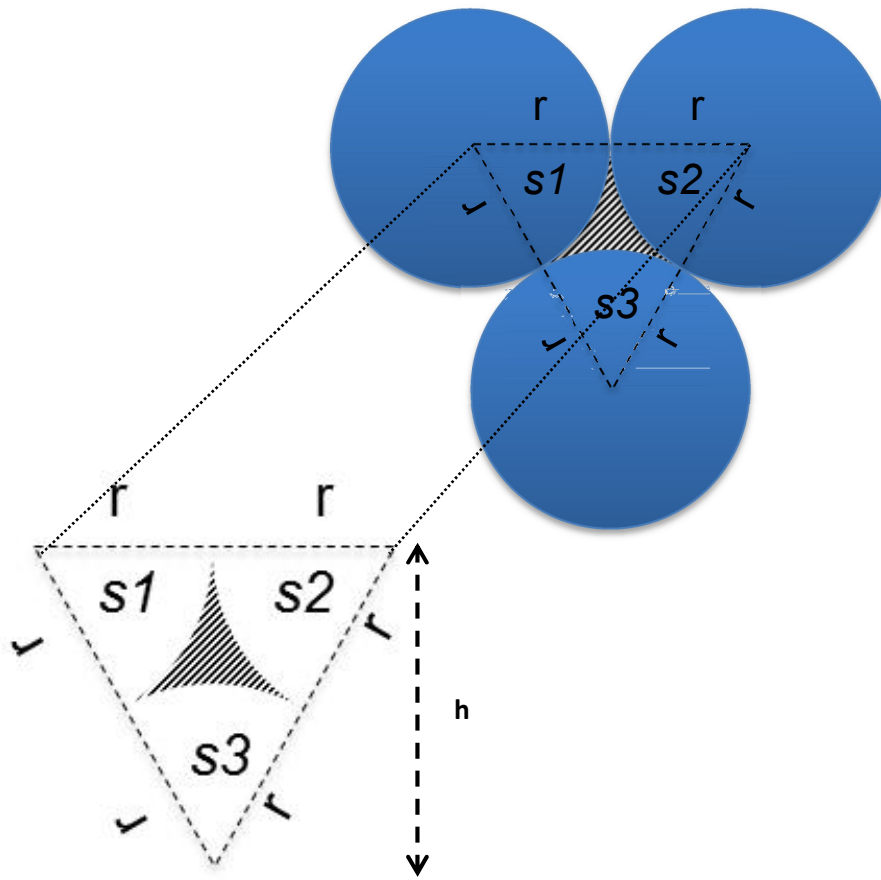


Figure 5.8 –Effective pore size created by the glass beads.

Shaded area – pore, area A_p . $h = (3r^2)^{0.5}$

The cells were allowed to settle for 30 minutes before the permeate valve was opened fully and a syringe loaded with air only was connected to the top. Air was pumped into the filter at controlled flow rates ranging from 0.5 mL min^{-1} (1000 LMH) to 60 mL min^{-1} (120,000 LMH). Once all of the liquid had permeated through the filter, the cells were recovered by backflushing the filter at 1 mL s^{-1} with 10 mL of DPBS.

Figure 5.10 shows the effect of the rate of flux on both the proportion of total cells recovered and the viability of the recovered cells. The results show that in all three runs the highest recoveries were achieved when processing the cells at 20,000 LMH (10 mL min^{-1}) however there was a significant degree of variation in all of the recovery measurements and so it was not possible to note any significant trends ($p = 0.255$). The lowest recoveries were observed when processing at the highest flow rate of 60 mL min^{-1} (120,000 LMH).

The viability of the recovered cells was also analysed using the ViCell XR. The results show that the cells recovered following filtration at a rate of 120,000 LMH had a significantly lower proportion of viable cells amongst those which were recovered, in comparison to filtrations carried out at 20,000 LMH ($p = 0.006$) and 1000 LMH ($p = 0.017$).

5.7. Effect of flux rate on cell quality

It was hypothesised that forcing the material through the filter at high flux rates may cause damage to the cells.

The cell death assay results show that there was no significant decrease in the proportion of viable cells with increased flux rates. There was also no significant

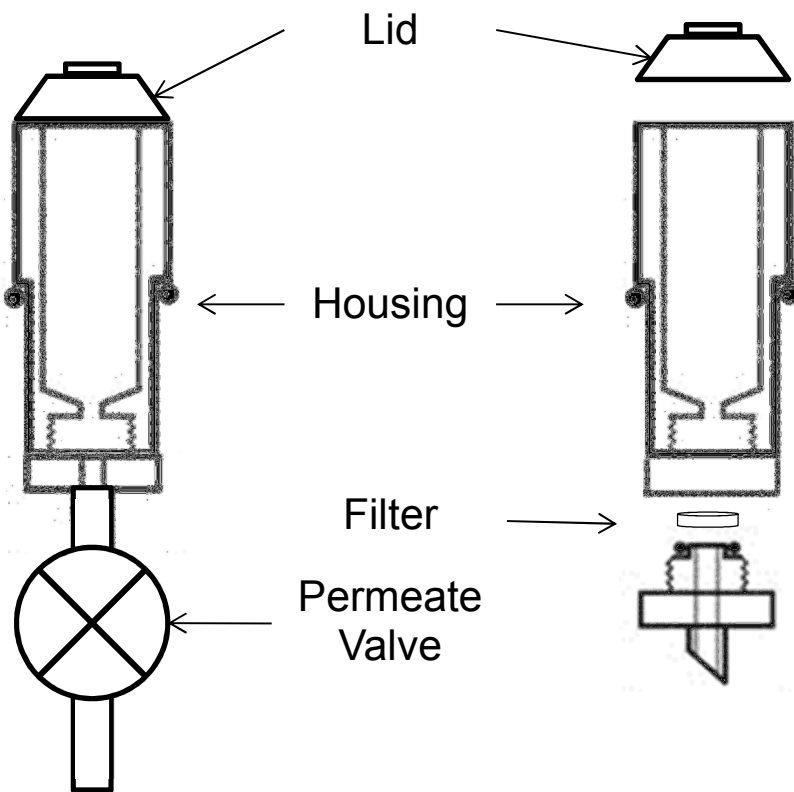


Figure 5.9 - Schematic drawing of gravity settling filtration set up.

Figure shows the apparatus set up used during the gravity settling experiments. Small scale depth filtration filter housings (Jackson et al., 2006) were adapted in house at the UCL Rapid Design and Fabrication Facility, fitting a perspex lid to the housings which allowed the connection of the housings to the syringe in order to control the rate of filtration.

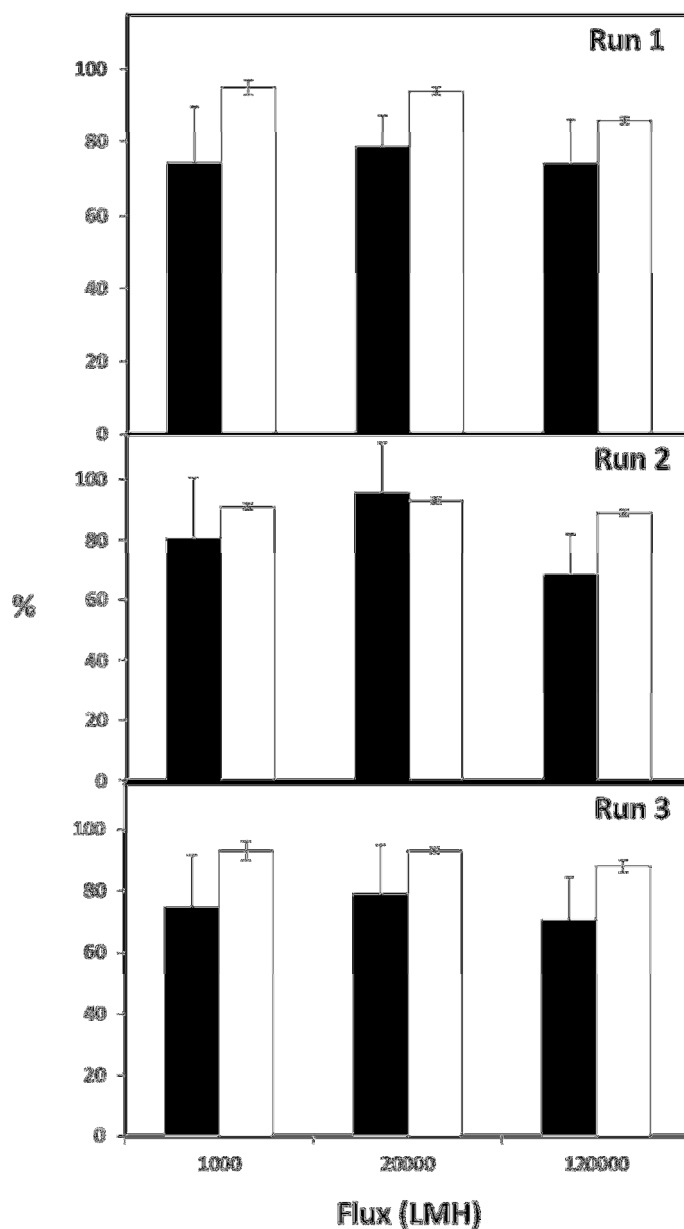


Figure 5.10 – Effect of filtration rate on the proportion of total cells recovered during gravity settling filtration.

Data shows the total cell recovery (□) and the viability of the recovered cells (■).

Results show the mean average \pm the range for three separate filtrations (z=3, n=3).

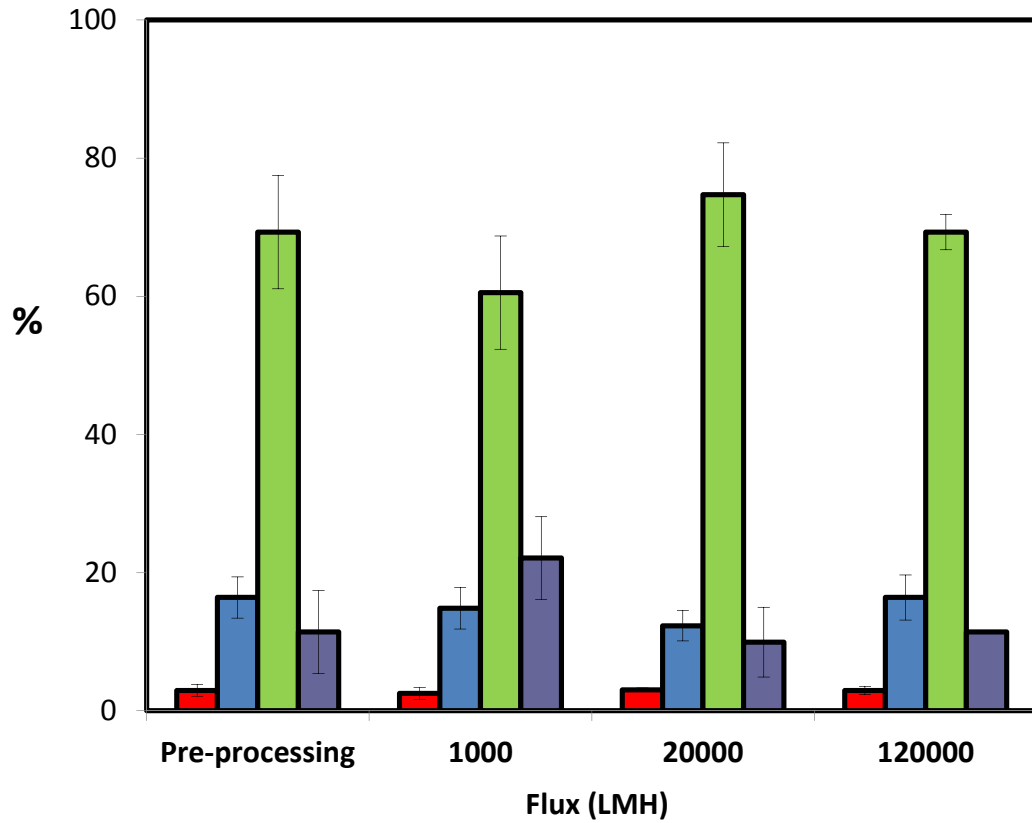


Figure 5.11 – Effect of flux rate during processing on the quality of recovered cells

All processing conditions were the same as in Figure 5.10. A caspase cell death assay was used to identify necrotic (■), late apoptotic (■), viable (■) and early apoptotic (■) cells. Results show the mean average \pm the range for three separate filtrations ($z=3$, $n=1$).

increase in damage to the cells post processing when compared to the non-filtered, pre-processing control.

5.8. Protein removal

Despite high recoveries, it was also important that the glass bead filtration method was capable of removing sufficient protein. 1mL of cell suspension at 1.5×10^6 cells mL^{-1} was loaded onto a filter topped with 5 layers of glass beads. The permeate was allowed to flow through at 20,000 LMH (10 mL min^{-1}) and the cells were recovered via backflushing with 10 mL of PBS at 1 mL s^{-1} (120,000 LMH).

Figure 5.12 shows that the glass bead filtration is as effective (if not more) than both the syringe filtration (without beads) and centrifugation at removing protein. On average the glass bead filtration removed 97% of the total protein.

Experiments were carried out to investigate the effect of a 5 mL ‘forward wash step’ (Figure 5.13).

1mL of cell suspension at 1.5×10^6 cells mL^{-1} was loaded onto a filter topped with 5 layers of glass beads. The permeate was allowed to flow through at 20,000 LMH (10 mL min^{-1}) and the cells were then forward washed with 5 mL of PBS at 10 mL min^{-1} . Cells were recovered via backflushing with 10 mL PBS at 1 mL s^{-1} (120,000 LMH).

Figure 5.13 shows that adding a forward wash step did not improve the levels of protein removal.

5.9. Effect of a glass bead ‘pre-filter’ during membrane filtration.

In section 5.2, the idea of using asymmetric membranes in place of the depth filters to increase the levels of cell recovery was proposed. However the initial results showed

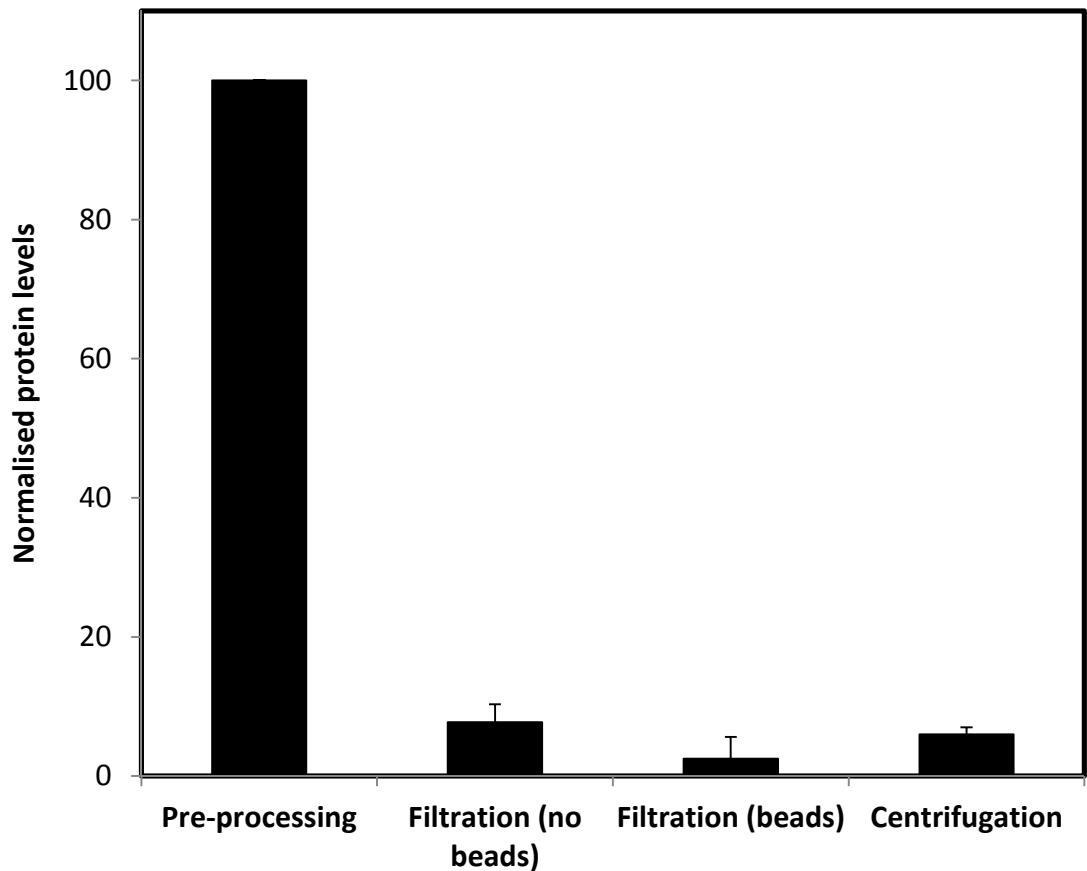


Figure 5.12 –Comparison of protein removal capacity for three different methods of primary recovery.

A BCA total protein assay was used to measure the amount of protein removed during processing. Processing conditions for the ‘bead’ filtration were the same as in Figure 5.10. For the ‘no- bead’ filtration, 5 mL of cell suspension at a concentration of 2×10^6 cells mL^{-1} was loaded at a constant flow rate of 150 LMH and recovered via backflushing with elution buffer at 45,000 LMH. During centrifugation, 5 mL of cell suspension at a concentration of 2×10^6 cells mL^{-1} was centrifuged at 800g for 5 mins and then resuspended in 5mL of elution buffer. Results show the mean average \pm the range for three separate filtrations ($z=3$, $n=3$).

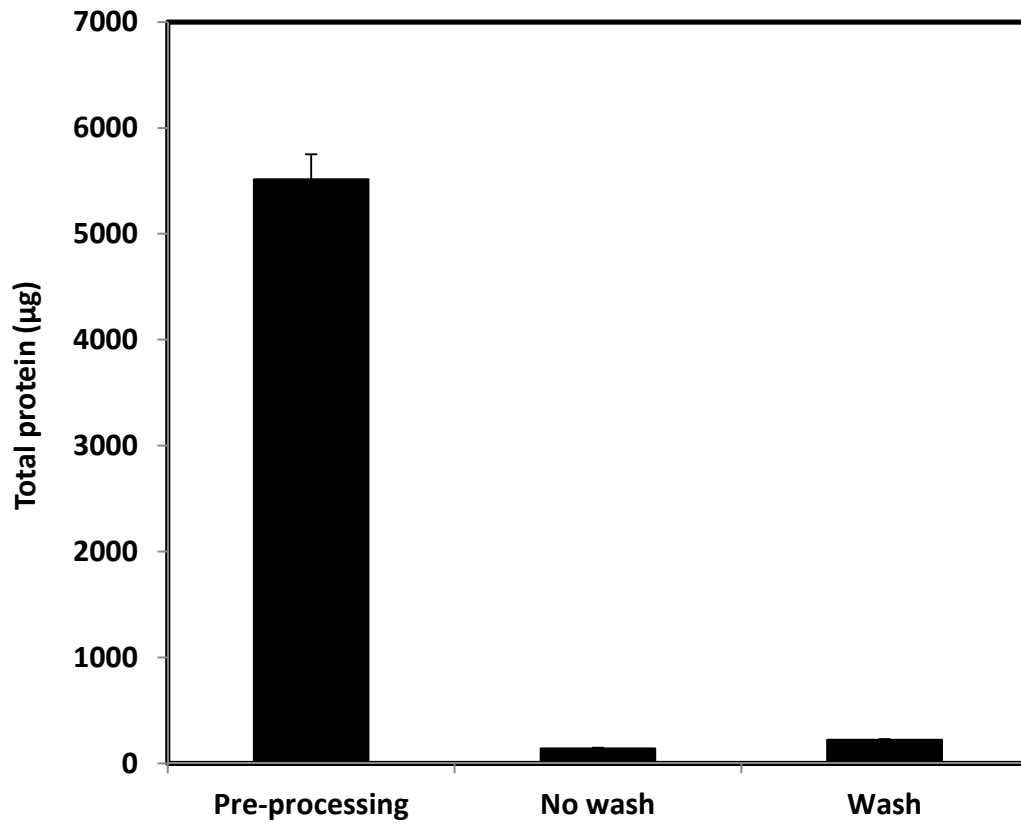


Figure 5.13 –Effect of a forward wash step on protein removal during ‘glass bead filtration’.

All processing conditions were the same as in Figure 5.10, however following loading the cells were gently forward washed with 5 mL of DPBS at 20,000 LMH. A BCA total protein assay was used to measure the amount of protein removed during processing. Results show the mean average \pm the range for three separate filtrations ($z=3$, $n=3$).

that during syringe filtration, high levels of cell loss (similar to the depth filtration losses) were observed.

It was not possible to use the gravity settling methods as the resistance of the blocked membrane was too high for filtration to take place. It was hypothesised that the glass bead pre-filter could be used to prevent the cells coming into contact with the membrane in order to increase the proportion of total cells recovered, as well as reducing the membrane resistance (by preventing fouling) and allowing filtration to take place.

Apparatus was set up as for the glass bead depth filtrations (Figure 5.9) however the filter was replaced with a 0.28 cm² membrane. The membrane was wetted with 1 mL of DPBS prior to loading. The glass beads were resuspended in 1 mL of DPBS with enough beads to provide approximately 5 bead layers (0.029g) between the membrane and the cells. The beads were loaded manually onto the membrane using a Gilson pipette and left to settle evenly across the membrane for 5 minutes

As with the depth filtration, 1 mL of HCA2 cell suspension was manually loaded into the top of the filter housing at a concentration of 2×10^6 cells mL⁻¹ using a pipette. The cells were then given 15 minutes to gravity settle onto the filter. Figure 5.14 shows the effect the glass bead pre-filter had on the total cell recovery for the membrane filtration.

The recoveries are compared to processes using syringe loading onto the same membrane type without the glass beads (gravity settling is not possible for membrane filtration without the glass beads due to extremely high membrane resistance). The recoveries are also compared to similar glass bead filtrations using the depth filters.

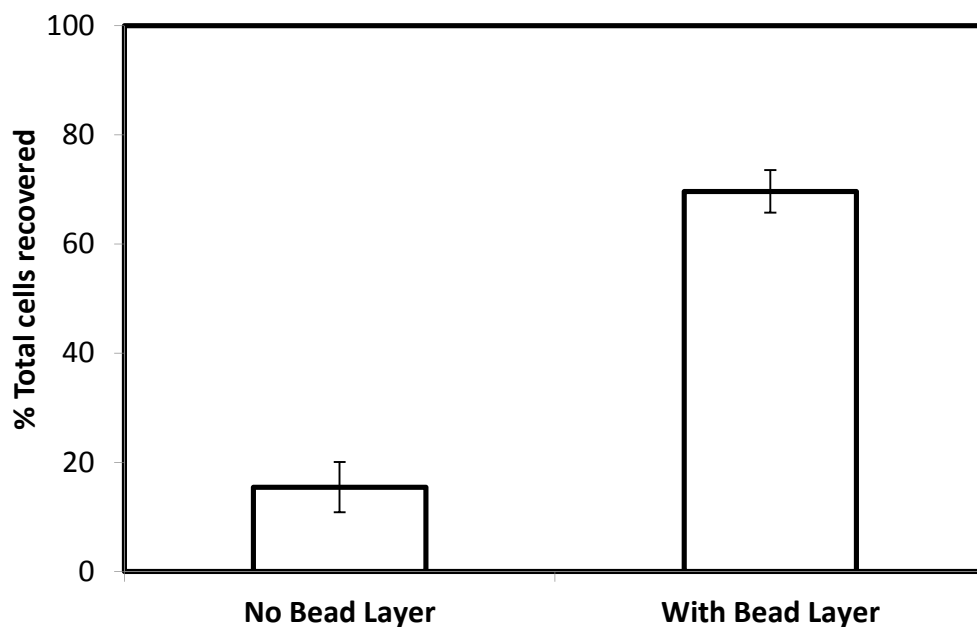


Figure 5.14 – Effect of glass bead ‘pre-filter’ on total cell recovery

5 layers of glass beads were added on top of the membrane prior to cell loading. 1mL of cell suspension (2×10^6 cells $\text{mL}^{-1} \equiv 8$ layers of 100% confluent cells) was added and cells were allowed to gravity settle onto the surface for 15 minutes. The permeate valve was then released and the permeate was pulled through under vacuum at 20,000LMH. Cells were recovered by backflushing with PBS at 120,000 LMH. The results show the mean value \pm 1sd for three separate filtrations ($z=3$, $n=3$).

The results showed that for membrane filtrations, the total cell recoveries are significantly increased compared to when there is no bead layer present and the cells are allowed to come into direct contact with the filter.

However the total cell recoveries for the glass bead membrane filtrations are slightly lower than the recoveries which were achieved using the glass beads with the depth filters.

5.9.1. Reasons for cell loss during membrane bead filtration

Although the glass beads did significantly increase the proportion of total cells recovered during the membrane filtration process, there was still a number of cells which were not recovered. A number of possible reasons for the cell loss were hypothesised. Possibly the most obvious theory for the reasons behind the cell loss is that the cells pass through the bead layers and are adhere to the membrane where they then become trapped. It was also hypothesised that the cells could be adhering to the beads meaning they are lost in the final stages of the process when the cells are separated from the glass beads. There was also the possibility that following recovery, cells are trapped within the bead 'pellet' as it settles. However this is unlikely to cause significant cell loss as the volume of liquid interspersed between the beads is insignificant in comparison to the backflush (~1% of volume) and therefore any cells trapped there should not have a significant effect on the proportion of cells recovered.

Scanning electron microscopy was used to identify the cells which remain trapped following the backflush step. The USD depth filter housings were loaded with a 0.28 cm² membrane and wetted with 1 mL of DPBS. The permeate valve was then closed and 0.029g (≈5 layers) of glass beads were added in 1 mL of DPBS to the surface of the membrane. Using the gravity settling filter method, 1 mL of cell suspension at a

concentration of 1.5×10^6 cells mL^{-1} was manually loaded using a Gilson pipette and the cells were allowed to settle for 15 minutes. The permeate valve was then opened and the filtrate was pulled through the membrane at a constant flow rate of 10 mL min^{-1} (20,000 LMH). Cells were then recovered by backflushing the filters with 10 mL of DPBS at a constant flow rate of 1 mL s^{-1} (45,000 LMH). The beads were allowed to gravity settle to the bottom of a centrifuge tube and the recovered cells were decanted off and counted. A control membrane was also set up and was processed in exactly the same way as described above however it was loaded with cDMEM only (no cells).

Once the filters were prepared they were fixed overnight along with the processed glass beads in 2% w/v PFA and 1% glutaraldehyde in 0.1M sodium cacodylate buffer (pH 7.3) at 21°C . before they were fractured and imaged.

Figure 5.15 shows the glass beads post processing. Images A and B are the beads used in the control process and have therefore not come into contact with the cells. It can be seen from images C and D that some of the cells have attached to the beads. However considering that there were approximately 200,000 glass beads and 300,000 missing cells we would expect the ratio of cells to beads to be higher than the images show. Image D shows that even when looking at group of over 50 beads, there are only a small proportion that have cells attached to them. It is unlikely that cells attaching to the glass beads is the main reason for the cell losses seen previously. Image C shows a single cell attached to the surface of a glass bead. It can be seen that the cells attach to the surface of the bead via cellular processes in the same way that the cells attached to the filters in section 4.1.4.

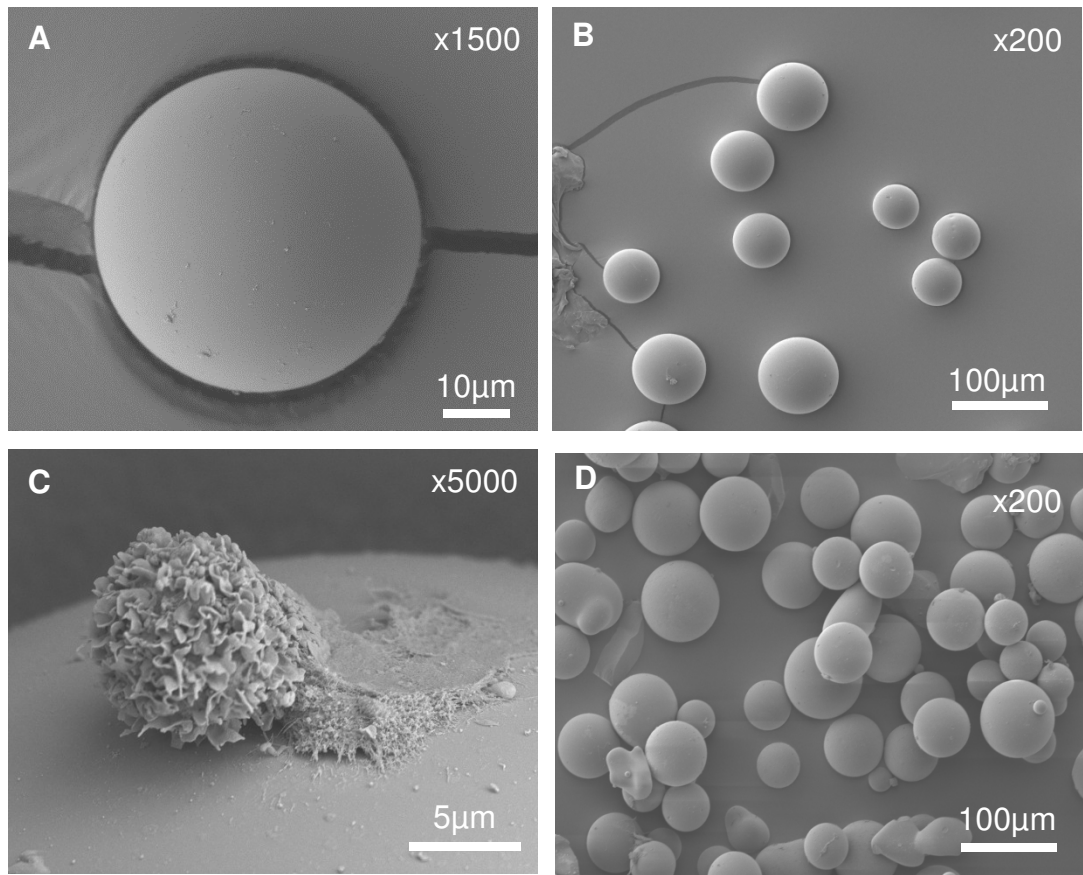


Figure 5.15 – SEM images of glass beads post filtration

The images show glass beads post processing. Images A and B were processed with CDMEM only and did not come into contact with cells. Images C and D show that post processing some of the cells have attached to individual beads.

5.9.2. Bead layers

In an attempt to improve the proportion of total cells recovered during the membrane filtration a number of processing factors were investigated and optimised. It was hypothesised that the number of layers of beads which make up the permeable 'pre-filter layer' in between the membrane and the cells could impact on the cell recovery. The membrane filtrations were carried out with glass bead pre-filters consisting of 1, 2, 4 and 8 layers of glass beads. The USD depth filter housings were loaded with a 0.28 cm² membrane and wetted with 1 mL of DPBS. The permeate valve was then closed and the glass beads were added in 1 mL of DPBS to the surface of the membrane. Using the gravity settling filter method, 1 mL of cell suspension at a concentration of 1.5x10⁶ cells mL⁻¹ was manually loaded using a Gilson pipette and the cells were allowed to settle for 15 mins. The permeate valve was then opened and the filtrate was pulled through the membrane at a constant flow rate of 10 mL min⁻¹ (20,000 LMH). Cells were then recovered by backflushing the filters with 10 mL of DPBS at a constant flow rate of 1 mL s⁻¹ (45,000 LMH). The beads were allowed to gravity settle to the bottom of a centrifuge tube and the recovered cells were decanted off and counted

Figure 5.16 shows the effect of the number of glass bead layers within the pre filter layer on the proportion of cells which are recovered. The results show that a single layer of glass beads was not enough to improve the recovery and the yield dropped to the levels previously observed before the glass beads were used (35%). A 2 layer deep glass bead pre filter provided the highest levels of recovery and appears to be the optimum pre-filter depth.

When the number of glass bead layers was increased beyond the optimum there was a significant drop in the total cell recovery. This was unexpected; however it could be due

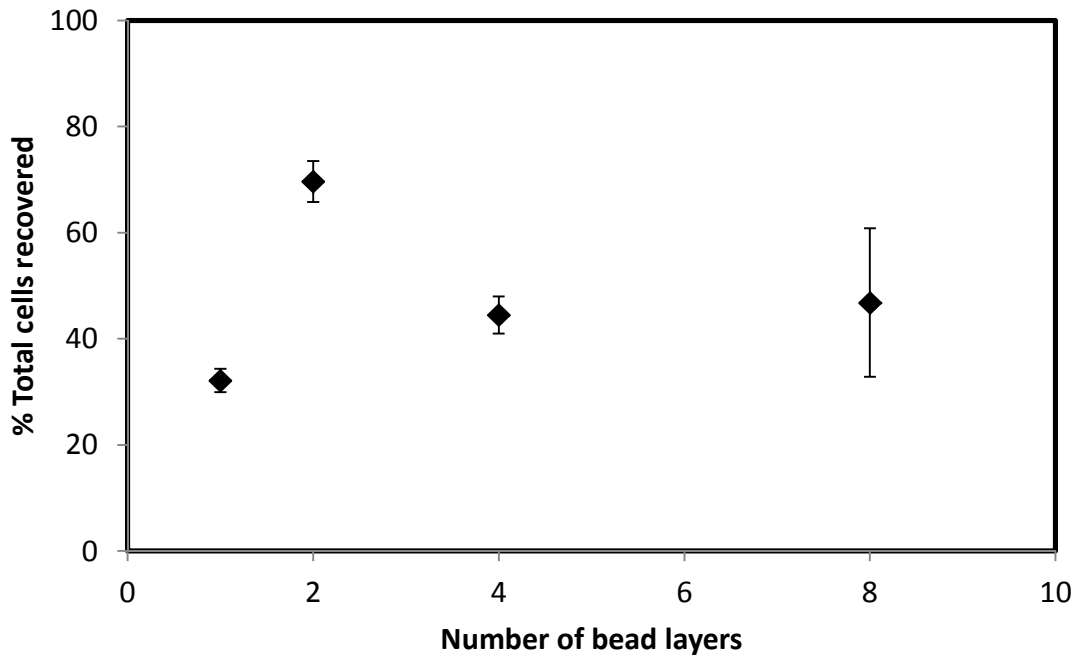


Figure 5.16 – Effect of glass bead pre-filter depth on the total cell recovery.

The membrane filtrations were carried out with glass bead pre-filters consisting of 1, 2, 4 and 8 layers of glass beads. Results show the mean average \pm 1sd ($z=3$, $n=3$).

to the increased numbers of bead layers creating a more complex matrix providing more opportunity for the cells to become trapped within it when the cells are separated from the beads post processing.

5.9.3. Effect of flux on the recovery of cells during glass bead membrane filtration

As part of the glass bead membrane filtration investigation, the rate of filtration was also explored. Similar studies with the glass bead depth filtration had shown that the rate of filtration had a significant effect on not only the proportion of total cells recovered but also the quality of the recovered cells.

Figure 5.17 shows the effect that the rate of filtration had on the recovery of the processed cells.

The results showed that as with the depth filtration, the lower filtration rates (1000 LMH) produced the highest levels of recovery. The proportion of total cells recovered decreased with both of the higher filtration rates (20,000 LMH and 120,000 LMH).

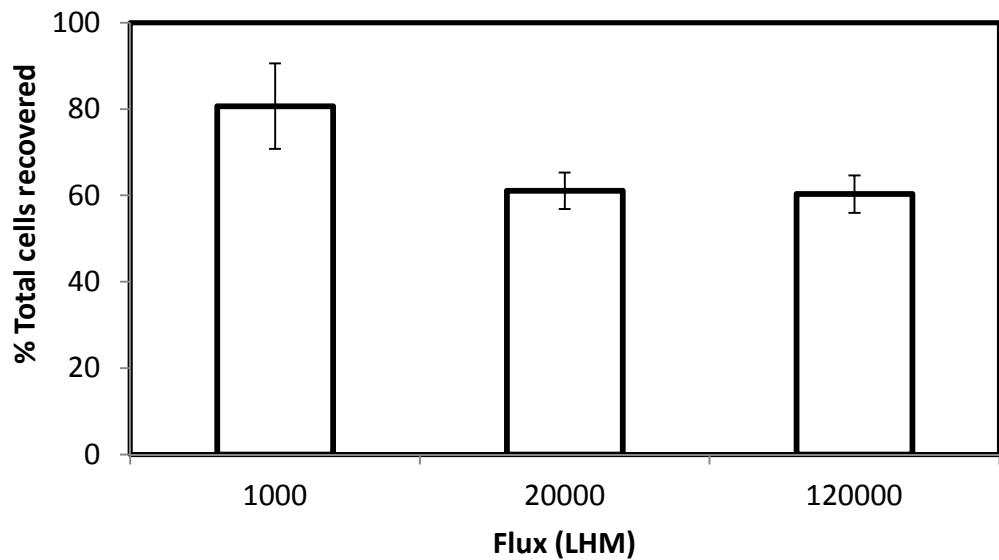


Figure 5.17 - Effect of filtration rate on the total cell recovery

Membranes (0.28 cm² diameter) were loaded into the housings and wetted with 1 mL of DPBS. The permeate valve was then closed and 5 layers of glass beads were added. 1 mL of cell suspension at a concentration of 1.5x10⁶ cells mL⁻¹ was manually loaded allowed to settle for 15 minutes. The permeate valve was then opened and the filtrate was pulled through at varying constant flow rates. Cells were backflushed with 10 mL of DPBS at a constant flow rate of 45,000 LMH. Results show the mean average ± 1sd (z=3, n=3).

5.10. Chapter discussion

Having developed some understanding of the mechanisms involved with recovery of cells using filtration, chapter 5 looked at using this knowledge to improve the levels of recovery as well as the quality of the recovered cells.

One of the main causes of cell loss was cells becoming trapped and entangled within the filter matrix. It was therefore logical that to improve the recoveries, cells must be prevented from entering the filter. It was hypothesised that using membranes with microscopic pores, smaller than the average diameter of the cells would mean the cells could not become trapped within the filter material.

'MMM' asymmetric super-micron membranes with a 5nm diameter pore were supplied by Pall Life Sciences. These membranes have an asymmetric pore structure and are designed specifically to be low binding on the retentate side to prevent cells and proteins from sticking to the membrane. The membranes were used as a direct replacement for the depth filters used previously; otherwise the process remained the same. Cells were loaded at a controlled flow rate and recovered via backflushing at high speeds with an elution buffer.

Figure 5.1 showed that the total cell recovery was higher when using a membrane ($26\% \pm 11\%$) in comparison to a depth filter ($14\% \pm 3\%$) however due to the lack of reproducibility this was not deemed statistically significant and the method still failed to recover a significant proportion of the cells. It was believed that the high levels of cell loss was due to the cells adhering to the membrane making them difficult to recover.

It was becoming clear that in order to prevent cell loss, the cells must be prevented from coming into contact with the filter material. The results from the gravity settling

experiments Figure 5.5 corroborated this theory. The gravity settling experiments were carried out to try and increase the proportion of cells residing on the surface of the filter (T_{SURF}) and therefore reduce the proportion of cells which enter the filter (T_{FILT}) and are difficult to recover. Results showed that if cells were allowed to settle onto the filter and no liquor was allowed to permeate through the filter, then a large proportion of those cells can be recovered. However as soon as the liquor is allowed to permeate through the filter, the cells become dragged into the filter and are difficult to recover. Controlling and reducing the rate of flow through the filter did improve the levels of recovery; however there was still a significant amount of cell loss.

The concept of using a pre-filter which would prevent the cells coming into contact with the filter and to which the cells would not adhere was proposed as a method for improving the cell recovery. Commercially available glass beads were a suitable choice as they were inexpensive, readily available and resistant to cell adherence (private communication).

Results showed (Figure 5.7) that by using the glass beads to prevent the cells coming into contact with the filter material, a large proportion of the cells were recovered ($84\% \pm 6\%$) and the viability of the recovered cells was also high (94%). Following recovery the beads were easily separated due to the fact they are much more dense than the cells, meaning that they settle at a higher rate and the cells can simply be decanted off. If this process were to be used in the manufacture of cells for therapy this process of removing the beads would have to be more rigorous to prevent glass beads being injected into the patient, this will be discussed further, in the future work section later in the thesis (chapter 6).

The glass beads significantly improved the yield of the depth filtration process and did not compromise the cell quality. The beads also had a significant impact on membrane filtrations (Figure 5.14) resulting in a fivefold increase in total cell recovery in comparison to a similar process without the glass beads.

The beads were on average 34 μm in diameter, which meant that assuming a 70% packing density they would create an equivalent pore size of 17 μm . Although this is slightly larger than the mean cell diameter, the fact that the beads are heterogeneous meant that in reality the packing density was probably higher than 70% making the pores less than 17 μm in diameter. There were also 5 layers of beads which prevented the cells from getting through to the filter or membrane.

There was still a small number of cells that were not recovered and it was hypothesised that this was due to cells adhering to the membrane or to the beads. SEM images (Figure 5.15) did appear to show some cells attached to the beads post processing, however it is unlikely that these numbers were significant enough to fully explain the cell loss. The mechanisms behind the cell loss would need to be investigated further in order to properly optimise the process.

As well as improving the levels of cell recovery, the glass bead filtration method was also demonstrated to be as effective (if not more) than both the syringe filtration (without beads) and centrifugation. On average the glass bead filtration removed 97% of the total protein (Figure 5.12).

An ultra scale-down filtration method for the primary recovery of adherent human cells for therapy, which is capable of recovering a significant amount of high quality cells has been demonstrated. The methods behind why cells are not recovered during processing are understood and this understanding has been used to inform and develop the process.

Chapter 6: Conclusion

6. Conclusion

The research focussed on the use of depth filtration as an alternative to centrifugation or TFF in the primary recovery of adherent cells for therapy. Batch centrifugation is an open process with inherent risk of contamination as well as variability between operators. It is also not scalable. TFF whilst providing a viable option for cell recovery, is a complex process requiring expensive equipment and materials. Research into TFF as a primary recovery step was on going within the lab team in parallel to this research and did prove more successful in terms of cell recovery when compared with depth filtration. For this body of research depth filtration was chosen initially as it is simple, well understood and has the potential to provide a one step, closed, scalable process for the recovery of cells for therapy.

During the early stages of the project it became clear that whilst the filters successfully captured the cells, it was then very difficult to recover a significant proportion of these. Imaging showed that the cells entangled themselves within the matrix of filter fibres demonstrating why recovery rates were so low.

As we began to better understand the mechanisms which affected recovery, it became more apparent that the depth filtration set up, which we had developed would not be a viable option as a primary recovery process. In my opinion a depth filtration process will not be capable of producing high levels of cell recovery if the cells are permitted to enter the filter matrix. This is obviously different to my opinion prior to the research; however I still believe the thought process behind initiating the research was sound. Depth filtration would provide a simple, one step, primary recovery process however without preventing the cells from entering the filter, the cell losses are such that it would not make the process viable.

This was the main reason that the later stages of the research focussed on preventing the cells from entering the filter either by settling the cells onto the surface of the filter, replacing the open matrix of filter fibres with a more closed membrane and finally using a bead layer to prevent the cells coming into contact with the filter.

Using the beads eventually proved successful and meant we had a filtration process that was capable of recovering a significant proportion of viable cells. To conclude, the research has produced a potential option for the primary recovery of adherent human cells for therapy, however more work is needed in order to assess the full suitability of this method as part of a large scale commercial manufacturing process.

Chapter 7: Future Work

7. Future Work

This body of research has explored the use of an ultra scale-down filtration device for the recovery of adherent cells for therapy. The initial aim of the research was to develop an ultra scale-down tool which was capable of recovering a high proportion of good quality cells.

A large proportion of this project was concerned with attempting to improve the levels of cell recovery. The quality of those cells which were recovered was investigated to a certain extent however the cell quality analysis was not as comprehensive as we would have liked. A number of the assays rely on a large number of cells to produce reliable results. This is a common issue when working with small quantities of cells in ultra scale-down devices and was further exacerbated by the high numbers of cells which were lost during processing. It was for this reason that a large amount of focus was given to improving the cell recoveries.

However, for this method to be fully utilised within a commercial manufacturing process, tools for measuring the key cell quality parameters of filtered cells will need to be further investigated. So far the membrane integrity of the recovered cells has been analysed to measure viability and a more in depth cell death assay has been used to look at changes in the apoptotic state of the cells post processing.

Future work would need to focus more around the key quality attributes that make the cells suitable for therapy such as do the cells still maintain the ability to differentiate (or if they have already been differentiated, do they maintain their differentiated state)? As described in section 1.3.4 there are a number of cell surface markers which can be analysed as a measure of these quality parameters.

The work would look at using the USD device to carry out multiple small-scale experiments over a wide range of processing conditions to look at the quality of the cells which are produced post processing and ultimately their effectiveness as a therapeutic agent.

Moving forward with the bead filtration method processing conditions such as load flow rate and flux, backflush flow rate and wash buffer volumes would need to be assessed based on their impact on the therapeutic potential of the cells. The impact of upstream processing conditions such as culture methods (i.e 2D or 3D) could also be analysed to look at its effect on the final product post primary recovery. Tools such as (design of experiment (DoE) software could be used to generate optimum processing conditions.

The research could even evolve around one specific cell therapy such as the CTX0E03 cells and their potential use in the treatment of stroke patients or a process using cells which require a differentiation step in the process such as human mesenchymal stem cells (hMSC's) which are differentiated to chondrocytes for use in osteo therapies. Using more clinically relevant cell lines such as these would also help to demonstrate whether or not there is potential for this method to be used in a commercial process as well as allowing further investigation into the effect of processing on the quality of the cells produced. It would also be important to look at the potential options for further downstream processing such as chromatography steps to see how the bead filtration primary recovery method impacts those processes. Using a clinically relevant manufacturing process such as the CTX0E03 process, we will gain more of an idea as to the feasibility of this method in a commercial process.

One factor which was shown to have an impact on cell quality was the length of time which cells were held prior to processing (section 4.2.2). When the cells were held in

suspensions for 24 hours prior to processing the recovered cells showed a significant drop in cell viability. However it was stated at the time that 24 hours is an extreme hold time (private communication indicated hold times of around 6 hours are more common in industry) and it may be that when held for a shorter period of time prior to processing, the impact might be less significant.

Improved understanding of the effect of processing conditions on key cell quality attributes as well how specific cell lines are affected during processing going forward will allow for further process optimisation and will assist with cell line selection.

A process of filtering the cells using a layer of glass beads on the surface of the filter led to significant improvements in cell recovery. Using this method we were not only able to recover the majority of the cells without impacting on the cell quality, but we were also able to remove a significant proportion of the total protein present pre-processing. However whilst carrying out these filtrations using the ultra scale-down device is beneficial due to the complexity and financial implications of culturing large numbers of adherent cells, moving forward it would be important to carry out filtrations on a similar scale to industrial manufacturing in order to compare the results and make the small scale experiments more relevant.

There are some basic theoretical calculations which can be done to envisage what the process would look like at a larger scale. On average the bead filtration process recovered 90% of the cells loaded. This means that to produce enough cells for a standard cell therapy dose of 1×10^7 cells, 1.11×10^7 cells would need to be loaded initially. Maintaining the same number of cells per area of filter material (5.36×10^6 cells cm^{-2}) would mean a filter of 2.07 cm^2 at large scale (this would increase further if more than one dose was being produced).

Using the ultra scale-down device for depth filtration we had five layers of glass beads which equated to 0.114 g of beads per cm² of filter area. This equates to 0.24 g of beads which would be needed to produce the standard therapeutic at large scale. Table 7.1 provides an overview of what a scaled-up bead filtration process would look like if it were used to produce enough cells for a typical cell therapy dose of 1×10^7 cells.

When conducting large scale investigations the main aim would be to look at how the process could be used to filter large volumes of feed stock. Currently the glass bead filtration method has been used to process volumes up to 5 mL. A typical process for the production of adherent cells for therapy may result in harvested cells, quenched in complete growth medium at a final volume of 25 L.

The scale-up experiments would be used to demonstrate the capability of the glass bead system to process this volume of material without compromising on the recovery or the quality of the recovered cells when compared to the small scale processes.

Cells produced at large scale can be of lower quality as they are damaged in the harsh environment of large scale bioreactors. The experiments carried out on the USD device thus far have all used feed stock which has been of a consistent nature in terms of viability and cell age. During the scale-up experiments it will be important to closely analyse the feed stock in terms of the quality of the cells (including cell death assay as well as initial membrane integrity testing), the age of the cells and the supplemented media in which they are cultured. A scaled up version of the bead filtration system could be used in tandem with newly developed bioreactors for adherent culture such as the iCellis to mimic a whole large scale production process.

Bead Filtration	USD	Large Scale (1x10⁷ cells)
Cells cm⁻²	5.36 x10 ⁶	5.36E x10 ⁶
Predicted total cell recovery (%)	90%	90%
Cells loaded	1.50 x10 ⁶	1.11 x10 ⁷
Filter required (cm²)	0.28	2.07
Beads (g cm⁻²)	0.114	0.114
Beads (g)	0.032	0.24

Table 7.1 – Theoretical scale up of bead filtration process

Chapter 8: Validation

The research shown has documented the development of a method for the primary recovery of adherent cells for therapy. The journey has seen the initial development of an ultra scale-down device capable of processing small quantities of human cells and the subsequent optimisation of this device and increased understanding of the mechanisms in play during processing. This knowledge has led to the development of a process which is able to take small quantities of harvested cell suspensions and recover them from the supplemented growth media and harvest enzyme solutions they exist in. By processing cells using this method a large proportion of good quality cells were recovered.

For this method of processing to be incorporated into a large scale process, producing high quality therapeutics for the commercial market there would need to be a thorough process of validation carried out first.

The FDA first proposed an approach to the regulation of cellular therapies in 1997 (FDA, 1997). The guidelines recognised the increased risk of damage or contamination of the cellular product during extensive processing which could potentially lead to changes in the biological activity and efficacy of the cellular therapy. It was acknowledged that because of this risk regulations relating to good manufacturing practice (GMP) would apply to the production of new cell therapies for market, in 2006 this led FDA to publish a new set of guidelines detailing good tissue practice for the preparation of cellular therapies for phase I clinical trials (Halme and Kessler, 2006).

In order for the process detailed in the research above to be incorporated into a commercial process for the production of cellular therapies it would have to undergo stringent process validation in order to ensure that the processed cells do not fall foul of any of the FDA guidelines. I believe the main risk would be that the processing changes

the biological properties of the cells which at best could render them ineffective and at worst could make them unsafe causing harm to the recipient.

As mentioned in the previous chapter (chapter 6) due to the restricted amount of material available (due to complexities associated with adherent cell culture and high cell loss during processing) it was not always possible to do extensive cell analysis post processing. At the most basic level cells were analysed to measure the proportion of viable and non-viable cells, there was also some more in depth analysis of apoptotic cells as well as image analysis of cell damage (SEM) and cell morphology.

Whilst parameters relating to cell viability are an important first indicator of cell quality a more in depth analysis would be needed to confirm the identity and the efficacy of the cells (identity is particularly important when processing cells which possess the ability to differentiate as it has been shown that processing stress can promote differentiation in certain types of cells (Yourek et al., 2010, Chowdhury et al., 2010, Dong et al., 2009)).

The markers used to measure these parameters would need to be identified during the early stages of process development and used to compile an extensive profile of the cellular product. Once this work has been carried out the process can then be developed to identify the optimum operating conditions and look at which conditions in particular can damage or change the cells if they are not tightly controlled; this is known as process validation.

In 2011 the FDA set out a number of guidelines detailing the main principles of process validation in the production of pharmaceuticals replacing the initial guidelines first published in May 1987 (Katz and Campbell, 2012). The 2011 guidelines define process validation as “the collection and evaluation of data, from the process design stage

through commercial production which establishes scientific evidence that a process is capable of consistently delivering quality product.”

In summary, the guidelines breakdown process validation into three main stages; process design, process qualification and continuous process verification. Process design (stage 1) details the need to define the process using a combination of scientific knowledge developed during the initial research and development phases and scale up studies of the lab scale experiments carried out initially.

The shear forces which the cells are exposed to are often not present at small scale and therefore in order to validate the process detailed in this research (glass bead layer filtration) there would be a need for a number of scale-up studies to ensure that the results produced at small scale can be replicated consistently at large scale.

Process qualification (phase 2) looks at whether or not the process is capable of consistently delivering a safe and effective product. The glass bead filtration process would need to be assessed further to evaluate whether or not it is fit for purpose. There are a number of potential problems associated with the process relating to the use of the glass beads themselves. Firstly the method for separating them from the cells post processing is very crude and so would need to be improved to ensure no beads were administered to the patients. It would also be necessary to ensure that the glass beads are completely inert and do not leach any chemicals or compounds into the cells which could potentially be harmful to the cells or even the recipient.

Leachables and extractables are an essential part of any process validation. The FDA guidelines on good manufacturing practice state that “Equipment shall be constructed so that surfaces that contact components, in-process materials, or drug products shall not be reactive, additive, or absorptive so as to alter the safety, identity, strength, quality, or

purity of the drug product beyond the official or other established requirements”. This means that not only the glass beads but also the filters and any other connectors and components which make up the filtration device must react or affect the cellular products in any way (Ding and Martin, 2008).

The final stage (stage 3) is continued process verification and this takes place during routine manufacturing of the therapy. The cells should be continually analysed to ensure consistent safety and quality and any results or knowledge gained from this should be used to continually validate the process.

References

ABERCROMBIE, M. & AMBROSE, E. J. 1962. The surface properties of cancer cells: a review. *Cancer Res*, 22, 525-48.

ACOSTA-MARTINEZ, J. P., PAPANTONIOU, I., LAWRENCE, K., WARD, S. & HOARE, M. 2010. Ultra scale-down stress analysis of the bioprocessing of whole human cells as a basis for cancer vaccines. *Biotechnology and Bioengineering*, 107, 953-963.

ÄHRLUND-RICHTER, L., DE LUCA, M., MARSHAK, D. R., MUNSIE, M., VEIGA, A. & RAO, M. 2009. Isolation and production of cells suitable for human therapy: challenges ahead. *Cell Stem Cell*, 4, 20-26.

AL-RUBEAI, M., SINGH, R. P., EMERY, A. N. & ZHANG, Z. 1995. Cell cycle and cell size dependence of susceptibility to hydrodynamic forces. *Biotechnology and Bioengineering*, 46, 88-92.

BAPTISTA, P. M. & ATALA, A. 2014. Regenerative medicine: the hurdles and hopes. *Translational Research*, 163, 255-258.

BECKMAN 2006. ViCell Instructions.

BEDNER, E., SMOLEWSKI, P., AMSTAD, P. & DARZYNKIEWICZ, Z. 2000. Activation of caspases measured in situ by binding of fluorochrome-labeled inhibitors of caspases (FLICA): correlation with DNA fragmentation. *Experimental Cell Research*, 259, 308-313.

BENCHERIF, S. A., SANDS, R. W., ALI, O. A., LI, W. A., LEWIN, S. A., BRASCHLER, T. M., SHIH, T. Y., VERBEKE, C. S., BHATTA, D., DRANOFF, G. & MOONEY, D. J. 2015. *Injectable cryogel-based whole-cell cancer vaccines*.

BERTHIAUME, F., MAGUIRE, T. J. & YARMUSH, M. L. 2011. Tissue engineering and regenerative medicine: history, progress, and challenges. *Annual Review of Chemical and Biomolecular Engineering*, 2, 403-430.

BLANCO, Y., SAIZ, A., CARRERAS, E. & GRAUS, F. 2005. Autologous haematopoietic-stem-cell transplantation for multiple sclerosis. *The Lancet Neurology*, 4, 54-63.

BRANDENBERGER, R., BURGER, S., CAMPBELL, A., FONG, T., LAPINSKAS, E. & ROWLEY, J. A. 2011. Cell therapy bioprocessing : integrating process and product

development for the next generation of biotherapeutics. *BioProcess International*, 9, 30-37.

BRETZNER, F., GILBERT, F., BAYLIS, F. & BROWNSTONE, R. 2011. Target populations for first in human embryonic stem cell research in spinal cord injury. *Cell Stem Cell*, 8, 468-475.

BURKE, P., LAI, L.-C. & KWAST, K. 2004. A rapid filtration apparatus for harvesting cells under controlled conditions for use in genome-wide temporal profiling studies. *Analytical Biochemistry*, 328, 29.

CADWELL, J. J. S. 2011. Production of recombinant proteins and monoclonal antibodies in hollow fiber bioreactors. *American Laboratory*, 43, 30-33.

CARMELO, J. G., FERNANDES-PLATZGUMMER, A., DIOGO, M. M., DA SILVA, C. L. & CABRAL, J. 2015. A xeno-free microcarrier-based stirred culture system for the scalable expansion of human mesenchymal stem/stromal cells isolated from bone marrow and adipose tissue. *Biotechnology journal*.

CARMEN, J., BURGER, S. R., MCCAMAN, M. & ROWLEY, J. A. 2011. Developing assays to address identity, potency, purity and safety: cell characterization in cell therapy process development. *Regenerative Medicine*, 7, 85-100.

CHEN, A. K. L., REUVENY, S. & OH, S. K. W. 2013. Application of human mesenchymal and pluripotent stem cell microcarrier cultures in cellular therapy: Achievements and future direction. *Biotechnology Advances*, 31, 1032.

CHOWDHURY, F., NA, S., LI, D., POH, Y.-C., TANAKA, T. S., WANG, F. & WANG, N. 2010. Material properties of the cell dictate stress-induced spreading and differentiation in embryonic stem cells. *Nat Mater*, 9, 82-88.

CHWASTIAK, L., EHDE, D. M., GIBBONS, L. E., SULLIVAN, M., BOWEN, J. D. & KRAFT, G. H. 2014. Depressive symptoms and severity of illness in multiple sclerosis: epidemiologic study of a large community sample. *American Journal of Psychiatry*.

COHEN, E. P., CHOPRA, A., O-SULLIVAN, I. & KIM, T. S. 2009. Enhancing cellular cancer vaccines. *Immunotherapy*, Vol. 1, 495-504.

COLMONE, A. 2015. Rethinking myelin-reactive T cells in multiple sclerosis. *Science Signaling*, 8, ec131-ec131.

CUNHA, B., AGUIAR, T., SILVA, M. M., SILVA, R. J. S., SOUSA, M. F. Q., PINEDA, E., PEIXOTO, C., CARRONDO, M. J. T., SERRA, M. & ALVES, P. M. 2015a. Exploring continuous and integrated strategies for the up- and downstream processing of human mesenchymal stem cells. *Journal of Biotechnology*, 213, 97-108.

CUNHA, B., PEIXOTO, C., SILVA, M. M., CARRONDO, M. J. T., SERRA, M. & ALVES, P. M. 2015b. Filtration methodologies for the clarification and concentration of human mesenchymal stem cells. *Journal of Membrane Science*, 478, 117-129.

DANPURE, C. J. 1984. Lactate dehydrogenase and cell injury. *Cell Biochemistry and Function*, 2, 144-148.

DARZYNKIEWICZ, Z. & POŻAROWSKI, P. 2007. All that glitters is not gold: All that FLICA binds is not caspase. A caution in data interpretation—and new opportunities. *Cytometry Part A*, 71A, 536-537.

DE GRUIJL, T. D., VAN DEN EERTWEGH, A. J., PINEDO, H. M. & SCHEPER, R. J. 2008. Whole-cell cancer vaccination: from autologous to allogeneic tumor- and dendritic cell-based vaccines. *Cancer Immunology, Immunotherapy*, 57, 1569-1577.

DELAHAYE, M. 2013. *An ultra scale-down study of recovery by centrifugation of human cells for therapy*. EngD, UCL (University College London).

DELAHAYE, M., LAWRENCE, K., WARD, S. J. & HOARE, M. 2015. An ultra scale-down analysis of the recovery by dead-end centrifugation of human cells for therapy. *Biotechnology and Bioengineering*, 112, 997-1011.

DEPALMA, A. 2014. Bioprocess scaleup focuses on quality.

DHONDALAY, G. K., LAWRENCE, K., WARD, S., BALL, G. & HOARE, M. 2014. Relationship between preparation of cells for therapy and cell quality using artificial neural network analysis. *Artificial Intelligence In Medicine*, 62, 119-127.

DING, W. & MARTIN, J. 2008. Implementing single-use technology in biopharmaceutical manufacturing. *BioProcess International*.

DIVE, C., GREGORY, C. D., PHIPPS, D. J., EVANS, D. L., MILNER, A. E. & WYLLIE, A. H. 1992. Analysis and discrimination of necrosis and apoptosis (programmed cell death) by multiparameter flow cytometry. *Biochimica et Biophysica Acta (BBA) - Molecular Cell Research*, 1133, 275-285.

DONG, J.-D., GU, Y.-Q., LI, C.-M., WANG, C.-R., FENG, Z.-G., QIU, R.-X., CHEN, B., LI, J.-X., ZHANG, S.-W., WANG, Z.-G. & ZHANG, J. 2009. Response of mesenchymal stem cells to shear stress in tissue-engineered vascular grafts. *Acta Pharmacol Sin*, 30, 530-536.

ELMORE, S. 2007. Apoptosis: A review of programmed cell death. *Toxicologic Pathology*, 35, 495-516.

FDA 1997. Proposed approach to regulation of cellular and tissue-based products. The Food and Drug Administration. *J Hematother*, 6, 195-212.

FELLOWS, C., MATTA, C., ZAKANY, R., KHAN, I. & MOBASHERI, A. 2016. Adipose, bone marrow and synovial joint-derived mesenchymal stem cells for cartilage repair. *Frontiers in genetics*, 7, 213.

GAUTHIER, J., CASTAGNA, L., GARNIER, F., GUILLAUME, T., SOCIE, G., MAURY, S., MAILLARD, N., TABRIZI, R., MARCHAND, T., MALFUSON, J., GAC, A., GYAN, E., MERCIER, M., BEGUIN, Y., DELAGE, J., TURLURE, P., MARCAIS, A., NGUYEN, S., DULERY, R., BAY, J., HUYNH, A., DAGUINDAU, E., CORNILLON, J., REGNY, C., MICHALLET, M., PEFFAULT DE LATOUR, R., YAKOUB-AGHA, I. & BLAISE, D. 2017. Reduced-intensity and non-myeloablative allogeneic stem cell transplantation from alternative HLA-mismatched donors for Hodgkin lymphoma: a study by the French Society of Bone Marrow Transplantation and Cellular Therapy. *Bone Marrow Transplant*.

GUNDOGDU, O., KOENDERS, M. A., WAKEMAN, R. J. & WU, P. 2003. Permeation through a bed on a vibrating medium: theory and experimental results. *Chemical Engineering Science*, 58, 1703-1713.

HALME, D. G. & KESSLER, D. A. 2006. FDA Regulation of stem cell based therapies. *New England Journal of Medicine*, 355, 1730-1735.

HANSEL, M. C., DAVILA, J. C., VOSOUGH, M., GRAMIGNOLI, R., SKVORAK, K. J., DORKO, K., MARONGIU, F., BLAKE, W. & STROM, S. C. 2016. The use of induced pluripotent stem cells for the study and treatment of liver diseases. *Current protocols in toxicology*. John Wiley & Sons, Inc.

HASSAN, S., SIMARIA, A., VARADARAJU, H., GUPTA, S., WARREN, K. & FARID, S. 2015. Allogeneic cell therapy bioprocess economics and optimization: downstream processing decisions. *Regenerative medicine*, 10, 591-609.

HE, X., FU, W. & ZHENG, J. 2012. Cell sources for trachea tissue engineering: past, present and future. *Regenerative Medicine*, 7, 851-863.

HITCHCOCK, T. 2009. Production of recombinant whole cell vaccines with disposable manufacturing systems. *BioProcess international*, 7, 36-47.

HOLLINSHEAD, A. C., HERBERMAN, R. B., JAFFURS, W. J., ALPERT, L. K., MINTON, J. P. & HARRIS, J. E. 1974a. Soluble membrane antigens of human malignant melanoma cells. *Cancer*, 34, 1235-1243.

HOLLINSHEAD, A. C., JAFFURS, W. T., ALPERT, L. K., HARRIS, J. E. & HERBERMAN, R. B. 1974b. Isolation and identification of soluble skin-reactive membrane antigens of malignant and normal human breast cells. *Cancer Research*, 34, 2961-2968.

HOARD, P., CHANDRA, A., MEDCALF, N. & WILLIAMS, D. J. 2014. Regulatory challenges for the manufacture and scale-out of autologous cell therapies.

HU, W., BERDUGO, C. & CHALMERS, J. J. 2011. The potential of hydrodynamic damage to animal cells of industrial relevance : current understanding. *Cytotechnology*, 63, 445-460.

HUGO, O. J., SHARDA, N., HENRY, S., JING, P., DONNA, T. & CLAUDY, M. 1994. Primary cultures of rat hepatocytes in hollow fiber chambers. *In Vitro Cellular & Developmental Biology. Animal*, 30A, 23-29.

ILIC, D. & OGILVIE, C. 2017. Concise review: Human embryonic stem cells—What have we done? What are we doing? Where are we going? *Stem cells*, 35, 17-25.

IRITANI, E., KATAGIRI, N. & NAKANO, D. 2012. Flux decline behaviors in inclined dead-end ultrafiltration of BSA solutions. *Chemical Engineering Journal*, 184, 98.

JACKSON, N. B., LIDDELL, J. M. & LYE, G. J. 2006. An automated microscale technique for the quantitative and parallel analysis of microfiltration operations. *Journal of Membrane Science*, 276, 31-41.

JAKAB, K., MARGA, F., NOROTTE, C. & FORGACS, G. 2015. 4. The promises of tissue engineering for organ building and banking. *Cryobiology*, 71, 165-166.

JEANNIE, L. D., DESMOND, F. L. & THOMAS, P. W. 1991. Depth Filtration of wastewater: Particle size and ripening. *Research Journal of the Water Pollution Control Federation*, 63, 228-238.

JONES 1985. An improved method to determine cell viability by simultaneous staining with fluorescein diacetate-propidium iodide. *The Journal of Histochemistry and Cytochemistry*, 33, 77-79.

JONES, S. D., LEVINE, H. L. & MCKEE, S. 2012. Cell Therapies. *Small*.

KATZ, P. & CAMPBELL, C. 2012. FDA 2011 Process validation guidance: Process validation revisited. *Journal of GXP Compliance*, 16, 18-29.

KATZ, T., AVIVI, I., BENYAMINI, N., ROSENBLATT, J. & AVIGAN, D. 2014. Dendritic cell cancer vaccines: from the bench to the bedside. *Rambam Maimonides medical journal*, 5.

KBI-BIOPHARMA. 2014. <http://www.kbibioharma.com/about-us/ksep-systems/> [Online]. [Accessed 08 January 2014].

KEIRAN, S. M., MERCEDES, L. & MEENHARD, H. 2006. Life isn't flat: Taking cancer biology to the next dimension. *In Vitro Cellular & Developmental Biology. Animal*, 42, 242-247.

KEMPNER, M. E. & FELDER, R. A. 2002. A review of cell culture automation. *Journal of the Association for Laboratory Automation*, 7, 56-62.

KERR, J. F. R., WINTERFORD, C. M. & HARMON, B. V. 1994. Apoptosis. Its significance in cancer and cancer therapy. *Cancer*, 73, 2013-2026.

KIM, J. B., SEBASTIANO, V., WU, G., ARAÚZO-BRAVO, M. J., SASSE, P., GENTILE, L., KO, K., RUAU, D., EHRICH, M. & VAN DEN BOOM, D. 2009. Oct4-induced pluripotency in adult neural stem cells. *Cell*, 136, 411-419.

KIROUAC, D. C. & ZANDSTRA, P. W. 2008. The systematic production of cells for cell therapies. *Cell Ctem Cell*, 3, 369-381.

KNOEPFLER, P. S. 2015. From bench to FDA to bedside: US regulatory trends for new stem cell therapies. *Advanced drug delivery reviews*, 82, 192-196.

KO, H. F. & BHATIA, R. 2012. Evaluation of single-use fluidized bed centrifuge system for mammalian cell harvesting. *Biopharm International*, 25, 34-40.

KOLLE, G., HO, M., ZHOU, Q., CHY, H. S., KRISHNAN, K., CLOONAN, N., BERTONCELLO, I., LASLETT, A. L. & GRIMMOND, S. M. 2009. Identification of

Human Embryonic Stem Cell Surface Markers by Combined Membrane-Polysome Translation State Array Analysis and Immunotranscriptional Profiling. *Stem Cells*, 27, 2446-2456.

KONG, S., AUCAMP, J. & TITCHENER-HOOKER, N. J. 2010. Studies on membrane sterile filtration of plasmid DNA using an automated multiwell technique. *Journal of Membrane Science*, 353, 144-150.

KONJEVIC, G., JURISIC, V. & SPUZIC, I. 2001. Association of NK cell dysfunction with changes in LDH characteristics of peripheral blood lymphocytes (PBL) in breast cancer patients. *Breast Cancer Res Treat*, 66, 255-63.

KREGEL, K. C. 2002. Invited review: heat shock proteins: modifying factors in physiological stress responses and acquired thermotolerance. *Journal of Applied Physiology*, 92, 2177-2186.

KÜHL, N. & RENSING, L. 2000. Heat shock effects on cell cycle progression. *Cellular and Molecular Life Sciences CMLS*, 57, 450-463.

KUMAR, V., ABBAS, A., FAUSTO, N. & MITCHELL, R. N. 2007. Robbins Basic Pathology. *Saunders Elsevier*, 516-22.

LAPINSKAS, E. 2010. Scaling up research to commercial manufacturing. *Chemical Engineering Progress*, 106, 44-49.

LASKA, M., BROOKS, R., GAYTON, M. & PUJAR, N. 2005. Robust scale-up of dead end filtration: impact of filter fouling mechanisms and flow distribution. *Biotechnology and Bioengineering*, 92, 308.

LEGRAND, C., BOUR, J. M., JACOB, C., CAPIAUMONT, J., MARTIAL, A., MARC, A., WUDTKE, M., KRETZMER, G., DEMANGEL, C., DUVAL, D. & ET AL. 1992. Lactate dehydrogenase (LDH) activity of the cultured eukaryotic cells as marker of the number of dead cells in the medium [corrected]. *J Biotechnol*, 25, 231-43.

LESCH, H., LESCH, H. P., HEIKKILA, K. M., LIPPONEN, E. M., VALONEN, P., MÜLLER, A., RÄSÄNEN, E., TUUNANEN, T., HASSINEN, M. M. & PARKER, N. R. 2015. Process development of adenoviral vector production in fixed bed bioreactor-from bench to commercial scale. *Human gene therapy*.

LEVY, M. S., COLLINS, I. J., YIM, S. S., WARD, J. M., TITCHENER HOOKER, N., AYAZI SHAMLOU, P. & DUNNILL, P. 1999. Effect of shear on plasmid DNA in solution. *Bioprocess Engineering*, 20, 7-14.

LI, Q., AUCAMP, J. P., TANG, A., CHATEL, A. & HOARE, M. 2012. Use of focused acoustics for cell disruption to provide ultra scale-down insights of microbial homogenization and its bioprocess impact-recovery of antibody fragments from rec E. coli. *Biotechnology and Bioengineering*, 109, 2059-2069.

LLUFRIU, S., SEPÚLVEDA, M., BLANCO, Y., MARÍN, P., MORENO, B., BERENQUER, J., GABILONDO, I., MARTÍNEZ-HERAS, E., SOLA-VALLS, N. & ARNAIZ, J.-A. 2014. Randomized placebo-controlled phase II trial of autologous mesenchymal stem cells in multiple sclerosis.

LOKHOV, P. G. & BALASHOVA, E. E. 2010. Cellular cancer vaccines: an update on the development of vaccines generated from cell surface antigens. *Journal of Cancer*, 1, 230.

MA, G., AUCAMP, J., GERONTAS, S., EARDLEY-PATEL, R., CRAIG, A., HOARE, M. & ZHOU, Y. 2010. Mimic of a large-scale diafiltration process by using ultra scale-down rotating disc filter. *Biotechnology Progress*, 26, 466-476.

MA, G., AUCAMP, J., GERONTAS, S., EARDLEY PATEL, R., CRAIG, A., HOARE, M. & ZHOU, Y. 2009. Mimic of a large-scale diafiltration process by using ultra scale-down rotating disc filter. *Biotechnology Progress*, 26, NA.

MACCHIARINI, P., JUNGEBLUTH, P., GO, T., ASNAGHI, M. A., REES, L. E., COGAN, T. A., DODSON, A., MARTORELL, J., BELLINI, S., PARNIGOTTO, P. P., DICKINSON, S. C., HOLLANDER, A. P., MANTERO, S., CONCONI, M. T. & BIRCHALL, M. A. 2008. Clinical transplantation of a tissue-engineered airway. *The Lancet*, 372, 2023-2030.

MALIK, N. 2012. Allogeneic versus autologous stem-cell therapy. *BioPharm International*, 25, 36-40.

MASON, C. & HOARE, M. 2007. Regenerative medicine bioprocessing : Building a conceptual framework based on early studies. *Tissue Engineering*, 13, 301-311.

MCCOY, R., HOARE, M. & WARD, S. 2009. Ultra scale-down studies of the effect of shear on cell quality; processing of a human cell line for cancer vaccine therapy. *Biotechnology Progress*, 25, 1448-1458.

MCCOY, R., WARD, S. & HOARE, M. 2010. Sub-population analysis of human cancer vaccine cells-ultra scale-down characterization of response to shear. *Biotechnology and Bioengineering*, 106, 584-597.

- MCSHARRY, B. P., JONES, C. J., SKINNER, J. W., KIPLING, D. & WILKINSON, G. W. G. 2001. Human telomerase reverse transcriptase-immortalized MRC-5 and HCA2 human fibroblasts are fully permissive for human cytomegalovirus. *Journal of General Virology*, 82, 855-863.
- MINAS, T. & PETERSON, L. 2000. Autologous chondrocyte transplantation. *Operative Techniques in Sports Medicine*, 8, 144-157.
- MORRISON, S. J. & SCADDEN, D. T. 2014. The bone marrow niche for haematopoietic stem cells. *Nature*, 505, 327-334.
- MOTHE, A. J. & TATOR, C. H. 2012. Advances in stem cell therapy for spinal cord injury. *The Journal of Clinical Investigation*, 122, 3824-3834.
- MUNSIE, M. & HYUN, I. 2014. A question of ethics: selling autologous stem cell therapies flaunts professional standards. *Stem cell research*, 13, 647-653.
- NEEDHAM, D., TING-BEALL, H. P. & TRAN-SON-TAY, R. 1991. A physical characterization of GAP A3 hybridoma cells: Morphology, geometry, and mechanical properties. *Biotechnology and Bioengineering*, 38, 838-852.
- NEREM, R. M. 2010. Regenerative medicine: the emergence of an industry. *Journal of The Royal Society Interface*, 7, S771-S775.
- NEWMAN, R. E., YOO, D., LEROUX, M. A. & DANILKOVITCH-MIAGKOVA, A. 2009. Treatment of inflammatory diseases with mesenchymal stem cells. *Inflamm Allergy Drug Targets*, 8, 110-23.
- NG, Y. C., BERRY, J. M. & BUTLER, M. 1996. Optimization of physical parameters for cell attachment and growth on macroporous microcarriers. *Biotechnology and Bioengineering*, 50, 627.
- OH, H., ITO, H. & SANO, S. 2016. Challenges to success in heart failure: Cardiac cell therapies in patients with heart diseases. *Journal of cardiology*, 68, 361-367.
- OZTURK, S., THRIFT, J., BLACKIE, J. & NAVEH, D. 1997. Real-time monitoring and control of glucose and lactate concentrations in a mammalian cell perfusion reactor. *Biotechnology and Bioengineering*, 53, 372-378.
- PANDIAN, R. P., KUTALA, V. K., PARINANDI, N. L., ZWEIER, J. L. & KUPPUSAMY, P. 2003. Measurement of oxygen consumption in mouse aortic

endothelial cells using a microparticulate oximetry probe. *Archives of Biochemistry and Biophysics*, 420, 169-175.

PATTASSERIL, J., VARADARAJU, H., LOCK, L. & ROWLEY, J. 2013. Downstream technology landscape for large-scale therapeutic cell processing. *BioProcess International*, 11, 10.

PETR, G. 2010. Proteolytically-cleaved fragments of cell-surface proteins from live tumor cells stimulate anti-tumor immune response in vitro. *Journal of Carcinogenesis & Mutagenesis*.

PETRIDES, D. 2003. Bioprocess Design and Economics. *Bioseparations Science and Engineering*. Oxford University Press.

POLLOCK, K., STROEMER, P., PATEL, S., STEVANATO, L., HOPE, A., MILJAN, E., DONG, Z., HODGES, H., PRICE, J. & SINDEN, J. D. 2006. A conditionally immortal clonal stem cell line from human cortical neuroepithelium for the treatment of ischemic stroke. *Experimental neurology*, 199, 143-155.

RAMIREZ-MONTAGUT, T. 2014. Cancer Vaccines. *Novel Approaches and Strategies for Biologics, Vaccines and Cancer Therapies*, 365.

RAVIV, L. & CARNIELI, O. 2014. Cell therapies–The challenges and possible solutions for transferring cell therapy from the bench to the industry. *Drug Dev. Deliv*, 3.

REYNOLDS, T., BOYCHYN, M., SANDERSON, T., BULMER, M., MORE, J. & HOARE, M. 2003. Scale-down of continuous filtration for rapid bioprocess design: Recovery and dewatering of protein precipitate suspensions. *Biotechnology and Bioengineering*, 83, 454-464.

ROWLEY, J., ABRAHAM, E., CAMPBELL, A., BRANDWEIN, H. & OH, S. 2012. Lot-size challenges of manufacturing adherent cells for therapy. *BioProcess International*, 10.

RUSSOTTI, G., OSAWA, A. E., SITRIN, R. D., BUCKLAND, B. C., ADAMS, W. R. & LEE, S. S. 1995. Pilot-scale harvest of recombinant yeast employing microfiltration: a case study. *Journal of Biotechnology*, 42, 235.

SOWEMIMO-COKER, S. O., ANDRADE, F., KIM, A. & PESCI, S. 2009. A simple filtration system for red blood cell depletion and volume reduction in routine processing of human umbilical cord blood. *Vox Sanguinis*, 96, 138-145.

STANOVICI, J., BRENNAN, M. A., VIDAL, L., TRICHET, V., ROSSET, P., LAYROLLE, P. & LE NAIL, L. R. 2016. Bone regeneration strategies with bone marrow stromal cells in orthopaedic surgery. *Current Research in Translational Medicine*, 64, 83-90.

STARZL, T. E. 2000. History of clinical transplantation. *World J Surg*, 24, 759-82.

STEVANATO, L., CORTELING, R. L., STROEMER, P., HOPE, A., HEWARD, J., MILJAN, E. A. & SINDEN, J. D. 2009. c-MycERTAM transgene silencing in a genetically modified human

neural stem cell line implanted into MCAo rodent brain. *BMC Neuroscience*, 10.

STROEMER, P., PATEL, S., HOPE, A., OLIVEIRA, C., POLLOCK, K. & SINDEN, J. 2009. The neural stem cell line CTX0E03 promotes behavioral recovery and endogenous neurogenesis after experimental stroke in a dose-dependent fashion. *Neurorehabilitation and neural repair*, 23, 895-909.

STROMER 1997. Trypan blue exclusion test of cell viability. *Current Protocols in Immunology*.

SZCZYPKA, M., SPLAN, D., WOOLLS, H. & BRANDWEIN, H. 2014. Single-use bioreactors and microcarriers. *BioProcess International*, 12, 3.

TAIT, A. S., AUCAMP, J. P., BUGEON, A. & HOARE, M. 2009. Ultra scale-down prediction using microwell technology of the industrial scale clarification characteristics by centrifugation of mammalian cell broths. *Biotechnology and Bioengineering*, 104, 321-331.

TAKAHASHI, K., TANABE, K., OHNUKI, M., NARITA, M., ICHISAKA, T., TOMODA, K. & YAMANAKA, S. 2008. Induction of pluripotent stem cells from adult human fibroblasts by defined factors. *Obstetrical & gynecological survey*, 63.

TAKAHASHI, K. & YAMANAKA, S. 2006. Induction of pluripotent stem cells from mouse embryonic and adult fibroblast cultures by defined factors. *Cell*, 126, 663-676.

THAN, N. N., TOMLINSON, C. L., HALDAR, D., KING, A. L., MOORE, D. & NEWSOME, P. N. 2016. Clinical effectiveness of cell therapies in patients with chronic liver disease and acute-on-chronic liver failure: a systematic review protocol. *Systematic Reviews*, 5, 100.

THOMAS, R. J., ANDERSON, D., CHANDRA, A., SMITH, N. M., YOUNG, L. E., WILLIAMS, D. & DENNING, C. 2009. Automated, scalable culture of human

embryonic stem cells in feeder-free conditions. *Biotechnology and Bioengineering*, 102, 1636-1644.

USULUDIN, S. B. M., CAO, X. & LIM, M. 2012. Co-culture of stromal and erythroleukemia cells in a perfused hollow fiber bioreactor system as an in vitro bone marrow model for myeloid leukemia. *Biotechnology and Bioengineering*, 109, 1248.

VAN WEZEL, A. L. 1967. Growth of cell-strains and primary cells on micro-carriers in homogeneous culture. *Nature*, 216, 64.

WENGER, R. H. 2000. Mammalian oxygen sensing, signalling and gene regulation. *Journal of Experimental Biology*, 203, 1253-1263.

WHITFORD SR, W. G., HARDY, J. C. & CADWELL, J. J. S. 2014. Single-use, continuous processing of primary stem cells. *BioProcess international*, 12, 26.

WIEGAND, C. & HIPLER, U.-C. 2008. Methods for the measurement of cell and tissue compatibility including tissue regeneration processes. *GMS Krankenhaushygiene interdisziplinär*, 3.

WONG, J. 2009. *Centrifugal recovery of embryonic stem cells for regenerative medicine bioprocessing*.

YOUREK, G., MCCORMICK, S. M., MAO, J. J. & REILLY, G. C. 2010. Shear stress induces osteogenic differentiation of human mesenchymal stem cells. *Regen Med*, 5, 713-24.

YOUSSEF, A. A., ROSS, E. G., BOLLI, R., PEPINE, C. J., LEEPER, N. J. & YANG, P. C. 2016. The promise and challenge of induced pluripotent stem cells for cardiovascular applications. *JACC: Basic to translational science*, 1, 510-523.

ZHOU, J. Y., ZHANG, Z. & QIAN, G. S. 2016. Mesenchymal stem cells to treat diabetic neuropathy: a long and strenuous way from bench to the clinic. *Cell Death Discovery*, 2, 16055.

ZHOU, L.-Q. & DEAN, J. 2015. Reprogramming the genome to totipotency in mouse embryos. *Trends in cell biology*, 25, 82-91.